



จุฬาลงกรณ์มหาวิทยาลัย
ทุนวิจัย
กองทุนรัชดาภิเษกสมโภช

รายงานการวิจัย

**การดื้อยาเออร์โลทินิบโปรตีน EGFR TK ที่มีการกลายพันธุ์
และค้นหาสารที่มีฤทธิ์ต้านมะเร็ง : การศึกษาด้วยคอมพิวเตอร์
และการทดลองในห้องปฏิบัติการ**

โดย

ผู้ช่วยศาสตราจารย์ ดร.ธัญญดา รุ่งโรจน์มงคล

กันยายน 2563

กิตติกรรมประกาศ

โครงการนี้ได้รับทุนอุดหนุนการวิจัยจากจุฬาลงกรณ์มหาวิทยาลัย (This research is funded by Chulalongkorn University: CU_GR_62_96_23_35)

บทคัดย่อ

(ภาษาไทย) ตัวรับการเจริญเติบโตของเซลล์ที่ผิว (EGFR) เป็นโปรตีนที่มีการแสดงออกมากในมะเร็งหลายชนิด ซึ่งได้รับการพิสูจน์ว่าเป็นโปรตีนเป้าหมายที่มีประสิทธิภาพสูงสำหรับยารักษาโรคมะเร็ง ในปัจจุบันยาเออร์โลทินิบ (erlotinib) จัดเป็นยาที่มีประสิทธิภาพในการยับยั้งการทำงานของโปรตีน EGFR ซึ่งได้นำมาใช้เป็นอันดับต้นๆ สำหรับผู้ป่วยโรคมะเร็ง แต่อย่างไรก็ตามเมื่อใช้ยาชนิดนี้ติดต่อกันเป็นระยะเวลา 9-13 เดือน มักจะเกิดการดื้อยาเนื่องจากการกลายพันธุ์ขั้นที่สอง T790M ของโปรตีน EGFR ที่บริเวณโดเมนไทโรซีนไคเนส (TK) ดังนั้นการค้นหาสารประกอบที่มีแนวโน้มว่ามีประสิทธิภาพต่อโปรตีนเป้าหมาย EGFR-TK พันธุ์กลาย จึงเป็นสิ่งที่สำคัญอย่างยิ่ง ในงานวิจัยนี้ผู้วิจัยได้ศึกษาผลของการกลายพันธุ์ของโปรตีน EGFR-TK ที่มีผลต่อการจับกับยาเออร์โลทินิบและค้นหาสารอนุพันธ์ใหม่ ๆ ที่มีประสิทธิภาพในการยับยั้งโปรตีนเป้าหมายของเซลล์มะเร็ง จากผลการศึกษาพบว่า การกลายพันธุ์ขั้นที่สอง T790M ส่งผลให้บริเวณวง quinazoline ของยาเออร์โลทินิบจับกับโปรตีนเป้าหมายได้ลดลงด้วยการสร้างพันธะไฮโดรเจนแบบอ่อนๆ เป็นสาเหตุหลักของการดื้อยา และจากการคัดกรองสารอนุพันธ์กลุ่มซัลโฟนิลเลตอินดิโนควิโนลีนที่มีการดัดแปลงโครงสร้างจำนวนทั้งสิ้น 26 ตัว ด้วยเทคนิคโมเลคิวลาร์ดอกกิ้งพบว่า มีสารอนุพันธ์จำนวน 23 ตัว ที่สามารถเข้าจับกับโปรตีนเป้าหมาย EGFR-TK ที่บริเวณ ATP binding site ได้ดี โดยสารกลุ่มนี้ 8 ตัว มีประสิทธิภาพในการยับยั้งการทำงานของเอนไซม์ EGFR (IC_{50} ในช่วง 1 - 23 nM) แต่มีสารอนุพันธ์เพียง 6 ตัวที่แสดงความเป็นพิษต่อเซลล์เซลล์มะเร็งในเซลล์มะเร็งผิวหนัง A431 และมะเร็งปอด A549 ด้วยค่า IC_{50} ในช่วง 10 - 36 μ M จึงเป็นกลุ่มสารที่น่าสนใจที่จะพัฒนาต่อไปเป็นยาต้านมะเร็งในอนาคต

(ภาษาอังกฤษ) Epidermal growth factor receptor (EGFR) overexpressed in many types of cancer has been proved as a high potential target for cancer therapy. Currently, erlotinib, a potent EGFR inhibitor, has been used as the first-line drug for cancer patients. However, acquired drug resistance caused by the secondary mutation T790M of EGFR tyrosine kinase (TK) domain develops inevitably after a median response duration of 9 to 13 months. Therefore, the searching for promising compounds effectively targeting mutated EGFR-TK has become an imperative necessity. In this present study, we aimed to study the source of drug resistance due to the secondary mutation T790M and to search for the newly potent compounds against EGFR-TK. From the results, such secondary mutation has caused the quinazoline ring, a core of tyrosine kinase inhibitors (TKIs), lower binding with EGFR with rather weak hydrogen bond formation. The docking results of a novel series of sulfonylate indino quinoline derivatives (26 compounds) suggested that the 23 compounds can interact well with EGFR-TK at the ATP-binding site. Among them, the 8 compounds exhibited the promising inhibitory activity against EGFR-TK with IC_{50} values of 1-23 nM, while only 6 compounds showed a high cytotoxicity with IC_{50} values of 10-36 μ M towards the A431 and A549 cancer cell lines. Therefore, these compounds could be novel small molecule inhibitors of EGFR-TK capable of exerting benefit for cancer treatment.

สารบัญ

| | หน้า |
|---------------------------------------|------|
| บทนำ | 1 |
| เนื้อเรื่อง อภิปราย/วิจารณ์ผลการทดลอง | 2 |
| สรุปผลการวิจัย | 4 |
| ภาคผนวก | 5 |
| ประวัตินักวิจัย | 8 |

บทนำ

โรคมะเร็งถูกจัดอันดับเป็นโรคร้ายแรงที่คร่าชีวิตคนทั่วโลก จากสถิติเมื่อปี พ.ศ. 2560 มีผู้เสียชีวิตจากโรคนี้นับถึง 8.8 ล้านคน ซึ่งสถานการณ์โรคมะเร็งของประเทศไทย พบว่าสาเหตุการตายสูงสุดเป็นอันดับ 1 ของคนไทย โดยมีผู้ป่วยเสียชีวิตจากโรคมะเร็งกว่า 60,000 ล้านคนต่อปี มะเร็งปอดถือเป็นสาเหตุลำดับต้นๆ ของการเสียชีวิตจากโรคมะเร็งทั่วโลก ในปัจจุบันมีผู้ป่วยประมาณ 85% ที่ได้รับการวินิจฉัยว่า เป็นมะเร็งปอดชนิด non-small cell cancer (NSCLC) ซึ่งอัตราการรอดชีวิต 5 ปีมีเพียง 17.8% เท่านั้น

ปัจจุบันโรคมะเร็งสามารถรักษาได้หลายวิธี เช่น การผ่าตัด รังสีรักษา เคมีบำบัด ฮอโมน โดยการรักษาเหล่านี้มีความเหมาะสมต่อชนิดมะเร็งและระยะโรคที่แตกต่างกัน แต่การรักษาเหล่านี้อาจส่งผลข้างเคียงต่างๆ เช่น การสูญเสียอวัยวะ การอักเสบของอวัยวะที่ได้รับรังสี การกดภูมิคุ้มกัน อาการคลื่นไส้หรืออาเจียน และผมร่วง ฯลฯ ในช่วงระยะเวลาที่สืบทอดมา มีการคิดค้นยารักษาใหม่ๆ ซึ่งคือยารักษาโรคมะเร็งที่ไม่มีผลฆ่าตัวเซลล์มะเร็งโดยตรง แต่สามารถควบคุมเซลล์มะเร็งได้จากการขัดขวางการเจริญเติบโตของเซลล์มะเร็ง โดยเซลล์ปกติจะได้รับผลกระทบจากการรักษาน้อยกว่าการรักษาด้วยเคมีบำบัด ดังนั้นจึงทำให้ผู้ป่วยมะเร็งมีอัตราการรอดชีวิตที่สูงกว่าและมีคุณภาพชีวิตที่ดีขึ้น ซึ่งยากลุ่มนี้จะออกฤทธิ์โดยรบกวนการทำงานของโมเลกุลเป้าหมาย (molecular targets) ที่มีความจำเพาะต่อการเจริญเติบโตและการแพร่กระจายของเซลล์มะเร็งนั้น แต่อย่างไรก็ตามเมื่อใช้ยาชนิดนี้ติดต่อกันเป็นระยะเวลานานประมาณ 9 ถึง 13 เดือน มักจะเกิดการดื้อยาขึ้น เนื่องจากการกลายพันธุ์ของโปรตีนเป้าหมายของเซลล์มะเร็งส่งผลให้ยาที่ใช้ในปัจจุบันมีประสิทธิภาพลดลง ดังนั้นการศึกษาผลของการดื้อยาและการค้นหาสารใหม่ๆ ที่อาจมีประสิทธิภาพดีกว่ายาเออร์โลทินิบจึงกลายเป็นประเด็นสำคัญที่ผู้วิจัยสนใจศึกษาในครั้งนี้

ผู้วิจัยจึงมุ่งค้นหาสารอนุพันธ์ใหม่ๆ ที่มีประสิทธิภาพในการยับยั้งการทำงานของเอนไซม์เป้าหมาย EGFR มากกว่ายามุ่งเป้าเออร์โลทินิบ เพื่อเป็นแนวทางในการพัฒนาไปสู่ยาด้านโรคมะเร็งที่มีประสิทธิภาพมากยิ่งขึ้น โดยมีวัตถุประสงค์โครงการ ดังนี้

1. ศึกษาผลของการกลายพันธุ์แบบ L858R และ T790M/L858R ในโดเมน TK ของโปรตีน EGFR ที่มีผลต่อการจับกับยามุ่งเป้าเออร์โลทินิบด้วยการจำลองเชิงพลวัตโมเลกุล
2. เพื่อค้นหาสารที่มีประสิทธิภาพในการยับยั้งโปรตีนเป้าหมายของเซลล์มะเร็งและทดสอบความเป็นพิษต่อเซลล์มะเร็งเพาะเลี้ยงที่มีการแสดงออกที่มากผิดปกติและก่อการกลายพันธุ์ของโปรตีน EGFR

เนื้อเรื่อง อภิปราย/วิจารณ์ผลการทดลอง

ได้ทำการวิจัยตามแผนในตาราง โดยรายละเอียดของวิธีการทดลอง ผลการทดลอง อภิปราย/วิจารณ์ผลการทดลอง ดังเอกสารแนบ (ผลงานตีพิมพ์ระดับนานาชาติจำนวน 2 ฉบับ และอยู่ในระหว่างเตรียมผลงานตีพิมพ์อีก 1 ฉบับ)

| กิจกรรม | ผลผลิต |
|---|--|
| 1. สร้างโมเดลของโดเมน TK ของโปรตีน EGFR ที่มีการกลายพันธุ์ชั้นแรกแบบ L858R และชั้นสองแบบ T790M/L858R และสร้างประจุ RESP ของยามุ่งเป้าเออร์โลทินิบด้วยวิธีทางควอนตัม | โมเดลโครงสร้างของโดเมน TK ของโปรตีน EGFR ที่มีการกลายพันธุ์ทั้งก่อนและหลังการดื้อยา โครงสร้างอิสระของสารยามุ่งเป้าเออร์โลทินิบใน gas phase และพารามิเตอร์สำหรับการจำลองพลวัตเชิงโมเลกุล |
| 2. ปรับเปลี่ยนสถานะต่างๆ ของระบบจำลอง และทำการจำลองพลวัตเชิงโมเลกุลของสารประกอบเชิงซ้อนที่อุณหภูมิ 310K เป็นเวลา 200 ns | โครงสร้างที่เก็บได้จากการคำนวณโดยวิธีการจำลองพลวัตเชิงโมเลกุล |
| 3. วิเคราะห์การยึดจับกันระหว่างยามุ่งเป้าเออร์โลทินิบกับโดเมน TK ของโปรตีน EGFR เช่น electrostatic interactions, vdW interactions, protein motion และ binding free energy เป็นต้น | ข้อมูลพื้นฐานเชิงโมเลกุลที่สำคัญ ความเข้าใจถึงพฤติกรรมของการจับระหว่างยามุ่งเป้าเออร์โลทินิบที่มีต่อโดเมน TK ของโปรตีน EGFR ที่มีการกลายพันธุ์ |
| 4. ศึกษาลักษณะ Pharmacophore ของสารต้นแบบเพื่อใช้เป็นต้นแบบสำหรับออกแบบลักษณะโครงสร้างสารใหม่ที่สามารถเข้าจับกับโปรตีน EGFR ได้ดีขึ้นโดยใช้โปรแกรม LigandScout | ทราบลักษณะ Pharmacophore ของสารต้นแบบที่เกิดขึ้น และสามารถใช้เป็นต้นแบบสำหรับการออกแบบสารใหม่ๆ ได้ |

| | |
|---|--|
| <p>5. สร้างโครงสร้าง 3 มิติของสารประกอบที่สนใจและศึกษา รูปแบบการเข้าจับระหว่างโครงสร้างสารประกอบกับโปรตีนเป้าหมาย EGFR ด้วยเทคนิค Molecular docking</p> | <p>ทราบความสามารถและรูปแบบการเข้าจับระหว่างสารกลุ่มไวนิลซัลโฟนและสารกลุ่มไทอะโซลเบสซาร์โคลกับโปรตีน EGFR</p> |
| <p>6. ศึกษายับยั้งการทำงานของโปรตีนเป้าหมายด้วยวิธีทางชีวเคมี enzymatic activity</p> | <p>ทราบถึงความสามารถของสารสารกลุ่มไวนิลซัลโฟนและสารกลุ่มไทอะโซลเบสซาร์โคลในการยับยั้งการทำงานของโปรตีนเป้าหมาย</p> |
| <p>7. ศึกษาความเป็นพิษต่อเซลล์มะเร็งโดยการทดสอบ MTT ASSAY ในเซลล์มะเร็งชนิดต่างๆ เทียบกับเซลล์ปกติ</p> | <p>ทราบถึงจำนวนของสารกลุ่มไวนิลซัลโฟนและสารกลุ่มไทอะโซลเบสซาร์โคลที่สามารถทำลายเซลล์มะเร็งได้และไม่เป็นพิษต่อเซลล์ปกติ</p> |
| <p>8. ตีพิมพ์ในวารสารงานวิจัย</p> | <p>ผลงานตีพิมพ์ในวารสารงานวิจัย 2 ฉบับ และอยู่ในระหว่างเตรียมส่งตีพิมพ์อีก 1 ฉบับ</p> |

สรุปผลการวิจัย

ได้ตีพิมพ์เผยแพร่ผลการวิจัยในวารสารทางวิชาการระดับนานาชาติจำนวน 2 ฉบับ และอยู่ในระหว่างเตรียมผลงานตีพิมพ์อีก 1 ฉบับ ดังนี้

ชื่อบทความ Identification of vinyl sulfone derivatives as EGFR tyrosine kinase inhibitor: In vitro and in silico studies

ชื่อวารสาร Molecules, 2021, 26, 2211

High impact factor (ระดับ) โปรตระบุ 3.267 (Q1 in Scopus database)

ชื่อบทความ Discovery of novel JAK2 and EGFR inhibitors from thiazole derivatives

ชื่อวารสาร RSC Medicinal Chemistry, 2021, 12, 430

High impact factor (ระดับ) โปรตระบุ pending (*recently changed the journal name from Med Chem Comm with impact factor 2.394, Q1 in Scopus database*)

ชื่อบทความ Source of lower anticancer-drug susceptibility due to T790M/L858R

EGFR mutation: Molecular dynamics and principle component analysis

ชื่อวารสาร Protein Science (in preparation)

High impact factor (ระดับ) โปรตระบุ 3.876

ภาคผนวก



Article

Identification of Vinyl Sulfone Derivatives as EGFR Tyrosine Kinase Inhibitor: In Vitro and In Silico Studies

Thitinan Aiebchun ¹, Panupong Mahalapbutr ², Atima Auepattanapong ³, Onnicha Khaikate ³, Supaphorn Seetaha ⁴, Lueacha Tabtimmai ⁵, Chutima Kuhakarn ³, Kiattawee Choowongkamon ^{4,*} and Thanyada Rungrotmongkol ^{1,6,*}

- ¹ Biocatalyst and Environmental Biotechnology Research Unit, Department of Biochemistry, Faculty of Science, Chulalongkorn University, Bangkok 10330, Thailand; thitinan1906@gmail.com
² Department of Biochemistry, Faculty of Medicine, Khon Kaen University, Khon Kaen 40002, Thailand; panupma@kku.ac.th
³ Department of Chemistry and Center of Excellence for Innovation in Chemistry (PERCH-CIC), Faculty of Science, Mahidol University, Bangkok 10700, Thailand; iceatma.12@gmail.com (A.A.); onnicha.khai@gmail.com (O.K.); chutima.kon@mahidol.ac.th (C.K.)
⁴ Department of Biochemistry, Faculty of Science, Kasetsart University, Chatuchak, Bangkok 10900, Thailand; supaporn.se@ku.th
⁵ Department of Biotechnology, Faculty of Applied Science, King Mongkut's University of Technology of North Bangkok, Bangkok 10800, Thailand; Lueacha.t@sct.kmutnb.ac.th
⁶ Program in Bioinformatics and Computational Biology, Faculty of Science, Chulalongkorn University, Bangkok 10330, Thailand
 * Correspondence: kiattawee.c@ku.th (K.C.); t.rungrotmongkol@gmail.com (T.R.); Tel: +66-2218-5426 (T.R.); Fax: +66-2218-5418 (T.R.)



Citation: Aiebchun, T.; Mahalapbutr, P.; Auepattanapong, A.; Khaikate, O.; Seetaha, S.; Tabtimmai, L.; Kuhakarn, C.; Choowongkamon, K.; Rungrotmongkol, T. Identification of Vinyl Sulfone Derivatives as EGFR Tyrosine Kinase Inhibitor: In Vitro and In Silico Studies. *Molecules* **2021**, *26*, 2211. <https://doi.org/10.3390/molecules26082211>

Academic Editor: Pascal Marchand

Received: 21 November 2020

Accepted: 7 April 2021

Published: 12 April 2021

Publisher's Note: MDPI stays neutral with regard to jurisdictional claims in published maps and institutional affiliations.



Copyright © 2021 by the authors. Licensee MDPI, Basel, Switzerland. This article is an open access article distributed under the terms and conditions of the Creative Commons Attribution (CC BY) license (<https://creativecommons.org/licenses/by/4.0/>).

Abstract: Epidermal growth factor receptor (EGFR), overexpressed in many types of cancer, has been proved as a high potential target for targeted cancer therapy due to its role in regulating proliferation and survival of cancer cells. In the present study, a series of designed vinyl sulfone derivatives was screened against EGFR tyrosine kinase (EGFR-TK) using in silico and in vitro studies. The molecular docking results suggested that, among 78 vinyl sulfones, there were eight compounds that could interact well with the EGFR-TK at the ATP-binding site. Afterwards, these screened compounds were tested for the inhibitory activity towards EGFR-TK using ADP-Glo™ kinase assay, and we found that only VF16 compound exhibited promising inhibitory activity against EGFR-TK with the IC₅₀ value of 7.85 ± 0.88 nM. In addition, VF16 showed a high cytotoxicity with IC₅₀ values of 33.52 ± 2.57, 54.63 ± 0.09, and 30.38 ± 1.37 μM against the A431, A549, and H1975 cancer cell lines, respectively. From 500-ns MD simulation, the structural stability of VF16 in complex with EGFR-TK was quite stable, suggesting that this compound could be a novel small molecule inhibitor targeting EGFR-TK.

Keywords: EGFR tyrosine kinase; vinyl sulfone derivatives; in silico study; kinase assay; cytotoxicity assay

1. Introduction

Cancer is a devastating disease characterized by uncontrolled growth and spread of abnormal cells and is the second leading cause of mortality worldwide [1]. Nowadays, there are many types of cancer treatment such as chemotherapy, radiation therapy and targeted therapy [2–4]. Targeted cancer therapy has become one of the highly effective for cancer treatment due to its specificity towards cancer cells [5]. The overexpression of epidermal growth factor receptor (EGFR) in cancer cells leads to abnormal signal transduction and is closely related to the occurrence of cancer. Therefore, it has become one of the most important protein targets for designing and developing kinase inhibitors that act on oncogenic EGFR [6].

Cite this: *RSC Med. Chem.*, 2021, 12, 430

Discovery of novel JAK2 and EGFR inhibitors from a series of thiazole-based chalcone derivatives†

Kamonpan Sanachai,^{‡a} Thitinan Aiebchun,^{‡a} Panupong Mahalapbutr,^{‡b} Supaphorn Seetaha,^c Lueacha Tabtimmai,^d Phornphimon Maitarad,^e Iakovos Xenikakis,^f Athina Geronikaki,^g Kiattawee Choowongkorn,^h and Thanyada Rungrotmongkol^{h,*ag}

The Janus kinase (JAK) and epidermal growth factor receptor (EGFR) have been considered as potential targets for cancer therapy due to their role in regulating proliferation and survival of cancer cells. In the present study, the aromatic alkyl-amino analogs of thiazole-based chalcone were selected to experimentally and theoretically investigate their inhibitory activity against JAK2 and EGFR proteins as well as their anti-cancer effects on human cancer cell lines expressing JAK2 (TF1 and HEL) and EGFR (A549 and A431). *In vitro* cytotoxicity screening results demonstrated that the HEL erythroleukemia cell line was susceptible to compounds 11 and 12, whereas the A431 lung cancer cell line was vulnerable to compound 25. However, TF1 and A549 cells were not sensitive to our thiazole derivatives. From kinase inhibition assay results, compound 25 was found to be a dual inhibitor against JAK2 and EGFR, whereas compounds 11 and 12 selectively inhibited the JAK2 protein. According to the molecular docking analysis, compounds 11, 12 and 25 formed hydrogen bonds with the hinge region residues Lys857, Leu932 and Glu930 and hydrophobically came into contact with Leu983 at the catalytic site of JAK2, while compound 25 formed a hydrogen bond with Met769 at the hinge region, Lys721 near a glycine loop, and Asp831 at the activation loop of EGFR. Altogether, these potent thiazole derivatives, following Lipinski's rule of five, could likely be developed as a promising JAK2/EGFR targeted drug(s) for cancer therapy.

Received 30th December 2020.
Accepted 25th January 2021

DOI: 10.1039/d0md00436g

rsc.li/medchem

Introduction

Cancer, a group of diseases characterized by uncontrolled growth and spread of abnormal cells,¹ is the second leading cause of mortality worldwide.² Among several types of cancer, myeloproliferative neoplasms and lung cancer are the leading

cause of cancer-related death globally.³ The known molecular targets for treating these cancers are the Janus kinases (JAKs) and the epidermal growth factor receptor (EGFR), since they play a major role in regulating proliferation and survival of cancer cells.^{4,5}

JAK, an intracellular tyrosine kinase, is activated by the cytokine(s) binding to its receptor, resulting in the activation of the downstream signal transducer and activator of transcription (STAT), which leads to its dimerization and translocation to the nucleus, promoting cell proliferation, apoptosis and differentiation.⁶ Among the four JAK family members (JAK1, JAK2, JAK3 and TYK2),⁷ JAK2 is a critical moderator for hormone-like cytokines such as growth hormone (GH), erythropoietin (EPO), thrombopoietin (TPO) and cytokine receptor ligands involved in hematopoietic cell development such as interleukin-3 (IL-3).⁸ JAK2 consists of seven homology regions (JH1 to JH7) and the catalytically active domain in JH1 is located at the carboxy-terminus, close to the pseudo-kinase domain in JH2. The overexpression of JAK2, especially the V617F variance in the JH2 domain, has been shown to be related to myeloproliferative disorders (by approximately 50% or more) such as polycythemia vera, essential thrombocythemia and myelofibrosis,^{9,10} indicating

^aStructural and Computational Biology Research Unit, Department of Biochemistry, Faculty of Science, Chulalongkorn University, Bangkok 10330, Thailand. E-mail: t.rungrotmongkol@gmail.com; Fax: +662 2185418; Tel: +662 2185426

^bDepartment of Biochemistry, Faculty of Medicine, Khon Kaen University, Khon Kaen 40002, Thailand

^cDepartment of Biochemistry, Faculty of Science, Kasetsart University, Bangkok 10900, Thailand

^dDepartment of Biotechnology, Faculty of Applied Science, King Mongkut's University of Technology of North Bangkok, Bangkok, Thailand

^eResearch Center of Nano Science and Technology, Shanghai University, Shanghai 200444, PR China

^fDepartment of Pharmaceutical Chemistry, School of Pharmacy, Aristotle University of Thessaloniki, Thessaloniki 54124, Greece

^gProgram in Bioinformatics and Computational Biology, Graduate School, Chulalongkorn University, Bangkok 10330, Thailand

^hElectronic supplementary information (ESI) available. See DOI: 10.1039/d0md00436g

[†] These authors contributed equally to this work.

1 **Source of lower anticancer-drug susceptibility due to**
2 **T790M/L858R EGFR mutation: Molecular dynamics and**
3 **principle component analysis**

4 Phakawat Chusuth¹, Supot Hannongbua², Thanyada Rungrotmongkol^{1,3}

5

6

7 ¹Biocatalyst and Environmental Biotechnology Research unit, Department of Biochemistry,
8 Faculty of Science, Chulalongkorn University, Bangkok 10330, Thailand

9 ²Computational Chemistry Center of Excellent, Department of Chemistry, Faculty of Science,
10 Chulalongkorn University, Bangkok 10330, Thailand

11 ³Program in Bioinformatics and Computational Biology, Faculty of Science, Chulalongkorn
12 University, Bangkok 10330, Thailand

13

14

15 Email: thanyada.r@chula.ac.th, trungrotmongkol@gmail.com

16 Phone: +66-2218-5426. Fax: +66-2218-5418.

17

18

19

20

21

22

23

ประวัตินักวิจัย

ชื่อ (ภาษาไทย) ธัญญดา รุ่งโรจน์มงคล

ชื่อ (ภาษาอังกฤษ) Thanyada Rungrotmongkol

วันเดือนปีเกิด 14 January 1979

สถานที่เกิด Ratchaburi province

สถานภาพการสมรส -

ตำแหน่งปัจจุบัน Assistant Professor in Chemistry

ที่อยู่หน่วยงาน / โทรศัพท์ / โทรศัพท์เคลื่อนที่

Department of Biochemistry, Faculty of Science, Chulalongkorn University

254 Phayathai Rd., Patumwan, Bangkok, 10330, Thailand

E-mail address: thanyada.r@chula.ac.th, t.rungrotmongkol@gmail.com

Phone Number: +66-2218-5426

ประวัติการศึกษา

| <u>Year</u> | <u>Degree</u> | <u>Institute</u> |
|-------------|--|----------------------|
| 2001 | B.Sc. in Chemistry (with First Class Honors) | Kasetsart University |
| 2006 | Ph.D. in Physical Chemistry | Kasetsart University |

ผลงานวิจัยเด่น เช่น วารสารวิชาการระดับนานาชาติ วารสารวิชาการระดับชาติ หนังสือนิพนธ์ (ในประเทศและต่างประเทศ)

1. T. Rungrotmongkol, S. Hannongbua* and A. J. Mulholland, Mechanistic study of HIV-1 reverse transcriptase at the active site based on QM/MM method, *Journal of Theoretical and Computational Chemistry* 2004; 3(4): 491-500.
2. T. Rungrotmongkol, A. J. Mulholland and S. Hannongbua*, Active site dynamics and combined quantum mechanics/ molecular mechanics (QM/ MM) modelling of a HIV-1 reverse transcriptase/DNA/dTTP complex, *Journal of molecular graphics and modelling* 2007; 26(1): 1-13.
3. M. Malaisree, T. Rungrotmongkol, P. Decha, P. Intharathep, O. Aruksakunwong, and S. Hannongbua*, Understanding of known drug-target interactions in the catalytic pocket of neuraminidase subtype N1, *Proteins* 2008; 71(4): 1908-191
4. P. Decha, T. Rungrotmongkol, P. Intharathep, M. Malaisree, O. Aruksakunwong, C. Laohpongspaisan, V. Parasuk, P. Sompornpisut, S. Pianwanit, S. Kokpol and S. Hannongbua*, Source of high pathogenicity of an avian influenza virus H5N1: Why H5 is better cleaved by furin, *Biophysical Journal* 2008; 95(1): 128-134.
5. V. Nukoolkarn, S. Saen-oon, T. Rungrotmongkol, S. Hannongbua, K. Ingkaninan, K. Suwanborirux*, Petrosamine, a potent anticholinesterase pyridoacridine alkaloid from a Thai marine sponge *Petrosia n. sp.*, *Bioorganic & Medicinal Chemistry* 2008; 16(13): 6560-6567.
6. T. Rungrotmongkol, P. Decha, M. Malaisree, P. Sompornpisut, and S. Hannongbua*, Comment on "Cleavage mechanism of the H5N1 hemagglutinin by trypsin and furin" [Amino Acids 2008, January 31, Doi: 10.1007/s00726-007-0611-3], *Amino Acids* 2008; 35: 511-512.

7. P. Intharathep, C. Laohpongspaisan, T. **Rungrotmongkol**, A. Loisuangsin, M. Malaisree, P. Decha, O. Aruksakunwong, K. Chuenpennit, N. Kaiyawet, P. Sompornpisut, S. Pianwanit, and S. Hannongbua*, How amantadine and rimantadine inhibit proton transport in the M2 protein channel, *Journal of Molecular Graphics and Modelling* **2008**; 27(3): 342-348.
8. T. **Rungrotmongkol**, V. Frecer, W. De-Eknamkul, S. Hannongbua, and S. Miertus*, Design and in silico screening of combinatorial library of oseltamivir analogs inhibiting neuraminidase of avian influenza virus H5N1. *Antiviral Research* **2009**; 82(1):51-8.
9. T. **Rungrotmongkol**, M. Malaisree, T. Udommaneethanakit and S. Hannongbua*, Comment on "Another look at the molecular mechanism of the resistance of H5N1 influenza A virus neuraminidase (NA) to oseltamivir (OTV)". *Biophysical Chemistry* **2009**; 141: 131-132.
10. C. Laohpongspaisan, T. **Rungrotmongkol**, P. Intharathep, M. Malaisree, P. Decha, O. Aruksakunwong, P. Sompornpisut, S. Hannongbua*, Why amantadine loses its function in influenza M2 mutants: MD simulations. *Journal of Chemical Information and Modeling* **2009**; 49(4):847-52.
11. T. **Rungrotmongkol**, P. Decha, P. Sompornpisut, M. Malaisree, P. Intharathep, N. Nunthaboot, T. Udommaneethanakit, O. Aruksakunwong, and S. Hannongbua*, Combined QM/MM mechanistic study of the acylation process in furin complexed with the H5N1 avian influenza virus hemagglutinin's cleavage site. *Proteins: Structure, Function, and Bioinformatics* **2009**; 76(1): 62-71
12. T. **Rungrotmongkol**, P. Intharathep, M. Malaisree, N. Nunthaboot, N. Kaiyawet, P. Sompornpisut, S. Payungporn, Y. Poovorawan, and S. Hannongbua*, Susceptibility of antiviral drugs against 2009 influenza A (H1N1) virus. *Biochemical and Biophysical Research Communications* **2009**; 385(3):390-4.
13. M. Malaisree^a, T. **Rungrotmongkol**^a, N. Nunthaboot, O. Aruksakunwong, P. Intharathep, P. Decha, P. Sompornpisut and S. Hannongbua*, Source of Oseltamivir Resistance in Avian Influenza H5N1 Virus with the H274Y Mutation. *Amino Acids* **2009**; 37(4):725-732.
14. T. Udommaneethanakit, T. **Rungrotmongkol**, U. Bren, V. Frecer and S. Miertus*, Dynamic Behavior of Avian Influenza A Virus Neuraminidase Subtype H5N1 in Complex with Oseltamivir, Zanamivir, Peramivir, and their Phosphonate Analogues, *Journal of Chemical Information and Modeling* **2009**; 49(10):2323-2332.
15. T. **Rungrotmongkol**, T. Udommaneethanakit, M. Malaisree, N. Nunthaboot, P. Intharathep, P. Sompornpisut and S. Hannongbua*, How does each substituent functional group of oseltamivir lose its activity against virulent H5N1 influenza mutants? *Biophysical Chemistry* **2009**; 145(1):29-36.
16. T. **Rungrotmongkol**, T. Udommaneethanakit, V. Frecer, and S. Miertus, Combinatorial design of avian influenza neuraminidase inhibitors containing pyrrolidine core with a reduced susceptibility to viral drug resistance, *Combinatorial Chemistry & High Throughput Screening* **2010**; 13(3):268-77.
17. N. Nunthaboot, T. **Rungrotmongkol**, M. Malaisree, P. Decha, N. Kaiyawet, P. Intharathep, P. Sompornpisut, Y. Poovorawan and S. Hannongbua*, Molecular insights into human receptor binding to 2009 H1N1 influenza A hemagglutinin, *Monatshefte für Chemie - Chemical Monthly* **2010**; 141(7):801-807.

18. T. Rungrotmongkol^a, M. Malaisree^a, N. Nunthaboot, P. Sompornpisut, and S. Hannongbua*, Molecular prediction of oseltamivir efficiency against probable influenza A (H1N1-2009) mutants: Molecular modelling approach, *Amino Acids* **2010**; 39(2):393-398.
19. S. Phongphanphanee, T. Rungrotmongkol, N. Yoshida, S. Hannongbua, F. Hirata*, Proton transport through the influenza A M2 channel: 3D-RISM study, *Journal of American Chemical Society* **2010**; 132(28):9782-9788.
20. N. Nunthaboot, T. Rungrotmongkol, M. Malaisree, N. Kaiyawet, P. Decha, P. Sompornpisut, and S. Hannongbua*, Evolution of human receptor binding affinity of h1n1 hemagglutinins from 1918 to 2009 pandemic influenza A virus, *Journal of Chemical Information and Modeling* **2010**;50(8): 1410-1417.
21. T. Rungrotmongkol*, N. Nunthaboot, M. Malaisree, N. Kaiyawet, P. Yotmanee, A. Meeprasert and S. Hannongbua, Molecular Insight into the Specific Binding of ADP-ribose to the nsP3 Macro Domains of Chikungunya and Venezuelan Equine Encephalitis Viruses: Molecular Dynamics Simulations and Free Energy Calculations, *Journal of Molecular Graphics and Modelling* **2010**;29(3):347–353.
22. U. Arsawang, O. Saengsawang, T. Rungrotmongkol, P. Sornmee, K. Wittayanarakul, T. Remsungnen and S. Hannongbua*, How do carbon nanotubes serve as carriers for gemcitabine transport in drug delivery system? *Journal of Molecular Graphics and Modelling* **2011**;29(5):591–596.
23. P. Intharathep, T. Rungrotmongkol, P. Decha, N. Nunthaboot, N. Kaiyawet, T. Kerdcharoen, P. Sompornpisut, and S. Hannongbua*, Evaluating how rimantadines control the proton gating of the Influenza A M2-proton port via allosteric binding outside of the M2-channel: MD simulations, *Journal of Enzyme Inhibition and Medicinal Chemistry* **2011**; 26(2):162-168.
24. T. Rungrotmongkol, U. Arsawang, C. Iamsamai, A. Vongachariya, S. Dubas, U. Ruktanonchai, A. Soottitawat and S. Hannongbua*, Increase dispersion and solubility of carbon nanotubes noncovalently modified by the polysaccharide biopolymer, chitosan: MD simulations, *Chemical Physics Letter* **2011**;507(1-3):134–137.
25. T. Rungrotmongkol^a, P. Yotmanee^a, N. Nunthaboot^a and S. Hannongbua*, Computational studies of influenza A virus at three important targets: hemagglutinin, neuraminidase and M2 protein, *Current Pharmaceutical Design* **2011**;17(17):1720-1739. (review article)
26. P. Sornmee, T. Rungrotmongkol, O. Saengsawang, U. Arsawang, T. Remsungnen and S. Hannongbua*, Understanding the molecular properties of doxorubicin filling inside and wrapping outside single-walled carbon nanotubes, *Journal of Computational and Theoretical Nanosciences* **2011**;8(8): 1385-1391.
27. J. Kongkamnerd, L. Cappelletti, A. Prandi, P. Seneci*, T. Rungrotmongkol, N. Jongaroonngamsang, P. Rojsitthisak, V. Frecer*, A. Milani, G. Cattoli, C. Terregino, I. Capua, L. Beneduce, A. Gallotta, P. Pengo, G. Fassina, S. Miertus, W. De-Eknamkul*, Synthesis and in vitro study of novel neuraminidase inhibitors against avian influenza virus, *Bioorganic & Medicinal Chemistry* **2012**;20(6): 2152–2157
28. P. Kongsune, T. Rungrotmongkol, N. Nunthaboot, P. Yotmanee, P. Sompornpisut, Y. Poovorawan, P. Wolschann and S. Hannongbua*, Molecular insights into the binding affinity and specificity of the

- hemagglutinin cleavage loop from four highly pathogenic H5N1 isolates towards the proprotein convertase furin, *Monatshefte für Chemie - Chemical Monthly* **2012**;143(5):853–860.
29. A. Meeprasert, W. Khuntawee, K. Kamlungso, N. Nunthaboot, T. Rungrotmongkol*, S. Hannongbua, Binding pattern of the long acting neuraminidase inhibitor laninamivir toward influenza A subtypes H5N1 and pandemic H1N1, *Journal of Molecular Graphics and Modeling* **2012**;38: 148-154.
 30. C. Rungnim, U. Arsawang, T. Rungrotmongkol*, S. Hannongbua, Molecular dynamics properties of varying amounts of the anticancer drug gemcitabine inside an open-ended single-walled carbon nanotube, *Chemical Physics Letter* **2012**; 550: 99-103.
 31. A. Vongachariya, C. Iamsamai, O. Saengsawang, T. Rungrotmongkol, S. Dubas, V. Parasuk and S. Hannongbua*, The surface curvature effect of single-walled carbon nanotube on its cation- π interaction with monovalent cations, *Journal of Computational and Theoretical Nanosciences* **2012**; 9(12), 2107-2112.
 32. W. Khuntawee, T. Rungrotmongkol* and S. Hannongbua. Molecular Dynamic Behavior and Binding Affinity of Flavonoid Analogues to the Cyclin Dependent Kinase 6/cyclin D Complex, *Journal of Chemical Information and Modeling* **2012**;52:76–83.
 33. C. Rungnim, T. Rungrotmongkol, S. Hannongbua*, H. Okumura, Replica exchange molecular dynamics simulation of chitosan for drug delivery system based on carbon nanotube, *Journal of Molecular Graphics and Modeling* **2013**; 39: 183-192.
 34. N. Kaiyawet, T. Rungrotmongkol* and S. Hannongbua, Probable polybasic residues inserted into the cleavage site of the highly pathogenic avian influenza A/H5N1 hemagglutinin: speculation of the next outbreak in humans, *International Journal of Quantum Chemistry* **2013**; 113(4), 569–573.
 35. P. Maitarad, D. Zhang*, R. Gao, L. Shi*, H. Li, L. Huang, T. Rungrotmongkol, J. Zhang, Combination of experimental and theoretical investigations of MnO_x/Ce_{0.9}Zr_{0.1}O₂ nanorods for selective catalytic reduction of NO with ammonia, *The Journal of Physical Chemistry C*, **2013**; 117(19): 9999–10006.
 36. R. Gao, D. Zhang*, P. Maitarad, L. Shi*, T. Rungrotmongkol, H. Li, J. Zhang, W. Cao, Morphology-dependent properties of MnO_x/ZrO₂-CeO₂ nanostructures for the selective catalytic reduction of NO with NH₃, *The Journal of Physical Chemistry C*, **2013**; 117 (20), 10502–10511.
 37. N. Nunthaboot^a, T. Rungrotmongkol^a, O. Aruksakunwong^a, S. Hannongbua*, Effects of protonation state of catalytic residues and ligands upon binding and recognition in targeted proteins of HIV-1 and influenza viruses, *Current Pharmaceutical Design* **2013**; 19(23), 4276-4290. (review article)
 38. N. Kaiyawet, T. Rungrotmongkol, S. Hannongbua*, Effect of halogen substitutions on dUMP to stability of thymidylate synthase/dUMP/mTHF ternary complex using molecular dynamics simulation, *Journal of Chemical Information and Modeling*, **2013**; 53 (6), 1315–1323
 39. T. Rungrotmongkol, A.J. Mulholland, S. Hannongbua*, QM/MM simulations indicate that Asp185 is the likely catalytic base in the enzymatic reaction of HIV-1 reverse transcriptase, *Medicinal Chemistry Communications*, **2014**; 5(5): 593-596.
 40. W. Sangpheak, W. Khuntawee, P. Wolschann, P. Pongsawasdi, T. Rungrotmongkol*, Enhanced stability of naringenin/2,6-dimethyl β -cyclodextrin inclusion complex: Molecular dynamics and free

- energy calculations based on MM- and QMPBSA/GBSA, *Journal of Molecular Graphics and Modeling*, **2014**; 50: 10–15.
41. A. Meeprasert, T. Rungrotmongkol, M.S. Li*, S Hannongbua*, In Silico screening for potent inhibitors against the NS3/4A protease of hepatitis C virus, *Current Pharmaceutical Design*, **2014**; 20(21), 3465-3477.
 42. A. Meeprasert, S. Hannongbua, T. Rungrotmongkol*, Key Binding and Susceptibility of NS3/4A Serine Protease Inhibitors against Hepatitis C Virus, *Journal of Chemical Information and Modeling*, **2014**, 54(4): 1208-17.
 43. P. Maitarad, J. Han, D. Zhanga*, L. Shi, S. Namuangruk, T. Rungrotmongkol, Structure-Activity Relationships of NiO on CeO₂ Nanorods for Selective Catalytic Reduction of NO with NH₃: Experimental and DFT Studies, *The Journal of Physical Chemistry C*, **2014**; 118 (18), 9612–9620.
 44. B. Nutho, W. Khuntawee, C. Rungnim, P. Pongsawasdi, P. Wolschann, A. Karpfen, N. Kungwan, T. Rungrotmongkol*, Binding mode and free energy prediction of fisetin/ β -cyclodextrin inclusion complex, *Beilstein Journal of Organic Chemistry*, **2014**; 10, 2789–2799.
 45. T. Udommaneethanakit, T. Rungrotmongkol, V. Frecer, M. Stanislav, U. Bren*, Drugs against Avian Influenza A Virus: Design of Novel Sulfonate Inhibitors of Neuraminidase N1, *Current Pharmaceutical Design*, **2014**; 20(21):3478-87.
 46. A. Sukswan, L. Lomlim, T. Rungrotmongkol, T. Nakpheng, F.L. Dickert, R. Suedee*, The Composite Nanomaterials containing (R)-Thalidomide-Molecularly Imprinted Polymers as a Recognition System for Enantioselective- Controlled Release and Targeted Drug Delivery, *Journal of Applied Polymer Science*, **2015**; 132 (18): no.41930
 47. M. Ratanasak, T. Rungrotmongkol, O. Saengawang, S. Hannongbua, V. Parasuk, Towards the design of new electron donors for Ziegler-Natta catalyzed propylene polymerization using QSPR modeling. *Polymer (United Kingdom)* **2015**; 56, 340-345.
 48. N. Kaiyawet, R. Lonsdale, T. Rungrotmongkol, A. Mulholland, S. Hannongbua*, High-Level QM/MM Calculations Support the Concerted Mechanism for Michael Addition and Covalent Complex Formation in Thymidylate Synthase, *Journal of Chemical Theory and Computation*, **2015**; 11 (2), 713–722.
 49. S. Sirikataramas*, A. Meeprasert, T. Rungrotmongkol, H. Fuji, T. Hoshino, M. Yamazaki, K. Saito*, Structural insight of DNA topoisomerases I from camptothecin-producing plants revealed by molecular dynamics simulations, *Phytochemistry*, **2015**; 113:50-6.
 50. P. Yotmanee, T. Rungrotmongkol, K. Wichapong, S. B. Choi, H. A. Wahab*, N. Kungwan, S. Hannongbua*, Binding specificity of polypeptide substrates in NS2B/NS3pro serine protease of dengue virus type 2: A molecular dynamics Study, *Journal of Molecular Graphics and Modeling* **2015**; 60, 24-33.
 51. S. Kongkaew, P. Yotmanee, T. Rungrotmongkol, N. Kaiyawet, A. Meeprasert, T. Kaburaki, H. Noguchi, F. Takeuchi, N. Kungwan, S. Hannongbua*, Molecular Dynamics Simulation Reveals the Selective Binding of Human Leukocyte Antigen Alleles Associated with Behçet's Disease, *PLoS One*, **2015**; 10(9).

52. W. Khuntawee, P. Wolschann, T. Rungrotmongkol*, J. Wong-ekkabut*, S Hannongbua, Molecular dynamics simulations of the interaction of Beta cyclodextrin with a lipid bilayer, *Journal of Chemical Information and Modeling*, **2015**, 55(9): 1894-1902.
53. C. Rungnim, S. Phunpee, M. Kunaseth, S. Namuangruk, K. Rungsardthong, T. Rungrotmongkol*, U. Ruktanonchai*, Co-solvation effect on the binding mode of the α -mangostin/ β -cyclodextrin inclusion complex, *Beilstein Journal of Organic Chemistry*, **2015**; 11, 2306–2317.
54. W. Sangpheak, J. Kicuntod, R. Schuster, T. Rungrotmongkol, P. Wolschann, N. Kuawan, H. Viernstein, M. Mueller*, P. Pongsawasdi*, Physical properties and biological activities of hesperetin and naringenin in complex with methylated β -cyclodextrin, *Beilstein Journal of Organic Chemistry*, **2015**; 11, 2763–2773.
55. J. Phanich, T. Rungrotmongkol*, D. Sindhikara, S. Phongphanphanee, N. Yoshida, F. Hirata,* N. Kungwan, S. Hannongbua, A 3D-RISM/RISM study of the oseltamivir binding efficiency with the wild-type and resistance-associated mutant forms of the viral influenza B neuraminidase, *Protein Science*, **2016**; 25(1), 147-158.
56. A. Meeprasert, S. Hannongbua, N. Kungwan, T. Rungrotmongkol*, Effect of D168V Mutation in NS3/4A HCV Protease on Susceptibilities of Faldaprevir and Danoprevir, *Molecular BioSystems*, **2016**, 12(12):3666-3673.
57. J. Kicuntod, W. Khuntawee, P. Wolschann, P. Pongsawasdi, N. Kuawan, T. Rungrotmongkol* Inclusion complexation of pinostrobin with various cyclodextrin derivatives, *Journal of Molecular Graphics and Modelling*, **2016**; 63, 91–98.
58. C. Rungnim, R. Chanajaree, T. Rungrotmongkol, S. Hannongbua, N. Kungwan, P. Wolschann, A. Karpfen*, V. Parasuk*, How strong is the edge effect in the adsorption of anticancer drugs on a graphene cluster?, *Journal of Molecular Modeling*, **2016**; 22(4)
59. W. Khuntawee, T. Rungrotmongkol, P. Wolschann, P. Pongsawasdi, N. Kungwan, H. Okumura*, S. Hannongbua* , Conformation study of ϵ -cyclodextrin: Replica exchange molecular dynamics simulations, *Carbohydrate Polymer*, **2016**, 141; 99–105.
60. N. Schaduangrat, J. Phanich, T. Rungrotmongkol, H. Lerdsamran, P. Puthavathana, S. Ubol*, The significance of naturally occurring neuraminidase quasispecies of H5N1 avian influenza virus on resistance to oseltamivir: a point of concern, *Journal of General Virology*, **2016**; 97(6):1311-23.
61. W. Karnsomwan, T. Rungrotmongkol, W. De-Eknamkul, S. Chamni*, *In silico* structural prediction of human steroid 5 α -reductase Type II, *Med. Chem. Res.* **2016**; 25(6), 1049-1056.
62. R. Daengngern, C. Prommin; T. Rungrotmongkol, V. Promarak, P. Wolschann, N. Kungwan* , Theoretical investigation of 2-(iminomethyl)phenol in the gas phase as a prototype of ultrafast excited-state intramolecular proton transfer, *Chemical Physics Letters*, **2016**; 657, 113-118.
63. C. Rungnim, T. Rungrotmongkol*, N. Kungwan, S. Hannongbua, Protein-protein interactions between SWCNT/chitosan/EGF and EGF receptor: A model of drug delivery system, *Journal of Biomolecular Structure & Dynamics*, **2016**, 34(9):1919-1929.

64. J. Phanich, T. Rungrotmongkol*, N. Kungwan, S. Hannongbua*, Role of R292K mutation in influenza H7N9 neuraminidase toward oseltamivir susceptibility: MD and MM/PB(GB)SA study, *Journal of Computer-Aided Molecular Design*, 2016, 30(10), 917-926
65. S. Tantong, O. Pringsulaka, K. Weerawanich, A. Meeprasert, T. Rungrotmongkol, R. Sarnthima, S. Roytrakul, S. Sirikantaramas. Two novel antimicrobial defensins from rice identified by gene coexpression network analyses. *Peptides*, 2016, 84, 7–16.
66. F.N. Sabri, H. Monajemi, S.M. Zain, P.S. Wai, T. Rungrotmongkol, V.S. Lee, Molecular conformation and UV-visible absorption spectrum of emeraldine salt polyaniline as a hydrazine sensor, *Integrated Ferroelectrics*, 2016, 175(1): 202-210.
67. C. Rungnim, T. Rungrotmongkol, R. Poo-arporn*, pH-controlled doxorubicin anticancer loading and release from carbon nanotube noncovalently modified by chitosan: MD simulations, *Journal of Molecular Graphics and Modelling*, 2016, 70, 70-76.
68. V.T. Phuong, T. Chokbunpiam*, S. Fritzsche, T. Remsungnen, T. Rungrotmongkol, C. Chmelik, J. Caro, S. Hannongbua*, Methane in Zeolitic Imidazolate Framework ZIF-90: Adsorption and Diffusion by Molecular Dynamics and Gibbs Ensemble Monte Carlo, *Microporous & Mesoporous Materials*, 2016, 235, 69–77.
69. W. Jetsadawisut, B. Nutho, A. Meeprasert, T. Rungrotmongkol*, N. Kungwan, P. Wolschann, S. Hannongbua*, Susceptibility of inhibitors against 3C Protease of Coxsackievirus A16 and Enterovirus A71 Causing Hand, Foot and Mouth Disease: A Molecular Dynamics Study, *Biophysical Chemistry*, 2016, 219, 9-16.
70. P. Wongpituk, B. Nutho, W. Panman, N. Kungwan, P. Wolschann, T. Rungrotmongkol*, N. Nunthaboot*, Structural dynamics and binding free energy of neral- cyclodextrins inclusion complexes: Molecular dynamics simulation, *Molecular Simulation*, 2017, 43(13–16), 1356–1363
71. W. Karnsomwan, P. Netcharonensirisuk, T. Rungrotmongkol, W. De-Eknamkul, S. Chamni*, Synthesis, Biological Evaluation and Molecular Docking of Avicequinone C Analogues as Potential Steroid 5 α -Reductase Inhibitors, *Chemical & Pharmaceutical Bulletin*, 2017, 65(3): 253-260.
72. D. Saeloh, M. Wenzel, T. Rungrotmongkol, L. Hamoen, S. Voravuthikunchai, V. Tipmanee*, Effects of rhodomyrton on Gram-positive bacterial tubulin homologue FtsZ, *Peer J.*, 2017, 2;5:e2962.
73. B. Nutho, N. Nunthaboot*, P. Wolschann, N. Kungwan, T. Rungrotmongkol*, Metadynamics supports molecular dynamics simulation-based binding affinities of eucalyptol and beta-cyclodextrins inclusion complexes, *RSC Advances*, 2017, 7(80), 50899-50911.
74. S. Thompho, T. Rungrotmongkol, Oraphan Saengsawang, S. Hannongbua*, A Computational Study of Adsorption of Divalent Metal Ions on Graphene Oxide, *Songklanakarin Journal of Science and Technology*, 2017, 39(6):773-778
75. W. Khuntawee, M. Kunaseth*, C. Rungnim, S. Intagorn, P. Wolschann, N. Kungwan, T. Rungrotmongkol*, S. Hannongbua, Comparison of Implicit and Explicit Solvation Models for Iota-Cyclodextrin Conformation Analysis from Replica Exchange Molecular Dynamics, *Journal of Chemical Information and Modeling*, 2017, 57 (4): 778-786.

76. B. Nutho, A. Meeprasert, M. Chulapa, N. Kungwan, T. Rungrotmongkol*, Screening of Hepatitis C NS5B polymerase Inhibitors Containing Benzothiadiazine Core: A Steered Molecular Dynamics, *Journal of Biomolecular Structure & Dynamics*, 2017; 35(8): 1743-1757.
77. S. Kruawan, M. Ratanasak, R. Chanajaree, T. Rungrotmongkol, O. Saengsawang, V. Parasuk, N. Kungwan, S. Hannongbua*, Ethylene insertion in the presence of new alkoxysilane electron donors for ziegler-natta catalyzed polyethylene, *Computational and Theoretical Chemistry*, 2017, 1112: 10-19.
78. S. Raza, G. Sanober, T. Rungrotmongkol, S.S. Azam*, The Vitality of Swivel Domain Motion in Performance of Enzyme I of Phosphotransferase System; A Comprehensive Molecular Dynamic Study, *Journal of Molecular Liquids*, 2017, 242: 1184-1198.
79. P. Mahalapbutr, P. Chusuth, N. Kungwan, W. Chavasiri, P. Wolschann, T. Rungrotmongkol*, Molecular recognition of naphthoquinone-containing compounds against human DNA topoisomerase II α ATPase domain: A molecular modeling study, *Journal of Molecular Liquids*, 2017, 247, 374-385.
80. K. Nusai*, P. Doungeedee, T. Rungrotmongkol, Study of drug likeness of praziquantel derivatives for the inhibition of thioredoxin peroxidase and aspartic protease in *opisthorchis viverrini* by molecular docking method, *KMITL Sci. Tech. J.*, 2017, 17(1): Jan.-Jun.
81. W. Panman, B. Nutho, S. Chamni, S. Dokmaisrijan, N. Kungwan, T. Rungrotmongkol*, Computational Screening of Fatty Acid Synthase Inhibitors Against Thioesterase Domain, *Journal of Biomolecular Structure and Dynamics* 2018, 36(15), 4114-4125
82. P. Mahalapbutr, B. Nutho, P. Wolschann, N. Kungwan, T. Rungrotmongkol*, Molecular Insights into Inclusion Complexes of Mansonone E and H Enantiomers with various β -cyclodextrins, *Journal of Molecular Graphics and Modeling*, 2018, 79, 72-80
83. N. Ehsan, S. Ahmad, R. Uddin, T. Rungrotmongkol, S.S. Azam*, Proteome-wide identification of epitope-based vaccine candidates against multi-drug resistant *Proteus mirabilis*, *Biologicals* 2018, 55, 27-37
84. S. Thompho, O. Saengsawang, T. Rungrotmongkol, N. Kungwan, S. Hannongbua*, Structure and Electronic Properties of Deformed Single-Walled Carbon Nanotubes: Quantum Calculations, *Structural Chemistry*, 2018, 29(1): 39-47
85. J. Kicuntod, W. Sangpheak, M. Mueller*, P. Wolschann, H. Viernstein, S. Yanaka, K. Kato, W. Chavasiri, P. Pongsawasdi, N. Kungwan, T. Rungrotmongkol*, Physical and biological properties of pinostrobin/ β -cyclodextrins inclusion complexes, *Scientia Pharmaceutica*, 2018, 86(5), 1-15.
86. P. Srivarangkul, W. Yuttithamnon, A. Suroengrit, S. Pankaew, K. Hengprasartporn, T. Rungrotmongkol, P. Phuwaphrisarisarn, A. Balasubramanian, R. Padmanabhan, S. Boonyasuppayakorn*, A novel flavanone derivative inhibits dengue virus fusion and infectivity, *Antiviral Research*, 2018, 151:27-38.
87. Y. Asad, S. Ahmad, T. Rungrotmongkol, S.S. Azam*, Immuno-informatics Driven Proteome-wide Investigation Revealed Novel Peptide-based Vaccine Targets Against Emerging Multiple Drug Resistant *Providencia stuartii*, *Journal of Molecular Graphics and Modeling*, 2018, 80, 238-250

88. S. Meephon, T. Rungrotmongkol, N. Kaiyawet, S. Puttamat, V. Pavarajarn*, Surface-dependence of adsorption and its influence on heterogeneous photocatalytic reaction: A case of photocatalytic degradation of linuron on zinc oxide, *Catalysis Letter*, **2018**, 148: 873-881.
89. S. Ahmad, S. Raza, Qurat-ul-Ain, T. Rungrotmongkol, S.S. Azam*, From phylogeny to protein dynamics: A computational hierarchy quest for potent drug identification against an emerging enteropathogen "Yersinia enterocolitica", *Journal of Molecular Liquids*, **2018**, 265: 372-389
90. C. Hanpaibool, T. Chakcharoensap, Arifin, Y. Hijikata, S. Irle, P. Wolschann, N. Kungwan, P. Pongsawasdi, P. Ounjai*, T. Rungrotmongkol*, Theoretical analysis of orientations and tautomerization of genistein in β -cyclodextrin, *Journal of Molecular Liquids*, **2018**, 265: 16-23.
91. T. Rungrotmongkol*, T. Chakcharoensap, P. Pongsawasdi, N. Kungwan, P. Wolschann, The inclusion complexation of daidzein with β -cyclodextrin and 2,6-dimethyl- β -cyclodextrin: a theoretical and experimental study, *Monatshefte fur Chemie - Chemical Monthly*, **2018**, 149(10), 1739-1747
92. N. Kongtaworn, N. Hirun, V. Tantishaiyakul, T. Rungrotmongkol, S. Dokmaisrijan*, Molecular Aggregation of Four Modified Xyloglucan Models in Aqueous Solution, *Chiang Mai University Journal of Natural Sciences*, **2018**, 45(5), 2201-2210
93. A. Maiuthed, N. Bhummaphan, S. Luanpitpong, A. Mutirangura, C. Apontewan, A. Meeprasert, T. Rungrotmongkol, Y. Rojanasakul, P. Chanvorachote*, Nitric oxide promotes cancer cell dedifferentiation by disrupting an Oct4: caveolin-1 complex: A new regulatory mechanism for cancer stem cell formation, *Journal of Biological Chemistry*, **2018**, 293 (35), 13534-13552, DOI: 10.1074/jbc.RA117.000287
94. N. Jiwalak, R. Daengngern, T. Rungrotmongkol, S. Jungsuttiwong, S. Namuangruk, N. Kungwan, S. Dokmaisrijan*, A spectroscopic study of indigo dye in aqueous solution: A combined experimental and TD-DFT study, *Journal of Luminescence*, **2018**, 204, 568-572
95. P. Kanyaboon, T. Saelee, A. Suroengrit, K. Hengphasatporn, T. Rungrotmongkol, W. Chavasiri, S. Boonyasuppayakorn*, Cardol triene inhibits dengue infectivity by targeting kl loops and preventing envelope fusion, *Scientific Report*, **2018**, 8(1):16643
96. J. Phanich, S. Threeracheep, N. Kungwan, T. Rungrotmongkol*, S. Hannongbua, Glycan binding and specificity of viral influenza neuraminidases by classical molecular dynamics and replica exchange molecular dynamics simulations, *Journal of Biomolecular Structure & Dynamics*, **2019**, 37(13):3354-3365
97. K. Hengphasatporn, N. Kungwan, T. Rungrotmongkol*, Binding pattern and susceptibility of epigallocatechin gallate against envelope protein homodimer of Zika virus: A molecular dynamics study, *Journal of Molecular Liquids*, **2019**, 274, 140-147
98. K. Sangpheak, M. Mueller, N. Darai, P. Wolschann*, C. Suwattanasophon, R. Ruga, W. Chavasiri, S. Seetaha, K. Choowongkamon, N. Kungwan, C. Rungnim, T. Rungrotmongkol*, Computational screening of chalcones acting against topoisomerase II α and their cytotoxicity towards cancer cell lines, *Journal of Enzyme Inhibition and Medicinal Chemistry*, **2019**, 34(1), 134-143
99. P. Mahalapbutr, K. Thitinanthavet, T. kedkham, N. Huy, T. Le, S. Dokmaisrijan, L. Huynh, N. Kungwan, T. Rungrotmongkol* , A theoretical study on the molecular encapsulation of luteolin and

- pinocembrin with various derivatized beta-cyclodextrins, *Journal of Molecular Structure*, **2019**, 1180, 480-490
- 100.S. Kongkaew, **T. Rungrotmongkol***, C. Punwong, H. Noguchi, F. Takeuchi, N. Kungwan, P. Wolschann, S. Hannongbua*, Interactions of HLA-DR and Topoisomerase I Peptide Modulated Genetic Risk for Diffuse Cutaneous Systemic Sclerosis, *Scientific Reports*, **2019**, 9, 745
- 101.H.A.A. Karim, **T. Rungrotmongkol**, S.M. Zain, N.A. Rahman, C. Tayapiwattana, V.S. Lee*, Designed Antiviral Ankyrin – A Computational Approach to Combat HIV-1 via Intracellular Pathway by Targetting the Viral Capsid of HIV-1, *Journal of Molecular Liquids*, **2019**, 277, 63-69
- 102.W. Panman, P. Mahalapbutr, O. Saengsawang, C. Rungnim, N. Kungwan, **T. Rungrotmongkol***, S. Hannongbua*, Conjugated biopolymer-assisted the binding of polypropylene toward single-walled carbon nanotube: A molecular dynamics simulation, *Chiang Mai University Journal of Natural Sciences*, **2019**, 46(X): 1-11
- 103.K. Kerdpol, J. Kicuntod, P. Wolschann, S. Mori, C. Rungnim, M. Kunaseth, H. Okumura, N. Kungwan*, **T. Rungrotmongkol***, Cavity Closure of 2-Hydroxypropyl- β -cyclodextrin: Replica Exchange Molecular Dynamics Simulations, *Polymers*, **2019**, 11, 145
- 104.J. Kammarabut, P. Mahalapbutr, B. Nutho, N. Kungwan, **T. Rungrotmongkol***, Lower susceptibility of asunaprevir against R155K and D168A single mutations in HCV NS3/4A protease by molecular dynamics simulation, *Journal of Molecular Graphics and Modelling*, **2019**, 89, 122-130
- 105.K. Sangpheak, L. Tabtimmai, S. Seetaha, C. Rungnim, W. Chavasirid, P. Wolschann, K. Choowongkamon, **T. Rungrotmongkol***, Biological evaluation and molecular dynamics simulation of chalcone derivatives as EGFR-tyrosine kinase inhibitors, *Molecules*, **2019**, 24(6), 1092
- 106.B. Nutho, A.J. Mulholland*, **T. Rungrotmongkol***, Quantum Mechanics/Molecular Mechanics (QM/MM) Calculations Support a Concerted Reaction Mechanism for the Zika Virus NS2B/NS3 Serine Protease with Its Substrate, *Journal of Physical Chemistry B*, **2019**, 123, 13, 2889-2903
- 107.P. Mahalapbutr, P. Wonganan*, W. Chavasiri, **T. Rungrotmongkol***, Butoxy mansonone G inhibits STAT3 and Akt signaling pathways in non-small cell lung cancers: Combined experimental and theoretical investigations, *Cancers*, **2019**, 11, 437
- 108.W. Hotarat, C. Rungnim, P. Wolschann, N. Kungwan, **T. Rungrotmongkol***, S. Hannongbua*, Encapsulation of alpha-mangostin and hydrophilic beta-cyclodextrins revealed by all-atom molecular dynamics simulations, *Journal of Molecular Liquids*, **2019**, 288, 110965
- 109.S. Meephon, **T. Rungrotmongkol**, S. Puttamat, V. Pavarajarn*, Heterogeneous photocatalytic degradation of diuron on zinc oxide: Influence of surface-dependent adsorption on kinetics, degradation pathway, and toxicity of intermediates, *Journal of Environmental Science*, **2019**, 84, 97-111
- 110.S. Ubonprasert, J. Jaroensuk, W. Pornthanakasem, N. Kamonsutthipajit, P. Wongpituk, P. Mee-udorn, **T. Rungrotmongkol**, O. Ketchart, P. Chitnumsub, U. Leartsakulpanich, P. Chaiyen, S. Maenpuen*, A flexible flap motif of human cytosolic serine hydroxymethyltransferase is important for quaternary structure stabilization, cofactor and substrate binding, and control of product release, *Journal of Biological Chemistry*, **2019**, 294(27):10490-10502

111. B. Nutho, A.J. Mulholland*, T. Rungrotmongkol*, Reaction Mechanism of Zika Virus NS2B/NS3 Serine Protease Inhibition by Dipeptidyl Aldehyde: A QM/MM Study, *Physical Chemistry Chemical Physics*, **2019**, 21(27), 14945-14956
112. P. Mahalapbutr, N. Darai, W. Panman, A. Opasmahakul, N. Kungwan, S. Hannongbua, T. Rungrotmongkol*, Atomistic mechanisms underlying the activation of G protein-coupled sweet receptor heterodimer mediated by sugar alcohol recognition: A molecular dynamics study, *Scientific Reports*, **2019**, 9, 10205
113. C. Yibcharoenporn, P. Chusuth, T. Rungrotmongkol, W. Chavasiri, V. Chatsudthipong, C. Muanprasat*, Discovery of a novel chalcone derivative inhibiting CFTR chloride channel via AMPK activation and its anti-diarrheal application, *Journal of Pharmacological Sciences*, **2019**, 140(3), 273
114. B. Nutho, T. Rungrotmongkol*, Binding Recognition of Substrates in NS2B/NS3 Serine Protease of Zika virus Revealed by Molecular Dynamics Simulations, *Journal of Molecular Graphics and Modelling*, **2019**, 2(92), 227-235
115. T. Kaburaki, H. Nakahara, T. Tanaka, K. Okinaga, H. Kawashima, Y. Hamasaki, T. Rungrotmongkol, S. Hannongbua, H. Noguchi, M. Aihara, F. Takeuchi, Lymphocyte proliferation induced by high-affinity peptides for HLA-B*51:01 in Behçet's uveitis, *PLoS ONE*, **2019**, 14(9), e0222384
116. P. Mahalapbutr, P. Wonganan, T. Charoenwongpaiboon, W. Chavasiri, M. Prousoontorn, T. Rungrotmongkol*, Inclusion complexes of mannosone G with β -cyclodextrins: Molecular modeling, phase solubility, characterization, and cytotoxicity. *Biomolecules*, **2019**, 9(10), 545
117. T. Boonma, B. Nutho, T. Rungrotmongkol, N. Nunthaboot*, Understanding of the drug resistance mechanism of hepatitis C virus NS3/4A to Paritaprevir due to D168N/Y mutations: A molecular dynamics simulation perspective, *Computational Biology and Chemistry*. **2019**, 83, 107154
118. K. Sanachai, P. Mahalapbutr, K. Choowongkamon, R.P. Poo-arporn, P. Wolschann, T. Rungrotmongkol*, Insights into the binding recognition and susceptibility of tofacitinib toward Janus kinases, *ACS Omega*, **2019**, 5, 369-377
119. C. Hanpaibool, M. Leelawiwat, K. Takahashi, T. Rungrotmongkol*, Source of oseltamivir resistance due to single E119D and double E119D/H274Y mutations in pdm09H1N1 influenza neuraminidase, *Journal of Computer-Aided Molecular Design*, **2020**, 34(1):27-37
120. S. Rattanaphan, T. Rungrotmongkol, P. Kongsunea*, Biogas improving by adsorption of CO₂ on modified and unmodified waste tea activated carbon, *Renewable Energy*, **2020**, 622-631
121. K. Hengphasatporn, A. Garon, P. Wolschann, T. Langer, S. Yasuteru, T.H.N. Thanh, W. Chavasiri, T. Saelee, S. Boonyasuppayakorn, T. Rungrotmongkol*, Multiple Virtual Screening Strategies for the Optimization of the Novel Compound Against Dengue Virus: A Drug Discovery Study, *Sci. Pharm.*, **2020**, 88, 2
122. A. Sangkaew, N. Samritsakulchai, K. Sanachai, T. Rungrotmongkol, W. Chavasiri, C. Yompakdee*, Novel human carbonic anhydrase isozyme II inhibitors from *Murraya paniculata* detected by a resazurin yeast-based assay, *Journal of Microbiology and Biotechnology*, **2020**, 30(4):552-560
123. S. Kitdumrongthum, S. Reabroi, K. Suksen, P. Tuchinda, B. Munyoo, P. Mahalapbutr, T. Rungrotmongkol, P. Ounjai, A. Chairoungdua*, Inhibition of topoisomerase II α and induction of DNA

- damage in cholangiocarcinoma cells by altholactone and its halogenated benzoate derivatives, *Biomedicine & Pharmacotherapy*, **2020**, *127*, 110149
- 124.K. Petsri, M. Yokoya, S. Tungsukruthai, T. Rungrotmongkol, B. Nutho, C. Vinayanuwattikun, N. Saito, M. Takehiro, R. Sato, P. Chanvorachote, Structure–Activity Relationships and Molecular Docking Analysis of Mcl-1 Targeting Renieramycin T Analogues in Patient-derived Lung Cancer Cells, *Cancers* **2020**, *12*(4), 875
- 125.K. Hengphasatporn, K. Plaimas, A. Suratane, P. Wongsriphisant, J.-M. Yang, Y. Shigeta, W. Chavasiri, S. Boonyasuppayakorn, T. Rungrotmongkol*, Target Identification using Homopharma and Network-based Method for Predicting Compounds against Dengue Virus-Infected Cell, *Molecules* **2020**, *25*(8), 1883
- 126.J. Kammarabutr, P. Mahalapbutr, H. Okumura, P. Wolschann, T. Rungrotmongkol*, Structural dynamics and susceptibility of anti-HIV drugs against HBV reverse transcriptase, *Journal of Biomolecular Structure and Dynamics* **2020**, *20*, 10-10
- 127.B. Nutho^a, P. Mahalapbutr^a, K. Hengphasatporn, N.C. Pattarangoon, N. Simanon, Y. Shigeta, S. Hannongbua, T. Rungrotmongkol*, Why Are Lopinavir and Ritonavir Effective against the Newly Emerged Coronavirus 2019? Atomistic Insights into the Inhibitory Mechanisms, *Biochemistry*, **2020**, *59*, 18, 1769–1779
- 128.E. Lythell, R. Suardiaz, P. Hinchliffe, C. Hanpaibool, S. Visitsatthawong, S. Oliveira, E. Lang, P. Surawatanawong, V.S. Lee, T. Rungrotmongkol, N. Fey, J. Spencer*, A.J. Mulholland*, Resistance to the “Last Resort” Antibiotic Colistin: A Single-Zinc Mechanism for Phosphointermediate Formation in MCR Enzymes, *Chem. Commun.*, **2020**, *56*, 6874–6877
- 129.W. Hotarat, B. Nutho, P. Wolschann, T. Rungrotmongkol*, S. Hannongbua*, Delivery alpha-mangostin using cyclodextrins through a biological membrane: Molecular dynamics simulation, *Molecules*, **2020**, *25*, 2532
- 130.B. Nutho, S. Pengthaisong, A. Tankrathok, V.S. Lee, J.R.K. Cairns*, T. Rungrotmongkol*, S. Hannongbua*, Structural and Energetic Basis for β -Glucosidase Specificity of Os3BGlu7 by High Structural Similarity of Glucoimidazole and Mannoimidazole Binding, *Biomolecules*, **2020**, *10*(6): 907
- 131.P. Mahalapbutr, V.S. Lee, T. Rungrotmongkol*, Binding hot spot and activation mechanism of maltitol and lactitol toward human T1R2-T1R3 sweet taste receptor, *Journal of Agricultural and Food Chemistry*, **2020**, *68*(30), 7974–7983
- 132.P. Mahalapbutra, M. Sangkhawasib, J. Kammarabutra, S. Chamni*, T. Rungrotmongkol*, Rosmarinic acid as a potent influenza neuraminidase inhibitor: In vitro and in silico study, *Current Topics in Medicinal Chemistry*, **2020**, *20*, 2046-2055
- 133.S. Boonyasuppayakorn*, T. Saelee, P. Visitchanakun, A. Leelahavanichkul, K. Hengphasatporn, Y. Shigeta, T.N.T. Huynh, J.J.H. Chu, T. Rungrotmongkol, W. Chavasiri, Dibromopinocembrin and dibromopinostrobin are potential anti-dengue leads with mild animal toxicity, *Molecules*, **2020**, *25*, 4154

- 134.P. Mahalapbutr, N. Kongtaworn, T. Rungrotmongkol*, Structural Insight into the Recognition of S-Adenosyl-L-Homocysteine and Sinefungin in SARS-CoV-2 Nsp16/Nsp10 RNA Cap 2'-O-Methyltransferase, *Computational and Structural Biotechnology Journal*, **2020**, 18, 2766-2773
- 135.N. Darai, P. Mahalapbutr, K. Sangpheak, C. Rungnim, P. Wolschann, N. Kungwan, T. Rungrotmongkol*, In silico screening of chalcones against Epstein-Barr virus nuclear antigen 1 protein, *Songklanakarin J. Sci. Technol.* **2020**, 42 (4), 802-810
- 136.H.S.H. Soe, P. Mahalapbutr, N. Kongtaworn, T. Rungrotmongkol, S. Chamni, P. Jansook*, The investigation of binary and ternary sulfobutylether- β -cyclodextrin inclusion complexes with asiaticoside in solution and in solid state, *Carbohydrate Research*, **2020**, 498, 108190
- 137.T. Somboon, P. Mahalapbutr, K. Sanachai, P. Maitarad, V.S. Lee, S. Hannongbua, T. Rungrotmongkol*, Computational study on peptidomimetic inhibitors against SARS-CoV-2 main protease, *Journal of Molecular Liquids*, **2021**, 322, 114999
- 138.Q. Sun, K. Jin, Y. Huang, J. Guo, T. Rungrotmongkol, P. Maitarad*, C. Wang*, Influence of conformational change of chain unit on the intrinsic negative thermal expansion of polymers, *Chinese Chemical Letters*, **2021** DOI: 10.1016/j.ccllet.2020.09.046
- 139.K. Verma, P. Mahalapbutr, A. Auepattanapong, O. Khaikate, C. Kuhakarn, K. Takahashi, T. Rungrotmongkol*, Molecular Dynamics Simulations on Sulfone Derivatives in Complex with DNA Topoisomerase II α ATPase Domain, *Journal of Biomolecular and Structure Dynamics*, **2021** DOI: 10.1080/07391102.2020.1831961
- 140.J. Jewboonchu, J. Saetang, D. Saeloh, T. Siriyong, T. Rungrotmongkol, S.P. Voravuthikunchai, V. Tipmanee*, Atomistic insight and modeled elucidation of conessine towards *Pseudomonas aeruginosa* efflux pump, *Journal of Biomolecular Structure and Dynamics*, **2021**, DOI: 10.1080/07391102.2020.1828169
- 141.T. Roongcharoen, S. Impeng, C. Chitpakdee, T. Rungrotmongkol, T. Jitwatanasirikul, S. Jungsuttiwong, S. Namuangruk*, Intrinsic property and catalytic performance of single and double metal atoms incorporated *g-C₃N₄* for O₂ activation: A DFT insight, *Applied Surface Science*, **2021**, 541, 148671
- 142.T. Tanawattanasuntorn, T. Thongpanchang, T. Rungrotmongkol, C. Hanpaibool, P. Graidist, V. Tipmanee*, (-)-Kusunokinin as a potential aldose reductase inhibitor: Equivalency observed via AKR1B1 dynamics simulation, *ACS Omega*, **2021**, 6, 1, 606-614
- 143.P. Murali, K. Verma, T. Rungrotmongkol, V.T. Perarasu, K. Ramanathan*, Targeting the Autophagy Specific Lipid Kinase VPS34 for Cancer Treatment: An Integrative Repurposing Strategy, *The Protein Journal*, **2021**, doi.org/10.1007/s10930-020-09955-4 (Quartile score: -, Impact factor 2018: 1.097)
- 144.T. Boonma, B. Nutho, N. Darai, T. Rungrotmongkol, N. Nunthaboot*, Exploring of paritaprevir and glecaprevir resistance due to A156T mutation of HCV NS3/4A protease: Molecular dynamics simulation study, *Journal of Biomolecular Structure & Dynamics*, **2021** 10.1080/07391102.2020.1869587 (Quartile score: Q2, Impact factor 2018: 2.924)
- 145.W. Innok, A. Hiranrat, N. Chana, T. Rungrotmongkol, P. Kongsune*, In silico and in vitro anti-AChE activity investigations of constituents from *Mytragyna speciosa* for Alzheimer's disease treatment, *Journal of Computer-Aided Molecular Design*, **2021**, doi.org/10.1007/s10822-020-00372-4

- 146.K. Karnchanapandh, C. Hanpaibool, P. Mahalapbutr, T. Rungrotmongkol*, Source of oseltamivir resistance due to single E276D, R292K, and double E276D/R292K mutations in H10N4 influenza neuraminidase, *Journal of Molecular Liquids*, **2021**, 326, 115294
- 147.K. sangpheak, D. Waraho-Zhmayev, K. Haonoo, S. Torpaiboon, T. Teachersripaiboon, T. Rungrotmongkol, R. Poo-arporn*, Investigation of interactions between binding residues and solubility of grafted humanized anti-VEGF IgG antibodies expressed as full-length format in the cytoplasm of a novel engineered E.coli SHuffle strain, *RCS Advances*, **2021** accepted
- 148.N. Bhat, B. Nutho, A. Vangnai, K. Takahashi, T. Rungrotmongkol*, Substrate binding mechanism of glycerophosphodiesterase towards organophosphate pesticides, *Journal of Molecular Liquids*, **2021**, 329 115526
- 149.K. Kerdpol, R. Daengngern, C. Sattayanon, S. Namuangruk, T. Rungrotmongkol, P. Wolschann, N. Kungwan*, S. Hannongbua*, Effect of Water Microsolvation on Excited-State Proton Transfer of 3-Hydroxyflavone Enclosed in γ -Cyclodextrin, *Molecules*, **2021**, 26(4), 843
- 150.K. Sanachai^a, T. Aiebchun^a, P. Mahalapbutr, S. Seetaha, L. Tabtimmai, P. Maitarad, I. Xenicacis, A. Geronikaki, K. Choowongkamon, T. Rungrotmongkol*, Discovery of novel JAK2 and EGFR inhibitors from thiazole derivatives, *RSC Medicinal Chemistry*, **2021** accepted (Prof#5)
- 151.K. Verman, P. Mahalapbutr, U. Suriya, T. Somboon, T. Aiebchun, L. Shi, P. Maitarad, T. Rungrotmongkol*, Exploring DNA GyraseB Inhibitors for the Treatment of Clostridium difficile Infection from PhytoHub database using Computational Strategy, *Brazilian Archives of Biology and Technology*, **2021**, accepted
- 152.H.E. Putri, B. Nutho, T. Rungrotmongkol, B. Sritularak, C., Vinayanuwattikun, P. Chanvorachote, A Bibenzyl Analogue DS-1 Inhibits MDM2-mediated p53 Degradation and Sensitizes Apoptosis in Lung Cancer Cells, *Phytomedicine*, **2021** accepted
- 153.T. Aiebchun, P. Mahalapbutr, A. Auepattanapong, O. Khaikate, S. Seetaha, L. Tabtimmai, C. Kuhakarn, K. Choowongkamon*, T. Rungrotmongkol*, Identification of vinyl sulfone derivatives as EGFR tyrosine kinase inhibitor: In vitro and in silico studies, *Molecules*, **2021** 26, 2211
- 154.P. Satapornpong, J. Pratoomwun, P. Rerknimitr, J. Klaewsongkram, N. Nakkam, T. Rungrotmongkol, P. Konyoung, N. Saksit, A. Mahakkanukrauh, W. Amornpinyo, U. Khunarkornsiri, T. Tempark, K. Wantavornprasert, P. Jinda, N. Koomdee, T. Jantararoungtong, T. Rerkpattanapipat, C.W. Wang, D. Naisbitt, W. Tassaneeyakul, M. Pirmohamed, W.H. Chung, C. Sukasem, HLA-B*13:01 is a predictive marker of dapsone-induced severe cutaneous adverse reactions in Thai patients, *Frontiers in Immunology*, **2021**, accepted
- 155.P. Mahalapbutr, C. Phongern, N. Kongtaworn, S. Hannongbua, T. Rungrotmongkol*, Molecular encapsulation of a key odor-active 2-acetyl-1-pyrroline in aromatic rice with β -cyclodextrin derivatives, *Journal of Molecular Liquids*, **2021** accepted

| | |
|------------------|---|
| ชื่อโครงการวิจัย | การดื้อยาเออร์โลทินิบโปรตีน EGFR TK ที่มีการกลายพันธุ์ และค้นหาสารที่มีฤทธิ์ต้านมะเร็ง : การศึกษาด้วยคอมพิวเตอร์และการทดลองในห้องปฏิบัติการ |
| แหล่งทุน | ทุนวิจัย กองทุนรัชดาภิเษกสมโภช ประจำปีงบประมาณ 2562 |
| หัวหน้าโครงการ | ผู้ช่วยศาสตราจารย์ ดร.ธัญญา รุ่งโรจน์มงคล |
| ส่วนงาน | ภาควิชาชีวเคมี คณะวิทยาศาสตร์ |

แบบสรุปผลการดำเนินงาน *

1. ผลการดำเนินงานตั้งแต่เดือน ตุลาคม พ.ศ. 2562 ถึงเดือน กันยายน พ.ศ. 2563

2. สรุปทศย่อ

(ภาษาไทย) ตัวรับการเจริญเติบโตของเซลล์ที่ผิว (EGFR) เป็นโปรตีนที่มีการแสดงออกมากในมะเร็งหลายชนิด ซึ่งได้รับการพิสูจน์ว่าเป็นโปรตีนเป้าหมายที่มีประสิทธิภาพสูงสำหรับยารักษาโรคมะเร็ง ในปัจจุบันยาเออร์โลทินิบ (erlotinib) จัดเป็นยาที่มีประสิทธิภาพในการยับยั้งการทำงานของโปรตีน EGFR ซึ่งได้นำมาใช้เป็นอันดับต้นๆ สำหรับผู้ป่วยโรคมะเร็ง แต่อย่างไรก็ตามเมื่อใช้ยาชนิดนี้ติดต่อกันเป็นระยะเวลา 9-13 เดือน มักจะเกิดการดื้อยาเนื่องจากการกลายพันธุ์ขั้นที่สอง T790M ของโปรตีน EGFR ที่บริเวณโดเมนไทโรซีนไคนเนส (TK) ดังนั้นการค้นหาสารประกอบที่มีแนวโน้มว่ามีประสิทธิภาพต่อโปรตีนเป้าหมาย EGFR-TK พันธุ์กลาย จึงเป็นสิ่งที่สำคัญอย่างยิ่ง ในงานวิจัยนี้ผู้วิจัยได้ศึกษาผลของการกลายพันธุ์ของโปรตีน EGFR-TK ที่มีผลต่อการจับกับยาเออร์โลทินิบและค้นหาสารอนุพันธ์ใหม่ ๆ ที่มีประสิทธิภาพในการยับยั้งโปรตีนเป้าหมายของเซลล์มะเร็ง จากผลการศึกษาพบว่า การกลายพันธุ์ขั้นที่สอง T790M ส่งผลให้บริเวณวง quinazoline ของยาเออร์โลทินิบจับกับโปรตีนเป้าหมายได้ลดลงด้วยการสร้างพันธะไฮโดรเจนแบบอ่อนๆ เป็นสาเหตุหลักของการดื้อยา และจากการคัดกรองสารอนุพันธ์กลุ่มซัลโฟนิลเลตอินดิโนควิโนลีนที่มีการดัดแปลงโครงสร้างจำนวนทั้งสิ้น 26 ตัว ด้วยเทคนิคโมเลคิวลาร์ดอกกิ้งพบว่า มีสารอนุพันธ์จำนวน 23 ตัว ที่สามารถเข้าจับกับโปรตีนเป้าหมาย EGFR-TK ที่บริเวณ ATP binding site ได้ดี โดยสารกลุ่มนี้ 8 ตัว มีประสิทธิภาพในการยับยั้งการทำงานของเอนไซม์ EGFR (IC_{50} ในช่วง 1 - 23 nM) แต่มีสารอนุพันธ์เพียง 6 ตัวที่แสดงความเป็นพิษต่อเซลล์เซลล์มะเร็งในเซลล์มะเร็งผิวหนัง A431 และมะเร็งปอด A549 ด้วยค่า IC_{50} ในช่วง 10 - 36 μ M จึงเป็นกลุ่มสารที่น่าสนใจที่จะพัฒนาต่อไปเป็นยาต้านมะเร็งในอนาคต

(ภาษาอังกฤษ) Epidermal growth factor receptor (EGFR) overexpressed in many types of cancer has been proved as a high potential target for cancer therapy. Currently, erlotinib, a potent EGFR inhibitor, has been used as the first-line drug for cancer patients. However, acquired drug resistance caused by the secondary mutation T790M of EGFR tyrosine kinase (TK) domain develops inevitably after a median response duration of 9 to 13 months. Therefore, the searching for promising compounds effectively targeting mutated EGFR-TK has become an imperative necessity. In this present study, we aimed to study the source of drug resistance due to the secondary mutation T790M and to search for the newly potent compounds against EGFR-TK. From the results, such secondary mutation has caused the quinazoline ring, a core of tyrosine kinase inhibitors (TKIs), lower binding with EGFR with rather weak hydrogen bond formation. The docking results of a novel series of sulfonlate indino quinoline derivatives (26 compounds) suggested that the 23 compounds can interact well with EGFR-TK at the ATP-binding site. Among them, the 8 compounds exhibited the promising inhibitory activity against EGFR-TK with IC_{50} values of 1-23 nM, while only 6 compounds showed a high cytotoxicity with

IC₅₀ values of 10-36 μ M towards the A431 and A549 cancer cell lines. Therefore, these compounds could be novel small molecule inhibitors of EGFR-TK capable of exerting benefit for cancer treatment.

3. หลักการ ความสำคัญ ความเป็นมา :

โรคมะเร็งถูกจัดอันดับเป็นโรคร้ายแรงที่คร่าชีวิตคนทั่วโลก จากสถิติเมื่อปี พ.ศ. 2560 มีผู้เสียชีวิตจากโรคนี้นับถึง 8.8 ล้านคน ซึ่งสถานการณ์โรคมะเร็งของประเทศไทย พบว่าสาเหตุการตายสูงสุดเป็นอันดับ 1 ของคนไทย โดยมีผู้ป่วยเสียชีวิตจากโรคมะเร็งกว่า 60,000 ล้านคนต่อปี มะเร็งปอดถือเป็นสาเหตุลำดับต้นๆ ของการเสียชีวิตจากโรคมะเร็งทั่วโลก ในปัจจุบันมีผู้ป่วยประมาณ 85% ที่ได้รับการวินิจฉัยว่า เป็นมะเร็งปอดชนิด non-small cell cancer (NSCLC) ซึ่งอัตราการรอดชีวิต 5 ปีมีเพียง 17.8% เท่านั้น

ปัจจุบันโรคมะเร็งสามารถรักษาได้หลายวิธี เช่น การผ่าตัด รังสีรักษา เคมีบำบัด ฮอรัโมน โดยการรักษาเหล่านี้มีความเหมาะสมต่อชนิดมะเร็งและระยะโรคที่แตกต่างกัน แต่การรักษาเหล่านี้อาจส่งผลข้างเคียงต่างๆ เช่น การสูญเสียอวัยวะ การอักเสบของอวัยวะที่ได้รับรังสี การกดภูมิคุ้มกัน อาการคลื่นไส้หรืออาเจียน และผมร่วง ฯลฯ ในช่วงระยะเวลาที่ผ่านไปผ่านมา มีการคิดค้นยารักษาใหม่ๆ เป้าหมายซึ่งคือยารักษาโรคมะเร็งที่ไม่มีผลฆ่าตัวเซลล์มะเร็งโดยตรง แต่สามารถควบคุมเซลล์มะเร็งได้จากการขัดขวางการเจริญเติบโตของเซลล์มะเร็ง โดยเซลล์ปกติจะได้รับผลกระทบจากการรักษาน้อยกว่าการรักษาด้วยเคมีบำบัด ดังนั้นจึงทำให้ผู้ป่วยมะเร็งมีอัตราการรอดชีวิตที่สูงกว่าและมีคุณภาพชีวิตที่ดีขึ้น ซึ่งยากลุ่มนี้จะออกฤทธิ์โดยรบกวนการทำงานของโมเลกุลเป้าหมาย (molecular targets) ที่มีความจำเพาะต่อการเจริญเติบโตและการแพร่กระจายของเซลล์มะเร็งนั้น แต่อย่างไรก็ตามเมื่อใช้ยาชนิดนี้ติดต่อกันเป็นระยะเวลานานประมาณ 9 ถึง 13 เดือน มักจะเกิดการดื้อยาขึ้น เนื่องจากการกลายพันธุ์ของโปรตีนเป้าหมายของเซลล์มะเร็งส่งผลให้ยาที่ใช้ในปัจจุบันมีประสิทธิภาพลดลง ดังนั้นการศึกษาผลของการดื้อยาและการค้นหาสารใหม่ๆ ที่อาจมีประสิทธิภาพดีกว่ายาเออร์โลทินิบจึงกลายเป็นประเด็นสำคัญที่ผู้วิจัยสนใจศึกษาในครั้งนี้

4. เป้าหมายการวิจัย

ค้นหาสารอนุพันธ์ใหม่ที่มีประสิทธิภาพในการยับยั้งการทำงานของเอนไซม์เป้าหมาย EGFR มากกว่า ยามุ่งเป้าเออร์โลทินิบ เพื่อเป็นแนวทางในการพัฒนาไปสู่ยาด้านโรคมะเร็งที่มีประสิทธิภาพมากยิ่งขึ้น

5. วัตถุประสงค์โครงการ :

1.1 ศึกษาผลของการกลายพันธุ์แบบ L858R และ T790M/L858R ในโดเมน TK ของโปรตีน EGFR ที่มีผลต่อการจับกับยามุ่งเป้าเออร์โลทินิบด้วยการจำลองเชิงพลวัตโมเลกุล

1.2 เพื่อค้นหาสารซัลโฟนิลเลตอินดิโนลีนที่มีประสิทธิภาพในการยับยั้งโปรตีนเป้าหมายของเซลล์มะเร็งและทดสอบความเป็นพิษต่อเซลล์มะเร็งเพาะเลี้ยงที่มีการแสดงออกที่มากผิดปกติและก่อการกลายพันธุ์ของโปรตีน EGFR

6. ผลการดำเนินงาน : ได้ดำเนินงานตามแผนงานที่ได้วางไว้ทุกประการ
 ได้เปลี่ยนแปลงแผนงานที่ได้วางไว้ดังนี้คือ

7. สรุปผลการดำเนินงาน

สรุปผลการดำเนินงานเมื่อเทียบกับแผนที่วางไว้และที่จะดำเนินงานแล้วเสร็จ
(ควรระบุผลผลิต/ผลที่คาดว่าจะได้รับให้ชัดเจนและผลผลิตที่ได้ซึ่งสามารถตรวจสอบและวัดได้ เช่น ผลงานตีพิมพ์ในวารสารวิชาการนานาชาติ/หนังสือ/สิทธิบัตร, ความก้าวหน้าในการสร้างทีมวิจัย, การนำผลจากโครงการไปใช้ประโยชน์ เป็นต้น)

ผลผลิตหลัก บทความทางวิชาการระดับนานาชาติที่จะนำผลงานไปเผยแพร่ (ไม่น้อยกว่า 1 บทความ)
 ชื่อบทความ Discovery of novel JAK2 and EGFR inhibitors from thiazole derivatives
 ชื่อวารสาร RSC Medicinal Chemistry (submitted)
 High impact factor (ระดับ) โปรรตระบุ 3.119

ชื่อบทความ Source of lower anticancer-drug susceptibility due to T790M/L858R
 EGFR mutation: Molecular dynamics and principle component analysis
 ชื่อวารสาร Protein Science (in preparation)
 High impact factor (ระดับ) โปรรตระบุ 3.876

ผลผลิตรอง (โปรรตระบุ)

| ผลผลิตที่ระบุไว้ | รายละเอียดของผลผลิต | จำนวนนับ | หน่วยนับ | ผลลัพธ์ที่ได้ | ผลกระทบที่ได้ |
|------------------|---------------------|----------|----------|---------------|---------------|
| | | | | | |
| | | | | | |
| | | | | | |
| | | | | | |

8. ผลผลิตเป็นไปตามข้อกำหนดในข้อเสนอโครงการ

เป็นไปตามข้อกำหนดทุกประการ ไม่เป็นไปตามข้อกำหนด เนื่องจาก

9. คาดว่าผลงานวิจัยที่ได้เป็นประโยชน์ต่อชุมชน สังคม และประเทศในด้าน (ทำเครื่องหมาย ✓ ในช่อง)

ด้านการพัฒนาที่ยั่งยืน ด้านสิ่งแวดล้อม ด้านพลังงาน

ด้านอื่นๆ (โปรรตระบุ)ด้านสุขภาพ.....



หมายเหตุ * จัดทำแยกจากรายงานฉบับสมบูรณ์/แนบพร้อมผลงานที่ได้รับการตีพิมพ์ในวารสารวิชาการระดับนานาชาติ

.....


(ผู้ช่วยศาสตราจารย์ ดร.ธัญญา รุ่งโรจน์มงคล)
 หัวหน้าโครงการ

Article

Identification of Vinyl Sulfone Derivatives as EGFR Tyrosine Kinase Inhibitor: In Vitro and In Silico Studies

Thitinan Aiebchun ¹, Panupong Mahalapbutr ², Atima Auepattanapong ³, Onnicha Khaikate ³, Supaphorn Seetaha ⁴, Lueacha Tabtimmai ⁵, Chutima Kuhakarn ³, Kiattawee Choowongkamon ^{4,*}, and Thanyada Rungrotmongkol ^{1,6,*}

- ¹ Biocatalyst and Environmental Biotechnology Research Unit, Department of Biochemistry, Faculty of Science, Chulalongkorn University, Bangkok 10330, Thailand; thitinan1906@gmail.com
 - ² Department of Biochemistry, Faculty of Medicine, Khon Kaen University, Khon Kaen 40002, Thailand; panupma@kku.ac.th
 - ³ Department of Chemistry and Center of Excellence for Innovation in Chemistry (PERCH-CIC), Faculty of Science, Mahidol University, Bangkok 10700, Thailand; iceatima.12@gmail.com (A.A.); onnicha.khai@gmail.com (O.K.); chutima.kon@mahidol.ac.th (C.K.)
 - ⁴ Department of Biochemistry, Faculty of Science, Kasetsart University, Chatuchak, Bangkok 10900, Thailand; supaporn.se@ku.th
 - ⁵ Department of Biotechnology, Faculty of Applied Science, King Mongkut's University of Technology of North Bangkok, Bangkok 10800, Thailand; Lueacha.t@sci.kmutnb.ac.th
 - ⁶ Program in Bioinformatics and Computational Biology, Faculty of Science, Chulalongkorn University, Bangkok 10330, Thailand
- * Correspondence: kiattawee.c@ku.th (K.C.); t.rungrotmongkol@gmail.com (T.R.); Tel.: +66-2218-5426 (T.R.); Fax: +66-2218-5418 (T.R.)



Citation: Aiebchun, T.; Mahalapbutr, P.; Auepattanapong, A.; Khaikate, O.; Seetaha, S.; Tabtimmai, L.; Kuhakarn, C.; Choowongkamon, K.; Rungrotmongkol, T. Identification of Vinyl Sulfone Derivatives as EGFR Tyrosine Kinase Inhibitor: In Vitro and In Silico Studies. *Molecules* **2021**, *26*, 2211. <https://doi.org/10.3390/molecules26082211>

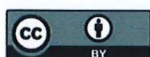
Academic Editor: Pascal Marchand

Received: 21 November 2020

Accepted: 7 April 2021

Published: 12 April 2021

Publisher's Note: MDPI stays neutral with regard to jurisdictional claims in published maps and institutional affiliations.



Copyright: © 2021 by the authors. Licensee MDPI, Basel, Switzerland. This article is an open access article distributed under the terms and conditions of the Creative Commons Attribution (CC BY) license (<https://creativecommons.org/licenses/by/4.0/>).

Abstract: Epidermal growth factor receptor (EGFR), overexpressed in many types of cancer, has been proved as a high potential target for targeted cancer therapy due to its role in regulating proliferation and survival of cancer cells. In the present study, a series of designed vinyl sulfone derivatives was screened against EGFR tyrosine kinase (EGFR-TK) using in silico and in vitro studies. The molecular docking results suggested that, among 78 vinyl sulfones, there were eight compounds that could interact well with the EGFR-TK at the ATP-binding site. Afterwards, these screened compounds were tested for the inhibitory activity towards EGFR-TK using ADP-Glo™ kinase assay, and we found that only VF16 compound exhibited promising inhibitory activity against EGFR-TK with the IC₅₀ value of 7.85 ± 0.88 nM. In addition, VF16 showed a high cytotoxicity with IC₅₀ values of 33.52 ± 2.57, 54.63 ± 0.09, and 30.38 ± 1.37 μM against the A431, A549, and H1975 cancer cell lines, respectively. From 500-ns MD simulation, the structural stability of VF16 in complex with EGFR-TK was quite stable, suggesting that this compound could be a novel small molecule inhibitor targeting EGFR-TK.

Keywords: EGFR tyrosine kinase; vinyl sulfone derivatives; in silico study; kinase assay; cytotoxicity assay

1. Introduction

Cancer is a devastating disease characterized by uncontrolled growth and spread of abnormal cells and is the second leading cause of mortality worldwide [1]. Nowadays, there are many types of cancer treatment such as chemotherapy, radiation therapy and targeted therapy [2–4]. Targeted cancer therapy has become one of the highly effective for cancer treatment due to its specificity towards cancer cells [5]. The overexpression of epidermal growth factor receptor (EGFR) in cancer cells leads to abnormal signal transduction and is closely related to the occurrence of cancer. Therefore, it has become one of the most important protein targets for designing and developing kinase inhibitors that act on oncogenic EGFR [6].

EGFR, a member of the ErbB family of receptor tyrosine kinases, plays important role in cellular signaling pathways, e.g., mitogen-activated protein kinase (MAPK), phosphoinositide 3-kinase (PI3K)/Akt, and signal transducer and activator of transcription (STAT) pathways that regulate key functions such as proliferation, survival, differentiation, and apoptosis [7]. EGFR is composed of an extracellular receptor domain, a single hydrophobic transmembrane region and an intracellular domain, which includes a juxta membrane domain [8], a tyrosine kinase (TK) domain and a C-terminal tyrosine-rich region [9]. The activation of EGFR-mediated signaling pathways begins with EGF binding to the extracellular domain, which activates the TK domain to phosphorylate at its C-terminal tail, and ultimately, initiates downstream signaling pathways [10,11]. Accordingly, targeting EGFR protein has been suggested as a promising strategy for targeted cancer therapy, since the EGFR is commonly overexpressed in many human cancers, including non-small cell lung, head, breast, bladder and ovarian carcinoma [12,13]. Consequently, inhibition of EGFR leads to the inhibition of cancer cells.

The clinically available drugs used as a tyrosine kinase inhibitor of EGFR (EGFR-TKI) such as erlotinib [14] and gefitinib [15]. The erlotinib is widely used in cancer patients for its inhibitory activity against EGFR exon 19 deletions or the L858R mutation [16,17]. However, these drugs have several side effects such as anemia, balance impairment, dizziness and headache. In addition, acquired drug resistance caused by the secondary mutation T790M of EGFR-TK domain develops inevitably after a median response duration of 9 to 13 months [18]. Therefore, the searching for promising compounds effectively targeting mutated EGFR-TK has become an imperative necessity [19,20].

Vinyl sulfone (VF) is an organic compound, where its core structure is similar to that of chalcones [21–24] (Figure 1). Previous study has shown that chalcone derivatives can inhibit EGFR activity with the IC_{50} value ranged from 10.3–15.4 μ M [25]. Thus, we hypothesized that VF derivatives can inhibit EGFR-TK activity in a manner similar to chalcones. In this study, we aimed to find new potential anti-cancer agents against EGFR-TK. A series of designed VF derivatives was initially screened by molecular docking technique. Subsequently, the kinase inhibition assay of the screened compounds against EGFR-TK was studied. Then, the *in vitro* cytotoxicity assay towards EGFR expressing lung carcinoma cell lines (A549 and A431) and T790M expressing lung cancer cell line (H1975) was conducted using MTT assay. Finally, the molecular dynamics simulation and free energy calculation were performed to investigate the structural and dynamics properties as well as the binding efficiency of the most potent VF in complex with EGFR-TK.

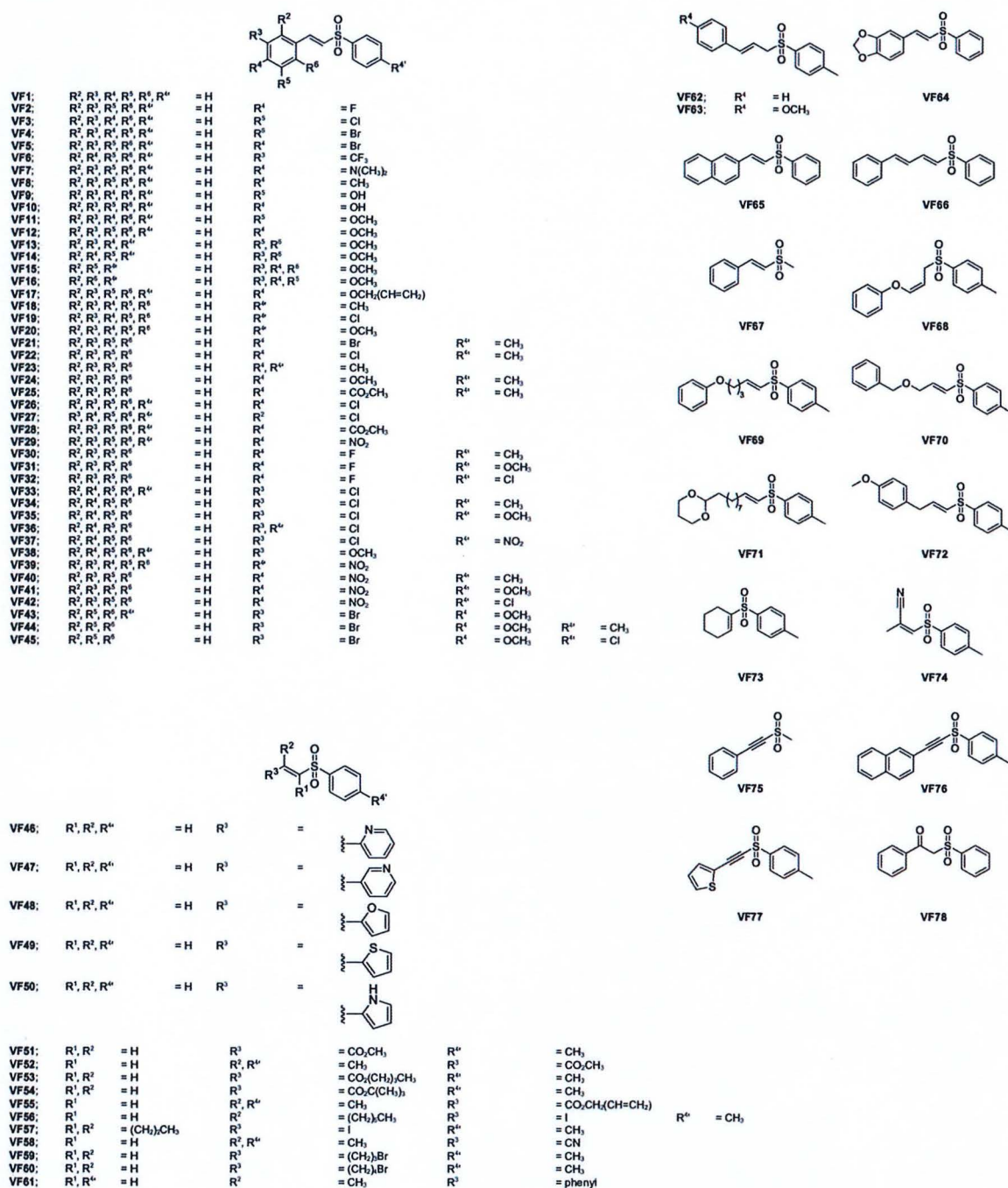


Figure 1. The chemical structures of VFs obtained from the previous study [21–24].

2. Results and Discussion

2.1. Molecular Docking

Initially, the 78 VFs (Figure 1) were investigated their binding mechanism using the CDOCKER module of Accelry Discovery Studio 3.0. Each compound was separately docked into the ATP-binding pocket of EGFR-TK complex. The interaction energy of erlotinib is -45.49 kcal/mol, while the interaction energy of all studied compounds is ranged from -43.47 to -21.61 kcal/mol. These results suggested that none of the vinyl sulfone derivatives is stronger than erlotinib. So, we cut off the compounds using the interaction energy lower than -37.5 kcal/mol, and we found eight VFs (VF15, VF16,

VF29, VF37, VF41, VF52, VF69 and VF71) that showed lower interaction energies than the others (Figure 2). These compounds can interact with important surrounding residues in ATP-binding pocket of EGFR-TK via H-bonding, pi interactions and van der Waals (vdW) forces (Figure 3). Interestingly, the sulfonate group of most compounds exhibited H-bond formation at the hinge region residue M769 (Figure 3A–I) [26,27] similar to erlotinib. The VF29, VF37, and VF41, which have nitro group as substituents, formed H-bond with T830 residue at A loop. Moreover, the matched vdW contacts between all VFs and erlotinib were as follows: (i) hinge region: T766, L768, P770, and G772 and (ii) A loop: K721, E731, T830, and D831. These results suggested that these eight VFs might be the potent candidate compounds acting against EGFR-TK.

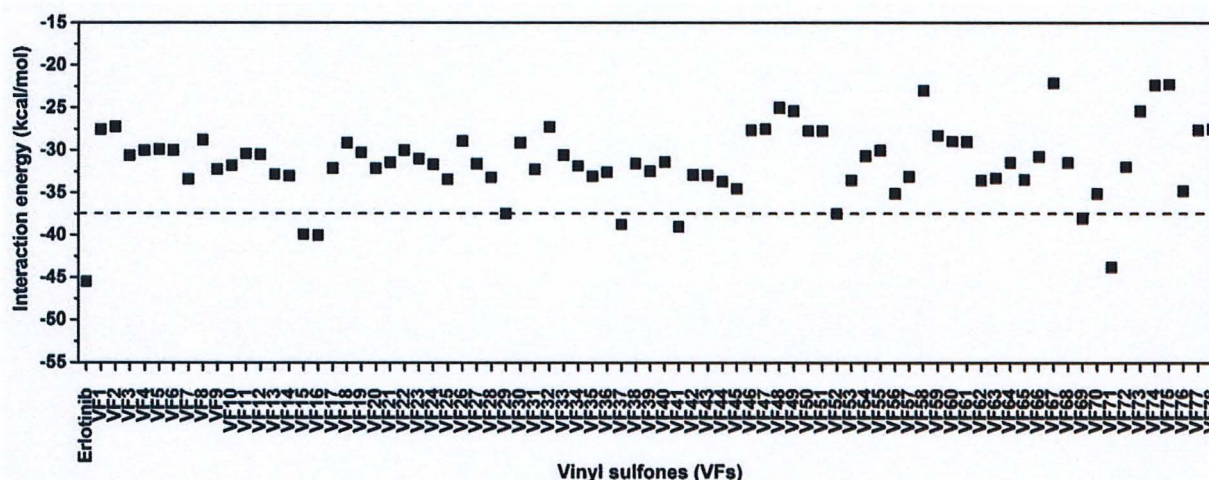


Figure 2. CDOCKER interaction energies of VFs and known drug erlotinib against EGFR-TK at ATP-binding site.

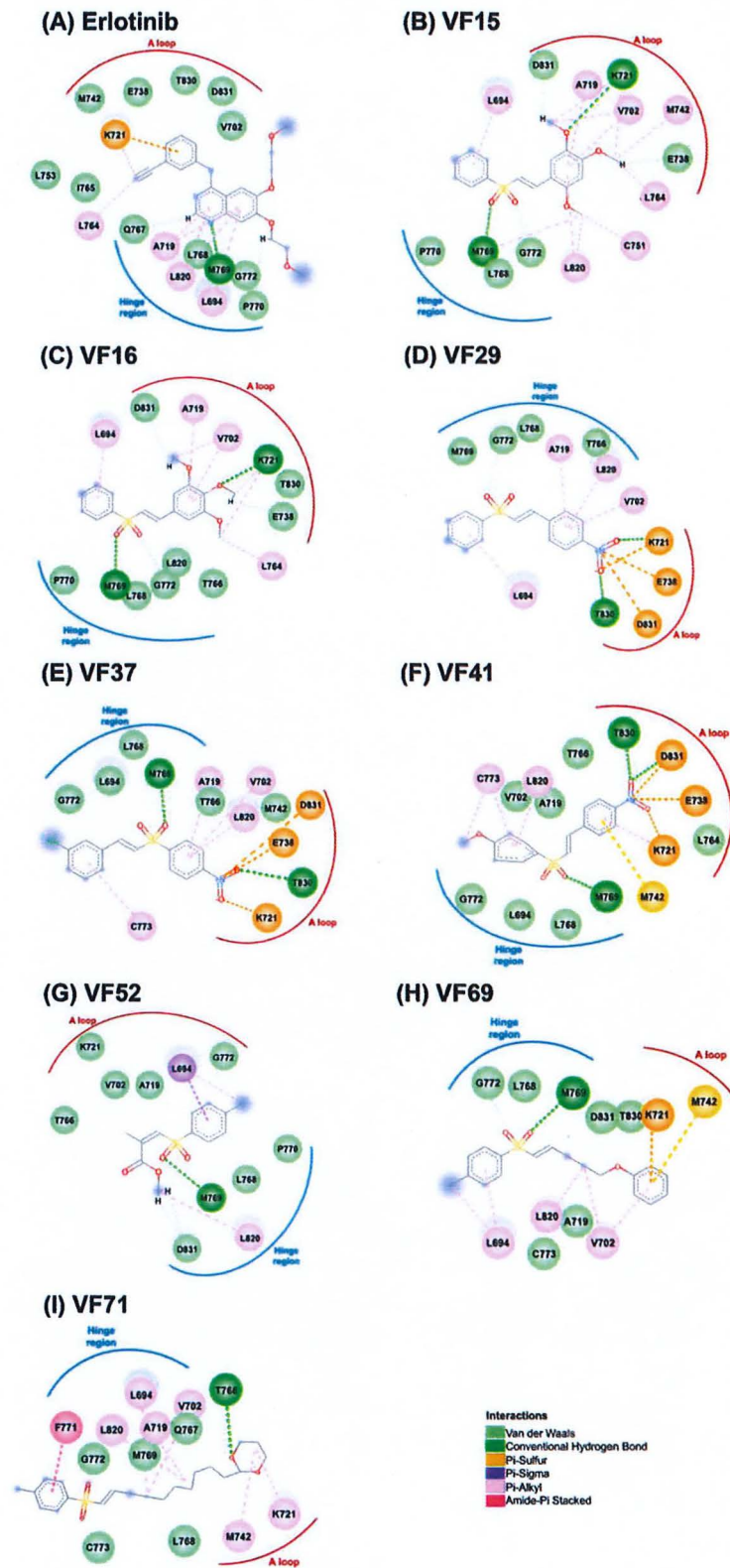


Figure 3. 2D interactions of EGFR-TK in complex with erlotinib (A) and VFs (B–I).

2.2. Drug-Likeness Prediction

Physical properties of the eight potent VFs were investigated in term of the drug-likeness by considering their physicochemical properties, including molecular weight (MW), the numbers of hydrogen bond donors (HBD) and acceptors (HBA), rotatable bond (RB), polar surface area (PSA) and lipophilicity (LogP) using the SwissADME web server [26]. The obtained results (Table 1) revealed that all VFs showed the acceptable value following the criteria: (i) $M_w \leq 500$ Da, (ii) $HBD \leq 5$ and $HBA \leq 10$, (iii) $RB \leq 10$, (iv) $PSA \leq 140$ Å, and (v) $LogP \leq 5$ [27]. Therefore, these VFs could likely be developed as promising novel EGFR-TK inhibitors.

Table 1. Predicted Lipinski's rule of five for the vinyl sulfones and the known drug. HBD, hydrogen bond donor; HBA, hydrogen bond acceptor; PSA, polar surface area.

| Compound | Lipinski's Rule of Five | | | | | | Drug-Likeness |
|------------------|-------------------------|---------------------|----------------------|---------------------|------------------------|----------------------|---------------|
| | MW (≤ 500 Da) | HBD (≤ 5) | HBA (≤ 10) | RB (≤ 10) | PSA (≤ 140 Å) | LogP (≤ 5) | |
| Erlotinib | 393.44 | 1 | 6 | 10 | 74.73 | 3.20 | Yes |
| VF15 | 334.39 | 0 | 5 | 6 | 70.21 | 2.76 | Yes |
| VF16 | 334.39 | 0 | 5 | 6 | 70.21 | 3.00 | Yes |
| VF29 | 291.32 | 2 | 4 | 4 | 86.22 | 2.32 | Yes |
| VF37 | 325.77 | 2 | 4 | 4 | 86.22 | 2.32 | Yes |
| VF41 | 321.35 | 2 | 5 | 5 | 95.45 | 2.66 | Yes |
| VF52 | 254.30 | 0 | 4 | 4 | 68.82 | 2.38 | Yes |
| VF69 | 316.41 | 0 | 3 | 7 | 51.75 | 3.26 | Yes |
| VF71 | 380.54 | 0 | 4 | 10 | 60.98 | 4.34 | Yes |

2.3. Inhibition of the EGFR-TK by Vinyl Sulfone Derivatives

Since the data shown above suggested that the eight VFs may be effective against EGFR-TK, we then investigated the EGFR-TKI inhibitory activity of the eight potent VFs and erlotinib at 1 μ M using ADP-Glo kinase assay (Figure 4A). Interestingly, we found that VF16 showed the highest EGFR-TK inhibitory activity (98.91%), which was higher than erlotinib (87.80%). Then, VF16 was selected to evaluate the half-maximal inhibitory concentration (IC_{50}) values. As shown in Figure 4B, the IC_{50} against EGFR-TK of VF16 is 7.85 ± 0.88 nM, which is significantly lower than the erlotinib (IC_{50} of 26.09 ± 5.42 nM). Additionally, the inhibitory activity of VF16 is greater than that of the chalcones that have been previously reported to inhibit EGFR activity (IC_{50} ranked from 10.3 to 15.4 μ M) [25].

In order to confirm the inhibition selectivity of VF16 towards EGFR-TK, we further performed kinase inhibition assay of VF16 against JAK3 and HER2 protein kinases because both kinases are one of the most studied kinase families [28,29]. The obtained results showed that VF16 showed very low inhibitory activity against JAK3 (IC_{50} of 158.45 ± 4.75 nM) and HER2 (IC_{50} of 312.00 ± 0.28 nM) (Figure S3) as compared to EGFR-TK (IC_{50} of 7.85 ± 0.88 nM), suggesting that VF16 was specific to EGFR-TK rather than JAK3 and HER2.

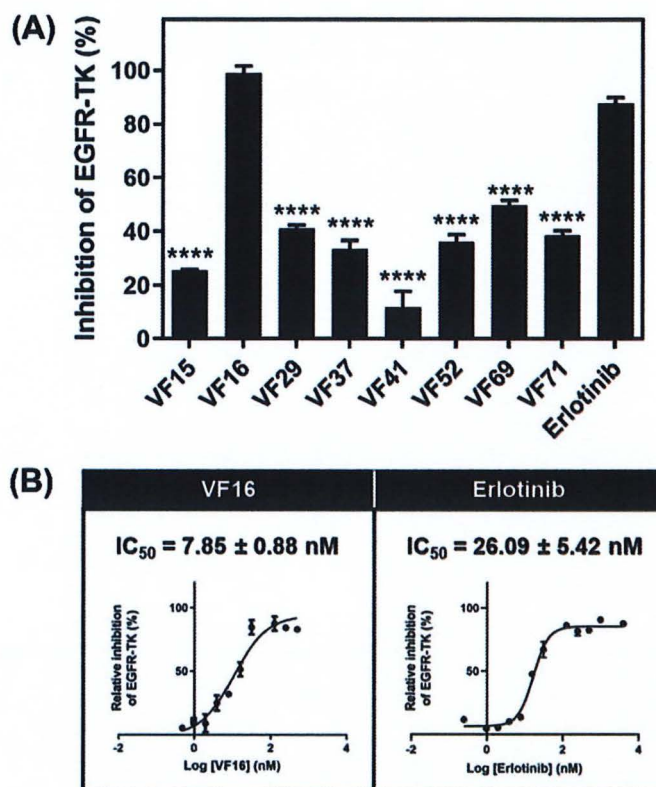


Figure 4. (A) Kinase inhibitory activity screening of VFs towards EGFR-TK at 1 μ M. **** $p \leq 0.0001$ vs. erlotinib. (B) Kinase inhibitory activity of VFs towards EGFR-TK. Data are represented as means \pm SEM from triplicate independent experiments.

2.4. Cytotoxicity

The VF16 was selected to evaluate IC₅₀ values against A549 and A431 cell lines overexpressing wild-type EGFR (A549 and A431) and mutant EGFR human lung cancer cell line (H1975) using MTT assay. The obtained results (Figure 5) revealed that the cytotoxic activity of VF16 against A549 (IC₅₀ of 54.63 \pm 0.09 μ M) and A431 (IC₅₀ of 33.52 \pm 2.57) was similar to that of erlotinib (IC₅₀ of 48.21 \pm 7.43 μ M and 27.19 \pm 6.93 μ M for A549 and A431, respectively). Note that VF16 inhibited the A431 cells better than A549 cells because (i) the EGFR expression level found in A431 cells is dramatically higher than that found in A549 [30] and (ii) A549 cells exhibits KRAS mutation, which constitutively activates downstream MAPK signaling pathways, causing a compensatory mechanism [31]. In H1975 cells, the VF16 (IC₅₀ of 30.38 \pm 1.37 μ M) was more susceptible than the erlotinib (IC₅₀ of 98.93 \pm 1.74 μ M) by ~3 times. The lower susceptibility of erlotinib towards T790M EGFR-expressing cells (H1975) compared to wild-type EGFR-expressing cells (A549 and A431) is in good agreement with the previous studies [32–34]. Altogether, these findings suggested that VF16 exhibited potent anti-lung cancer activity in all three lung cancer cell lines, which could be developed as a novel anti-lung cancer agent.

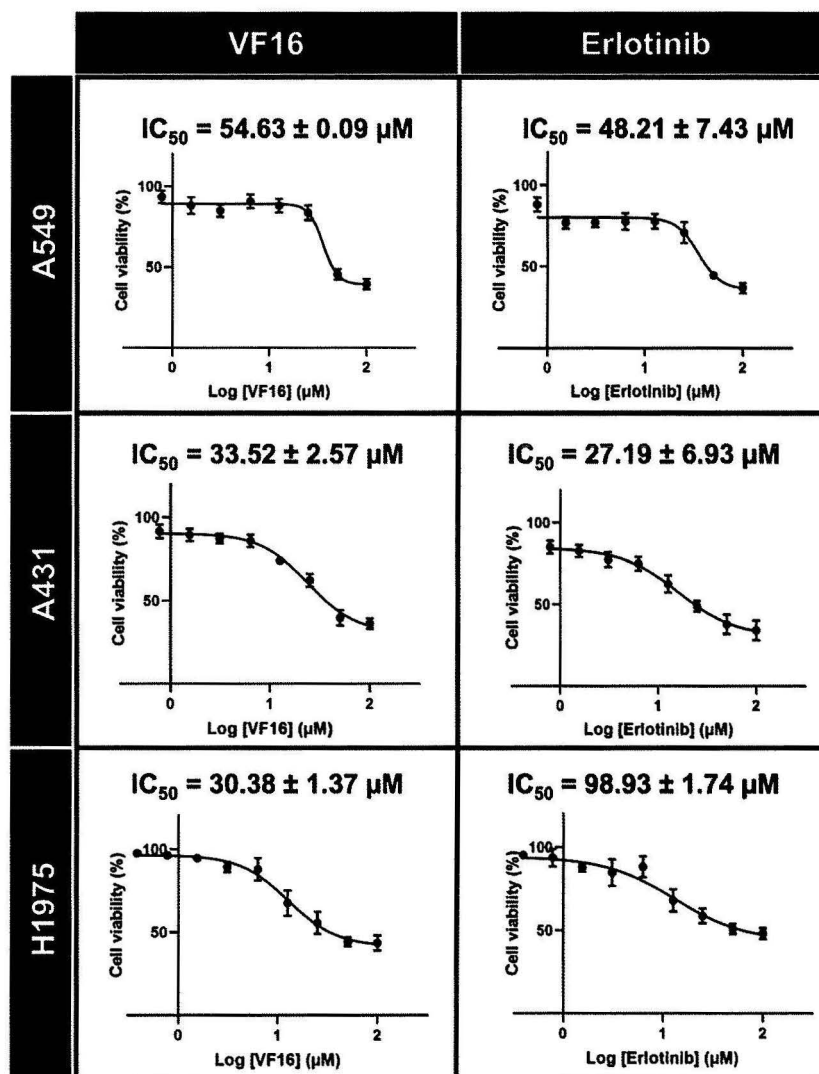


Figure 5. Cytotoxicity in three cancer cell lines (A549, A431, and H1975) after treated with various concentrations of VF16 compared to the known drug erlotinib for 72 h. Data are represented as means \pm SEM from triplicate independent experiments.

2.5. Molecular Dynamics Simulation

The structural stability of VF16 bound to the EGFR-TK domain was characterized using RMSD calculation plotted along the simulation time, and the obtained results are illustrated in Figure 6A. The RMSD values of VF16 were slightly fluctuated at the first 150 ns and then reached the equilibrium state after 250 ns with an average RMSD value of ~ 0.5 – 2 \AA . In the case of whole protein and backbone of protein, the RMSD values were slightly fluctuated at the first 100 ns then showed the stable values along the last stage of MD simulation with an average RMSD value of ~ 2 – 3.5 \AA .

In addition, the MD trajectories of this system were selected for further analysis in terms of: (i) the number of H-bond and (ii) number of contact atom within the 3.5 \AA sphere of VF16, respectively. The number of intermolecular hydrogen bonds and intermolecular contacts between VF16 and its surrounding residues was computed along 500 ns MD simulation represented in Figure 6A. According to the results, we found that VF16 formed two H-bonds with the M769 and C797, in which the C797 could form stronger H-bond than the M769. In addition, we found ~ 10 intermolecular contacts steadily formed between VF16 and EGFR-TK. These findings suggested that our simulation model was stable. In this

work, the MD trajectories from 300 to 500 ns were thus extracted for further analysis in terms of ΔG_{bind} values (kcal/mol) and key binding residues of VF16 against EGFR-TK.

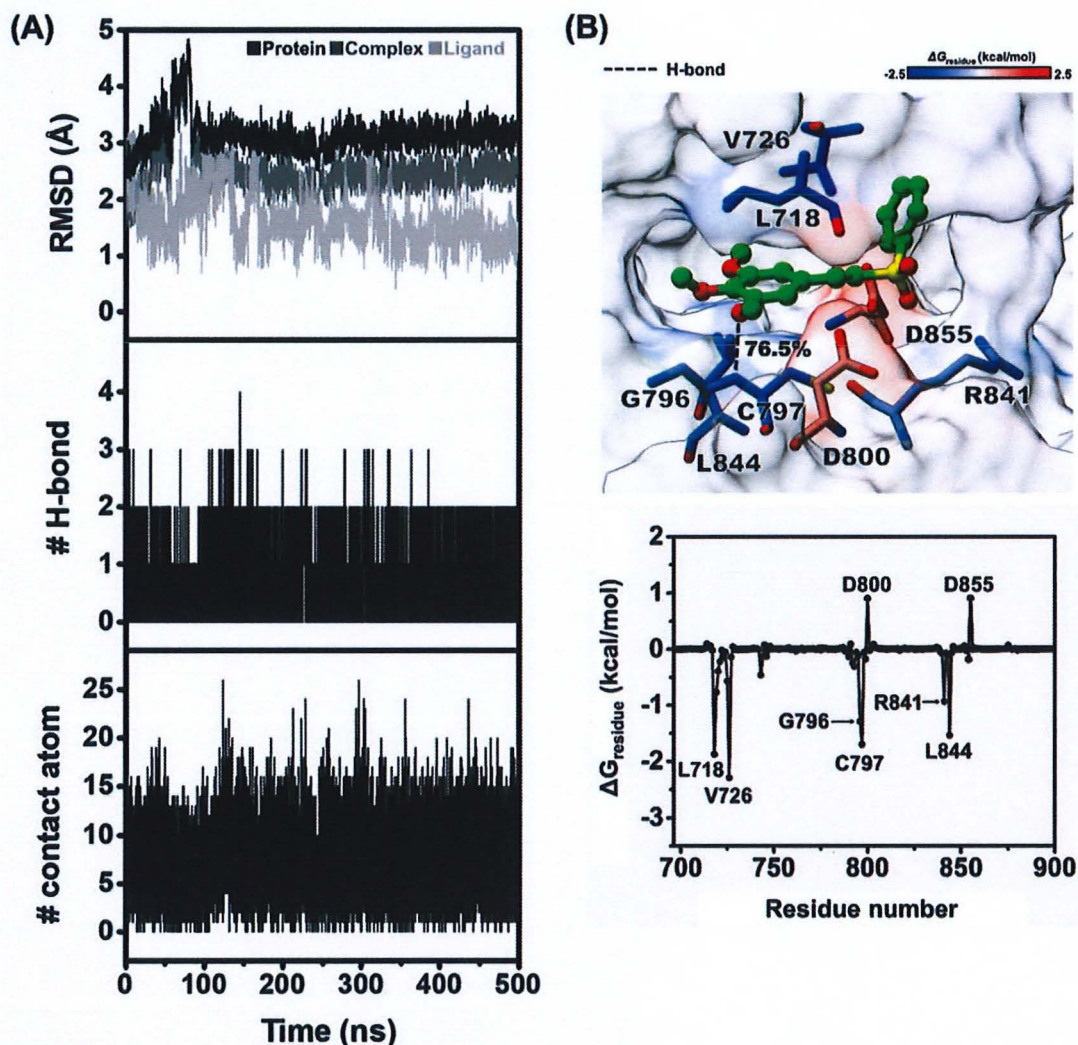


Figure 6. (A) All-atom RMSD, number of H-bonds, and number of contacts atom of VF16 in complex with EGFR-TK plotted along the 500 ns MD simulation. (B) Binding orientation of VF16 inside the ATP-binding pocket of EGFR-TK. The contributing residues involved in ligand binding are colored according to their $\Delta G_{\text{residue}}$ values, where the highest to lowest free energies are shaded from blue to red, respectively (H-bond interaction represented by black dash line) and per-residue decomposition free energy of the VF16 complex with EGFR-TK.

2.6. Binding Affinity and Key Residues for VF16/EGFR-TK Complex

The free energy calculation based on MM-GBSA method was applied to predict the binding affinity of VF16/EGFR-TK complex. We found that the ΔG_{bind} of VF16 is almost identical to the ΔG_{Exp} (Table 2). To investigate the key residues of EGFR-TK for VF16 binding, the per-residue decomposition free energy ($\Delta G_{\text{residue}}$) based on the MM-GBSA method was applied on the 100 snapshots over the last 200 ns MD simulation. Note that among residues 695–1018, only residues 695–900 are shown in Figure 6B, where the binding orientation of VF16 inside the ATP-binding pocket of EGFR-TK is shown in Figure 6B. The obtained results revealed that there were eight residues (L718, V726, G796, C797, D800, R841, L844, and D855) that were important for the binding of VF16. The binding residues of VF16 observed in this work were also found as a major interaction in erlotinib/EGFR-TK

complex (including L718, A743, L792, M793, G796, and L844) [35,36]. Figure 6B showed binding orientation inside the ATP-binding pocket of VF16/EGFR-TK complex, and we found that the -OCH₃ moiety of VF16 strongly formed H-bond with C797 and weakly formed H-bond with M769. This is in good agreement with the previous reports showing that H-bond formation with M769 is the main interaction of erlotinib and gefitinib in complex with wild-type EGFR and mutant EGFR [37–40].

Table 2. The MM-GBSA ΔG_{bind} and its energy components (kcal/mol).

| Energy Component | ΔG_{bind} (kcal/mol) |
|------------------------------------|-------------------------------------|
| ΔE_{vdW} | -38.99 ± 0.29 |
| ΔE_{ele} | -12.95 ± 0.55 |
| ΔG_{gas} | -51.94 ± 0.68 |
| ΔG_{solv} | 24.69 ± 0.53 |
| ΔG_{bind} | -8.74 ± 0.32 |
| $\Delta G_{\text{Exp}}^{\text{a}}$ | -10.13 ± 0.88 |

^a Experimental binding free energies (ΔG_{Exp}) was converted from the IC₅₀ value using the Cheng-Prusoff equation of $\Delta G_{\text{Exp}} = RT \ln(\text{IC}_{50})$ [41].

3. Materials and Methods

3.1. Interaction Energies between Vinyl Sulfone Derivatives and the ATP-Binding Site of EGFR-TK by Molecular Docking Technique

The crystal structure of EGFR complexed with erlotinib (PDB ID: 1M17) [39] was downloaded from Protein Data Bank (PDB). The 3D structure of the drug (erlotinib) was obtained from the ZINC database, whilst the 3D structures of vinyl sulfone derivatives were generated using the Gaussian 09 program. Note that the vinyl sulfone derivatives were constructed according to their availability from previous study [21–24]. All the ligands were optimized using the Gaussian 09 program (HF/6–31d) as per the standard protocol [42–44]. The protonation state of all studied ligands was characterized using the ChemAxon [45].

For system validation, the crystalized ligands were defined as a center in the active site for redocking using CDocker programs and the results are shown in Supplementary Figure S1. The docking protocols of EGFR system was set as 15 Å for sphere docking and docked into the binding pocket with 100 independent runs. The binding between protein and compounds/drug was visualized using the Accelrys Discovery Studio 3.0 (Accelrys Inc., Cambridge, UK) and UCSF Chimera package [46].

3.2. Predicted Physicochemical Properties

Physicochemical features such as hydrogen bond donors, hydrogen bond acceptors and drug-likeness play an important role in drug discovery and development [47]. Herein, such properties of the potent compounds were calculated in comparison with known drugs (erlotinib) using web-based applications SwissADME (www.swissadme.ch/) (accessed on 19 June 2020) [26].

3.3. Chemical Reagents and Cell Lines

The ADP-Glo™ Kinase Assay kit was purchased from Promega (Madison, WI, USA). EGFR and HER2 was obtained from the previous report [48]. JAK3 (SRP0173) were purchased from Sigma-Aldrich (Darmstadt, Germany). The series of vinyl sulfone derivatives were kindly provided by Dr. Chutima Kuhakarn from Department of Chemistry and Center of Excellence for Innovation in Chemistry (PERCH-CIC), Faculty of Science, Mahidol University [21–24]. Note that, due to limited amounts of vinyl sulfones obtained from previous study, we performed EGFR kinase and cytotoxicity assays as well as binding pattern study at the molecular level on only 78 vinyl sulfone derivatives (Figure 1). The lung carcinoma A549 (ATCC CCL-185) and A431 (ATCC CRL-1555) cell lines were purchased from the American Type Cell Culture Collection (ATCC,

Manassas, VA, USA). The EGFR mutated human lung cancer cell line (H1975) was provided by Dr. Chanida Vinayanuwattikun from Department of Medicine, Chulalongkorn University. Dulbecco's modified Eagle's medium (DMEM), RPMI-1640 medium, fetal bovine serum (FBS), penicillin-streptomycin (Pen-Strep) and trypsin were purchased from Life Technologies (California, USA). 3-(4,5-dimethylthiazol-2-yl)-2,5-diphenyltetrazolium bromide (MTT) and dimethyl sulfoxide (DMSO) were purchased from Sigma-Aldrich (Darmstadt, Germany).

3.4. Inhibition of the EGFR-TK by Vinyl Sulfone Derivatives

The selected sulfone derivatives that had the interaction energy lower or equal than erlotinib and physicochemical properties showed the acceptable value, were screened for their ability to inhibit the tyrosine kinase activity of the EGFR using the ADP-GloTM kinase assay as previously reported [25,49]. The first 8 μ L of buffer (40 mM Tris-HCl pH 7.5, 20 mM MgCl₂, and 0.1 mg/mL bovine serum albumin) was added to a 384-well plate. Then, 5 μ L of EGFR enzymes (1.25 ng/ μ L) and 2 μ L of inhibitors were added, followed by 10 μ L of a mixture of 5 μ M ATP and 2.5 μ M poly(glu-tyr), and incubated for 1 h at room temperature. Next, 5 μ L of the ADP-Glo reagent was added and incubated for 40 min, after that, 10 μ L of kinase detection reagent was added and incubated at room temperature for 30 min to convert the ADP to ATP. The ATP was then detected by measuring the luminescence using a microplate reader (Infinite M200 microplate reader, Tecan, Männedorf, Switzerland). All assays were performed in triplicate. The relative inhibition (%) of inhibitors were then calculated compared to the control with no inhibitor as shown in Equation (1):

$$\% \text{Relative inhibition} = \frac{[(\text{positive} - \text{negative}) - (\text{sample} - \text{negative})]}{(\text{positive} - \text{negative})} \times 100 \quad (1)$$

From this equation, the positive is the addition of the enzyme in the reaction, while the negative is without the enzyme in the reaction.

3.5. Cell Cultures

The A549 and A431 cells were grown in complete DMEM medium supplemented with 10% (v/v) FBS, 100 U/mL penicillin and 100 μ g/mL streptomycin. All cells were maintained at 37 °C in a 5% (v/v) CO₂, 95% (v/v) air humidified incubator while H1975 cells was grown in complete RPMI-1640 medium at 37 °C in a 5% (v/v) CO₂, 95% (v/v) air humidified incubator.

3.6. Cytotoxicity in Cancer Cell Lines

The in vitro cytotoxicity activity of vinyl sulfone derivatives against the A549, A431 and H1975 cell lines were evaluated using the MTT assay. The first 100 μ L of A549 (5000 cells/well), A431 (5000 cells/well) and H1975 (5000 cells/well) cells suspension was seeded per well in a 96-well microplate and incubated at 37 °C overnight, cells were treated with compounds and known drug (erlotinib) different concentration. Then, incubated for 72 h. Subsequently, the MTT solution (5 mg/mL) was added in A549, A431 and H1975 cells and incubated at 37 °C for 3 h. The medium was removed and 50 μ L of DMSO was added to each well to lyse the cells. Finally, the absorbance was measured at 570 nm using a microplate reader (Infinite M200 microplate reader, Tecan, Männedorf, Switzerland).

3.7. Molecular Dynamics Simulation

The starting crystal structure of EGFR-TK (PDB ID: 1M17) [39] was obtained from Protein Data Bank (PDB). The 3D structure of vinyl sulfone derivatives and known drug inhibitor (EGFR-TK) of EGFR-TK were generated and optimized HF/6-31G(d) method implemented in the Gaussian09 software [42-44]. The protein-ligand complexes were generated using the CDocker module accordance the standard protocol [50]. The docked VFs/EGFR-TK complex with lowest interaction energy and binding pattern similar to

the erlotinib (Figure S2) was selected as the initial structure for performing the Molecular Dynamics Simulation studies. The electrostatic potential (ESP) charges were consequently calculated with the same level of theory and were then fitted into restrained ESP (RESP) charges using the ANTECHAMBER module of AMBER16 [44,51,52]. The FF14SB [53] and GAFF [42,54] force fields were applied for protein and VF16, respectively. All missing hydrogen atoms of protein and ligand were added using LEaP module and were then minimized in order to remove the bad contacts. Each system was neutralized by the counter ions and immersed in a TIP3P water [55] box that extended at least 13 Å from the protein surface. Afterward, the complexes were energy-minimized by 1500 interactions of steepest descent (SD) and conjugated gradient (CG) methods using AMBER16 with the AMBER ff14SB force field.

The simulations are carried out under periodic boundary condition with NPT ensemble using a time step of 2 fs. The short-range cutoff for nonbonded interactions is set as 10 Å, whilst the Particle Mesh Ewald (PME) summation approach is applied to treat long-range electrostatic interaction [56,57]. Temperature and pressure are controlled by Berendsen weak coupling algorithm. The SHAKE algorithm is used to constrain all covalent bonds involving hydrogen atoms [58]. The simulated models are then heated up to 310 K for 100 ps and are continuously held at this temperature for another 100 ns or until the simulations have reached equilibrium. Finally, the structural and dynamics behaviors of each complex will be analyzed, including root mean square deviation (RMSD), number of H-bonds between the ligand and EGFR-TK and number of contact atom via the cptraj module [59]. Besides, the MM-GBSA and ΔG_{bind} , residue were calculated by the MM-PBSA.py module [58,59].

3.8. Statistical Analysis

The data are represented as mean \pm standard error of mean (SEM). Differences between groups were compared using one-way ANOVA, followed by Tukey's test for multiple comparisons. The differences in means were determined at the confidence level $p \leq 0.05$.

4. Conclusions

This work combined the computational and experiment techniques to identify new EGFR inhibitor based on vinyl sulfone derivatives. Eight vinyl sulfones from molecular docking technique were tested the inhibitory activity against EGFR-TK and cell-based assay in three cancer cell lines (A549, A431, and H1975 cell lines). The results showed that VF16 can inhibit EGFR-TK activity better than the approved drug erlotinib and showed higher cytotoxicity against A431 cell line than A549 cell line. Additionally, showed high cytotoxicity against H1975 cell lines. From MD simulations, our simulation model of VF16/EGFR are stable. In addition, VF16 showed strongest H-bond with C797, and the key residues responsible for VF16 binding were L718, V726, G796, C797, D800, R841, L844, and D855, in which these binding residues were also found in a major interaction between erlotinib and EGFR-TK. Thus, VF16 could be developed as a promising new anti-cancer drug targeting EGFR-TK.

Supplementary Materials: Figure S1: Superimposition of ligands between X-ray structure and CDocker docking, Figure S2: Binding pose between VF16 and known drug within EGFR-TK, Figure S3: The IC₅₀ curves of kinase inhibitory activity of VF16 against EGFR-TK, JAK3, and HER2.

Author Contributions: T.R., K.C., T.A., P.M. conceived and designed the experiments. T.A. conducted theoretical and experimental studies. A.A., O.K. and C.K. synthesized all compounds. T.A., P.M., T.R., K.C., L.T., and S.S. analyzed the data. T.A. wrote the original manuscript. All authors reviewed and edited the manuscript. All authors have read and agreed to the published version of the manuscript.

Funding: This work was financially supported by Ratchadaphiseksomphot Endowment Fund (Grant No. CU_GR_62_96_23_35 for T.R.). T.A. thanks the 90th Anniversary of Chulalongkorn University Fund (Ratchadaphiseksomphot Endowment Fund, GCUGR1125633082M). C.K. thanks

the Thailand Research Fund (BRG6180005) and the Center of Excellence for Innovation in Chemistry, Ministry of Higher Education, Science, Research and Innovation.

Data Availability Statement: Data contained in the manuscript are available from the authors.

Acknowledgments: We would like to thank Siwaporn Boonyasuppayakorn, Department of Microbiology, Faculty of Medicine, Chulalongkorn University for supporting cell culture laboratory.

Conflicts of Interest: The authors declared no conflict of interest.

Sample Availability: Samples of the compounds are available from the authors.

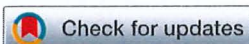
References

1. Siegel, R.L.; Miller, K.D.; Jemal, A. Cancer statistics, 2019. *CA Cancer J. Clin.* **2019**, *69*, 7–34. [[CrossRef](#)] [[PubMed](#)]
2. Araujo, D.V.; Watson, G.A.; Oliva, M.; Heirali, A.; Coburn, B.; Spreafico, A.; Siu, L.L. Bugs as Drugs: The Role of Microbiome in Cancer Focusing on Immunotherapeutics. *Cancer Treat. Rev.* **2020**, *92*, 102125. [[CrossRef](#)] [[PubMed](#)]
3. Huang, M.; Shen, A.; Ding, J.; Geng, M. Molecularly targeted cancer therapy: Some lessons from the past decade. *Trends Pharmacol. Sci.* **2014**, *35*, 41–50. [[CrossRef](#)] [[PubMed](#)]
4. Sharma, S.V.; Settleman, J. Oncogene addiction: Setting the stage for molecularly targeted cancer therapy. *Genes Dev.* **2007**, *21*, 3214–3231. [[CrossRef](#)]
5. Ke, X.; Shen, L. Molecular targeted therapy of cancer: The progress and future prospect. *Front. Lab. Med.* **2017**, *1*, 69–75. [[CrossRef](#)]
6. Wee, P.; Wang, Z. Epidermal Growth Factor Receptor Cell Proliferation Signaling Pathways. *Cancers* **2017**, *9*, 52. [[CrossRef](#)]
7. Holbro, T.; Hynes, N.E. ErbB receptors: Directing key signaling networks throughout life. *Annu. Rev. Pharmacol. Toxicol.* **2004**, *44*, 195–217. [[CrossRef](#)]
8. Choowongkamon, K.; Carlin, C.R.; Sonnichsen, F.D. A structural model for the membrane-bound form of the juxtamembrane domain of the epidermal growth factor receptor. *J. Biol. Chem.* **2005**, *280*, 24043–24052. [[CrossRef](#)]
9. Flynn, J.F.; Wong, C.; Wu, J.M. Anti-EGFR Therapy: Mechanism and Advances in Clinical Efficacy in Breast Cancer. *J. Oncol.* **2009**, *2009*, 526963. [[CrossRef](#)]
10. Seshacharyulu, P.; Ponnusamy, M.P.; Haridas, D.; Jain, M.; Ganti, A.K.; Batra, S.K. Targeting the EGFR signaling pathway in cancer therapy. *Expert Opin. Ther. Targets* **2012**, *16*, 15–31. [[CrossRef](#)]
11. Fitzgerald, T.L.; Lertpiriyapong, K.; Cocco, L.; Martelli, A.M.; Libra, M.; Candido, S.; Montalto, G.; Cervello, M.; Steelman, L.; Abrams, S.L.; et al. Roles of EGFR and KRAS and their downstream signaling pathways in pancreatic cancer and pancreatic cancer stem cells. *Adv. Biol. Regul.* **2015**, *59*, 65–81. [[CrossRef](#)]
12. Ogiso, H.; Ishitani, R.; Nureki, O.; Fukai, S.; Yamanaka, M.; Kim, J.H.; Saito, K.; Sakamoto, A.; Inoue, M.; Shirouzu, M.; et al. Crystal structure of the complex of human epidermal growth factor and receptor extracellular domains. *Cell* **2002**, *110*, 775–787. [[CrossRef](#)]
13. Yang, C.H.; Chou, H.C.; Fu, Y.N.; Yeh, C.L.; Cheng, H.W.; Chang, I.C.; Liu, K.J.; Chang, G.C.; Tsai, T.F.; Tsai, S.F.; et al. EGFR over-expression in non-small cell lung cancers harboring EGFR mutations is associated with marked down-regulation of CD82. *Biochim. Biophys. Acta* **2015**, *1852*, 1540–1549. [[CrossRef](#)]
14. Wang, Y.; Schmid-Bindert, G.; Zhou, C. Erlotinib in the treatment of advanced non-small cell lung cancer: An update for clinicians. *Ther. Adv. Med. Oncol.* **2012**, *4*, 19–29. [[CrossRef](#)]
15. Maemondo, M.; Inoue, A.; Kobayashi, K.; Sugawara, S.; Oizumi, S.; Isobe, H.; Gemma, A.; Harada, M.; Yoshizawa, H.; Kinoshita, I.; et al. Gefitinib or Chemotherapy for Non-Small-Cell Lung Cancer with Mutated EGFR. *N. Engl. J. Med.* **2010**, *362*, 2380–2388. [[CrossRef](#)]
16. Liu, W.; Ning, J.F.; Meng, Q.W.; Hu, J.; Zhao, Y.B.; Liu, C.; Cai, L. Navigating into the binding pockets of the HER family protein kinases: Discovery of novel EGFR inhibitor as antitumor agent. *Drug Des. Devel. Ther.* **2015**, *9*, 3837–3851. [[CrossRef](#)]
17. Jackman, D.M.; Yeap, B.Y.; Sequist, L.V.; Lindeman, N.; Holmes, A.J.; Joshi, V.A.; Bell, D.W.; Huberman, M.S.; Halmos, B.; Rabin, M.S.; et al. Exon 19 deletion mutations of epidermal growth factor receptor are associated with prolonged survival in non-small cell lung cancer patients treated with gefitinib or erlotinib. *Clin. Cancer Res.* **2006**, *12*, 3908–3914. [[CrossRef](#)]
18. Cortot, A.B.; Janne, P.A. Molecular mechanisms of resistance in epidermal growth factor receptor-mutant lung adenocarcinomas. *Eur. Respir. Rev.* **2014**, *23*, 356–366. [[CrossRef](#)]
19. Tang, J.; Salama, R.; Gadgeel, S.M.; Sarkar, F.H.; Ahmad, A. Erlotinib resistance in lung cancer: Current progress and future perspectives. *Front. Pharmacol.* **2013**, *4*, 15. [[CrossRef](#)]
20. Politi, K.; Fan, P.D.; Shen, R.; Zakowski, M.; Varmus, H. Erlotinib resistance in mouse models of epidermal growth factor receptor-induced lung adenocarcinoma. *Dis. Model. Mech.* **2010**, *3*, 111–119. [[CrossRef](#)]
21. Katrun, P.; Hlekhilai, S.; Meesin, J.; Pohmakotr, M.; Reutrakul, V.; Jaipetch, T.; Soorukram, D.; Kuhakarn, C. PhI(OAc)₂ mediated decarboxylative sulfonylation of beta-aryl-alpha, beta-unsaturated carboxylic acids: A synthesis of (E)-vinyl sulfones. *Org. Biomol. Chem.* **2015**, *13*, 4785–4794. [[CrossRef](#)]
22. Katrun, P.; Chiampanichayakul, S.; Korworapan, K.; Pohmakotr, M.; Reutrakul, V.; Jaipetch, T.; Kuhakarn, C. PhI(OAc)₂/KI-Mediated Reaction of Aryl Sulfinates with Alkenes, Alkynes, and α,β -Unsaturated Carbonyl Compounds: Synthesis of Vinyl Sulfones and β -Iodovinyl Sulfones. *Eur. J. Org. Chem.* **2010**, *2010*, 5633–5641. [[CrossRef](#)]

23. Meesin, J.; Katrun, P.; Pareseecharoen, C.; Pohmakotr, M.; Reutrakul, V.; Soorukram, D.; Kuhakarn, C. Iodine-catalyzed Sulfonylation of Arylacetylenic Acids and Arylacetylenes with Sodium Sulfonates: Synthesis of Arylacetylenic Sulfones. *J. Org. Chem.* **2016**, *81*, 2744–2752. [CrossRef] [PubMed]
24. Meesin, J.; Katrun, P.; Reutrakul, V.; Pohmakotr, M.; Soorukram, D.; Kuhakarn, C. Decarboxylative sulfonylation of arylpropionic acids with sulfonic acids: Synthesis of (E)-vinyl sulfones. *Tetrahedron* **2016**, *72*, 1440–1446. [CrossRef]
25. Sangpheak, K.; Tabtimmai, L.; Seetaha, S.; Rungnim, C.; Chavasiri, W.; Wolschann, P.; Choowongkamon, K.; Rungrotmongkol, T. Biological Evaluation and Molecular Dynamics Simulation of Chalcone Derivatives as Epidermal Growth Factor-Tyrosine Kinase Inhibitors. *Molecules* **2019**, *24*, 1092. [CrossRef] [PubMed]
26. Daina, A.; Michielin, O.; Zoete, V. SwissADME: A free web tool to evaluate pharmacokinetics, drug-likeness and medicinal chemistry friendliness of small molecules. *Sci. Rep.* **2017**, *7*, 42717. [CrossRef]
27. Lipinski, C.A. Lead- and drug-like compounds: The rule-of-five revolution. *Drug Discov. Today Technol.* **2004**, *1*, 337–341. [CrossRef]
28. Fink, B.E.; Vite, G.D.; Mastalerz, H.; Kadow, J.F.; Kim, S.H.; Leavitt, K.J.; Du, K.; Crews, D.; Mitt, T.; Wong, T.W.; et al. New dual inhibitors of EGFR and HER2 protein tyrosine kinases. *Bioorg. Med. Chem. Lett.* **2005**, *15*, 4774–4779. [CrossRef]
29. Parganas, E.; Wang, D.; Stravopodis, D.; Topham, D.J.; Marine, J.-C.; Teglund, S.; Vanin, E.F.; Bodner, S.; Colamonici, O.R.; van Deursen, J.M.; et al. Jak2 Is Essential for Signaling through a Variety of Cytokine Receptors. *Cell* **1998**, *93*, 385–395. [CrossRef]
30. Liu, W.J.; Liu, X.J.; Xu, J.; Li, L.; Li, Y.; Zhang, S.H.; Wang, J.L.; Miao, Q.F.; Zhen, Y.S. EGFR-targeting, beta-defensin-tailored fusion protein exhibits high therapeutic efficacy against EGFR-expressed human carcinoma via mitochondria-mediated apoptosis. *Acta Pharmacol. Sin.* **2018**, *39*, 1777–1786. [CrossRef]
31. Demiray, A.; Yaren, A.; Karagenc, N.; Bir, F.; Demiray, A.; Karagür, E.; Tokgün, O.; Elmas, L.; Akça, H. The Frequency of EGFR and KRAS Mutations in the Turkish Population with Non-small Cell Lung Cancer and their Response to Erlotinib Therapy. *Balk. J. Med. Genet.* **2018**, *21*, 21–26. [CrossRef]
32. Hirano, T.; Yasuda, H.; Tani, T.; Hamamoto, J.; Oashi, A.; Ishioka, K.; Arai, D.; Nukaga, S.; Miyawaki, M.; Kawada, I.; et al. In vitro modeling to determine mutation specificity of EGFR tyrosine kinase inhibitors against clinically relevant EGFR mutants in non-small-cell lung cancer. *Oncotarget* **2015**, *6*, 38789–38803. [CrossRef]
33. Li, Y.; Song, Z.; Jin, Y.; Tang, Z.; Kang, J.; Ma, X. Novel Selective and Potent EGFR Inhibitor that Overcomes T790M-Mediated Resistance in Non-Small Cell Lung Cancer. *Molecules* **2016**, *21*, 1462. [CrossRef]
34. Sharma, V.K.; Nandekar, P.P.; Sangamwar, A.; Pérez-Sánchez, H.; Agarwal, S.M. Structure guided design and binding analysis of EGFR inhibiting analogues of erlotinib and AEE788 using ensemble docking, molecular dynamics and MM-GBSA. *RSC Adv.* **2016**, *6*, 65725–65735. [CrossRef]
35. Liu, B.; Bernard, B.; Wu, J.H. Impact of EGFR point mutations on the sensitivity to gefitinib: Insights from comparative structural analyses and molecular dynamics simulations. *Proteins* **2006**, *65*, 331–346. [CrossRef]
36. Doss, G.P.; Rajith, B.; Chakraborty, C.; NagaSundaram, N.; Ali, S.K.; Zhu, H. Structural signature of the G719S-T790M double mutation in the EGFR kinase domain and its response to inhibitors. *Sci. Rep.* **2014**, *4*, 5868. [CrossRef]
37. Martinez-Jimenez, F.; Overington, J.P.; Al-Lazikani, B.; Marti-Renom, M.A. Rational design of non-resistant targeted cancer therapies. *Sci. Rep.* **2017**, *7*, 46632. [CrossRef]
38. Stamos, J.; Sliwkowski, M.X.; Eigenbrot, C. Structure of the epidermal growth factor receptor kinase domain alone and in complex with a 4-anilinoquinazoline inhibitor. *J. Biol. Chem.* **2002**, *277*, 46265–46272. [CrossRef]
39. Ahmed, M.; Sadek, M.M.; Abouzid, K.A.; Wang, F. In silico design: Extended molecular dynamic simulations of a new series of dually acting inhibitors against EGFR and HER2. *J. Mol. Graph. Model.* **2013**, *44*, 220–231. [CrossRef]
40. Cheng, H.C. The power issue: Determination of KB or Ki from IC50: A closer look at the Cheng–Prusoff equation, the Schild plot and related power equations. *J. Pharmacol. Toxicol. Methods* **2001**, *46*, 61–71. [CrossRef]
41. Mahalapbutr, P.; Thitinanthavet, K.; Kedkham, T.; Nguyen, H.; Theu, L.; Dokmaisrijan, S.; Huynh, L.; Kungwan, N.; Rungrotmongkol, T. A theoretical study on the molecular encapsulation of luteolin and pinocembrin with various derivatized beta-cyclodextrins. *J. Mol. Struct.* **2019**, *1180*, 480–490. [CrossRef]
42. Kammarabutr, J.; Mahalapbutr, P.; Nutho, B.; Kungwan, N.; Rungrotmongkol, T. Low susceptibility of asunaprevir towards R155K and D168A point mutations in HCV NS3/4A protease: A molecular dynamics simulation. *J. Mol. Graph. Model.* **2019**, *89*, 122–130. [CrossRef]
43. Sanachai, K.; Mahalapbutr, P.; Choowongkamon, K.; Poo-Arporn, R.P.; Wolschann, P.; Rungrotmongkol, T. Insights into the Binding Recognition and Susceptibility of Tofacitinib toward Janus Kinases. *ACS Omega* **2020**, *5*, 369–377. [CrossRef]
44. Marvin Was Used for Drawing, Displaying and Characterizing Chemical Structures, Substructures and Reactions, Marvin 17.21.0, ChemAxon. Available online: <https://www.chemaxon.com> (accessed on 19 June 2020).
45. Pettersen, E.F.; Goddard, T.D.; Huang, C.C.; Couch, G.S.; Greenblatt, D.M.; Meng, E.C.; Ferrin, T.E. UCSF chimera-A visualization system for exploratory research and analysis. *J. Comput. Chem.* **2004**, *25*, 1605–1612. [CrossRef]
46. Cheng, F.; Li, W.; Zhou, Y.; Shen, J.; Wu, Z.; Liu, G.; Lee, P.W.; Tang, Y. admetSAR: A Comprehensive Source and Free Tool for Assessment of Chemical ADMET Properties. *J. Chem. Inf. Model.* **2012**, *52*, 3099–3105. [CrossRef]
47. Seetaha, S.; Ratanabunyong, S.; Choowongkamon, K. Expression, purification, and characterization of the native intracellular domain of human epidermal growth factor receptors 1 and 2 in Escherichia coli. *Appl. Microbiol. Biotechnol.* **2019**, *103*. [CrossRef]

48. Mahalapbutr, P.; Wonganan, P.; Charoenwongpaiboon, T.; Prousoontorn, M.; Chavasiri, W.; Rungrotmongkol, T. Enhanced Solubility and Anticancer Potential of Mansonone G By beta-Cyclodextrin-Based Host-Guest Complexation: A Computational and Experimental Study. *Biomolecules* **2019**, *9*, 545. [[CrossRef](#)]
49. Mahalapbutr, P.; Nutho, B.; Wolschann, P.; Chavasiri, W.; Kungwan, N.; Rungrotmongkol, T. Molecular insights into inclusion complexes of mansonone E and H enantiomers with various beta-cyclodextrins. *J. Mol. Graph. Model.* **2018**, *79*, 72–80. [[CrossRef](#)]
50. Phanich, J.; Rungrotmongkol, T.; Kungwan, N.; Hannongbua, S. Role of R292K mutation in influenza H7N9 neuraminidase toward oseltamivir susceptibility: MD and MM/PB(GB)SA study. *J. Comput. Aided Mol. Des.* **2016**, *30*, 917–926. [[CrossRef](#)]
51. Maier, J.A.; Martinez, C.; Kasavajhala, K.; Wickstrom, L.; Hauser, K.E.; Simmerling, C. ff14SB: Improving the Accuracy of Protein Side Chain and Backbone Parameters from ff99SB. *J. Chem. Theory Comput.* **2015**, *11*, 3696–3713. [[CrossRef](#)]
52. Sangpheak, W.; Khuntawee, W.; Wolschann, P.; Pongsawasdi, P.; Rungrotmongkol, T. Enhanced stability of a naringenin/2,6-dimethyl beta-cyclodextrin inclusion complex: Molecular dynamics and free energy calculations based on MM- and QM-PBSA/GBSA. *J. Mol. Graph. Model.* **2014**, *50*, 10–15. [[CrossRef](#)] [[PubMed](#)]
53. Jorgensen, W.L.; Chandrasekhar, J.; Madura, J.D.; Impey, R.W.; Klein, M.L. Comparison of simple potential functions for simulating liquid water. *J. Chem. Phys.* **1983**, *79*, 926–935. [[CrossRef](#)]
54. Chari, R.; Jerath, K.; Badkar, A.V.; Kalonia, D.S. Long- and short-range electrostatic interactions affect the rheology of highly concentrated antibody solutions. *Pharm. Res.* **2009**, *26*, 2607–2618. [[CrossRef](#)] [[PubMed](#)]
55. York, D.M.; Darden, T.A.; Pedersen, L.G. The effect of long-range electrostatic interactions in simulations of macromolecular crystals: A comparison of the Ewald and truncated list methods. *J. Chem. Phys.* **1993**, *99*, 8345–8348. [[CrossRef](#)]
56. Ryckaert, J.-P.; Ciccotti, G.; Berendsen, H.J.C. Numerical integration of the cartesian equations of motion of a system with constraints: Molecular dynamics of n-alkanes. *J. Comput. Phys.* **1977**, *23*, 327–341. [[CrossRef](#)]
57. Roe, D.R.; Cheatham, T.E., III. PTRAJ and CPPTRAJ: Software for Processing and Analysis of Molecular Dynamics Trajectory Data. *J. Chem. Theory Comput.* **2013**, *9*, 3084–3095. [[CrossRef](#)]
58. Genheden, S.; Ryde, U. The MM/PBSA and MM/GBSA methods to estimate ligand-binding affinities. *Expert Opin. Drug Discov.* **2015**, *10*, 449–461. [[CrossRef](#)]
59. Sulea, T.; Cui, Q.; Purisima, E.O. Solvated Interaction Energy (SIE) for Scoring Protein–Ligand Binding Affinities. 2. Benchmark in the CSAR-2010 Scoring Exercise. *J. Chem. Inf. Model.* **2011**, *51*, 2066–2081. [[CrossRef](#)]

RESEARCH ARTICLE

View Article Online
View Journal | View IssueCite this: *RSC Med. Chem.*, 2021, 12,
430Discovery of novel JAK2 and EGFR inhibitors from
a series of thiazole-based chalcone derivatives†Kamonpan Sanachai,^{†a} Thitinan Aiebchun,^{†a} Panupong Mahalapbutr,^{†b}
Supaphorn Seetaha,^c Lueacha Tabtimmai,^d Phornphimon Maitarad,^e
Iakovos Xenikakis,^f Athina Geronikaki,^f
Kiattawee Choowongkorn^e and Thanyada Rungrotmongkol^{e*ag}

The Janus kinase (JAK) and epidermal growth factor receptor (EGFR) have been considered as potential targets for cancer therapy due to their role in regulating proliferation and survival of cancer cells. In the present study, the aromatic alkyl-amino analogs of thiazole-based chalcone were selected to experimentally and theoretically investigate their inhibitory activity against JAK2 and EGFR proteins as well as their anti-cancer effects on human cancer cell lines expressing JAK2 (TF1 and HEL) and EGFR (A549 and A431). *In vitro* cytotoxicity screening results demonstrated that the HEL erythroleukemia cell line was susceptible to compounds **11** and **12**, whereas the A431 lung cancer cell line was vulnerable to compound **25**. However, TF1 and A549 cells were not sensitive to our thiazole derivatives. From kinase inhibition assay results, compound **25** was found to be a dual inhibitor against JAK2 and EGFR, whereas compounds **11** and **12** selectively inhibited the JAK2 protein. According to the molecular docking analysis, compounds **11**, **12** and **25** formed hydrogen bonds with the hinge region residues Lys857, Leu932 and Glu930 and hydrophobically came into contact with Leu983 at the catalytic site of JAK2, while compound **25** formed a hydrogen bond with Met769 at the hinge region, Lys721 near a glycine loop, and Asp831 at the activation loop of EGFR. Altogether, these potent thiazole derivatives, following Lipinski's rule of five, could likely be developed as a promising JAK2/EGFR targeted drug(s) for cancer therapy.

Received 30th December 2020,
Accepted 25th January 2021

DOI: 10.1039/d0md00436g

rsc.li/medchem

Introduction

Cancer, a group of diseases characterized by uncontrolled growth and spread of abnormal cells,¹ is the second leading cause of mortality worldwide.² Among several types of cancer, myeloproliferative neoplasms and lung cancer are the leading

cause of cancer-related death globally.³ The known molecular targets for treating these cancers are the Janus kinases (JAKs) and the epidermal growth factor receptor (EGFR), since they play a major role in regulating proliferation and survival of cancer cells.^{4,5}

JAK, an intracellular tyrosine kinase, is activated by the cytokine(s) binding to its receptor, resulting in the activation of the downstream signal transducer and activator of transcription (STAT), which leads to its dimerization and translocation to the nucleus, promoting cell proliferation, apoptosis and differentiation.⁶ Among the four JAK family members (JAK1, JAK2, JAK3 and TYK2),⁷ JAK2 is a critical moderator for hormone-like cytokines such as growth hormone (GH), erythropoietin (EPO), thrombopoietin (TPO) and cytokine receptor ligands involved in hematopoietic cell development such as interleukin-3 (IL-3).⁸ JAK2 consists of seven homology regions (JH1 to JH7) and the catalytically active domain in JH1 is located at the carboxy-terminus, close to the pseudo-kinase domain in JH2. The overexpression of JAK2, especially the V617F variance in the JH2 domain, has been shown to be related to myeloproliferative disorders (by approximately 50% or more) such as polycythemia vera, essential thrombocythemia and myelofibrosis,^{9,10} indicating

^a Structural and Computational Biology Research Unit, Department of Biochemistry, Faculty of Science, Chulalongkorn University, Bangkok 10330, Thailand. E-mail: t.rungrotmongkol@gmail.com; Fax: +662 2185418; Tel: +662 2185426

^b Department of Biochemistry, Faculty of Medicine, Khon Kaen University, Khon Kaen 40002, Thailand

^c Department of Biochemistry, Faculty of Science, Kasetsart University, Bangkok 10900, Thailand

^d Department of Biotechnology, Faculty of Applied Science, King Mongkut's University of Technology of North Bangkok, Bangkok, Thailand

^e Research Center of Nano Science and Technology, Shanghai University, Shanghai 200444, PR China

^f Department of Pharmaceutical Chemistry, School of Pharmacy, Aristotle University of Thessaloniki, Thessaloniki 54124, Greece

^g Program in Bioinformatics and Computational Biology, Graduate School, Chulalongkorn University, Bangkok 10330, Thailand

† Electronic supplementary information (ESI) available. See DOI: 10.1039/d0md00436g

‡ These authors contributed equally to this work.

that JAK2 is an important target for the treatment of myeloproliferative diseases.

EGFR, a member of the ErbB family of receptor tyrosine kinases,¹¹ is composed of an extracellular domain, a single hydrophobic transmembrane region, an intracellular tyrosine kinase (TK) domain,¹² and a C-terminal tyrosine-rich region.¹³ The EGFR signaling pathways are triggered by the specific growth factors (such as EGF and TGF α) to the extracellular domain, activating autophosphorylation and subsequently initiating downstream signaling pathways, responsible for cell proliferation, survival, differentiation and apoptosis evasion.^{10,11,14,15} Importantly, more than 60% of non-small cell lung cancer have been involved in the overexpression of EGFR;¹⁶ therefore, targeting this protein is an important strategy for lung cancer treatment. As shown in Fig. 1A and B, the sequence identity and similarity of (i) the overall structure and (ii) the conserved regions (catalytic loop, hinge region, glycine-rich loop (G loop) and activation loop (A loop)) between JAK2 and EGFR are 29% and 46% as well as 54% and 71%, respectively.

To date, several JAK2 and EGFR inhibitors have been reported such as lestaurinib,¹⁷ momelotinib,¹⁸ and gandotinib¹⁹ for JAK2 as well as erlotinib²⁰ and gefitinib²¹ for EGFR. Among them, ruxolitinib is widely used in clinical treatment for bone marrow cancer (IC₅₀ against JAK2 is 4.5 nM),^{22,23} while erlotinib has been the first-line drug for lung cancer patients harboring wild-type EGFR (IC₅₀ against EGFR is 2.6 nM).^{24,25} However, these drugs have several side effects, e.g., anemia, balance impairment and dizziness.^{26,27} Moreover, acquired drug resistances of ruxolitinib (V617F/L983F) and erlotinib (T790M) have been detected after 1.5

year treatment.^{28–30} Accordingly, discovery of novel JAK2 and EGFR inhibitors is critically needed.

Thiazoles are a class of heterocyclic compounds containing sulfur and nitrogen atoms at positions 1 and 3, respectively. Thiazole derivatives were reported to exert anti-cancer activity against several types of cancer and were identified as JAK2 and EGFR inhibitors.³¹ Trifluoromethylphenyl thiazole amine inhibited the proliferation of HMC-1.1 cells, which are hematopoietic progenitors in the bone marrow, with an IC₅₀ value of 138 nM.³² In addition, the 4,5-dimethyl thiazole analog potentially inhibited JAK2 activity (IC₅₀ = 2.5 nM) and the JAK2 dependent cell line (SET-2; IC₅₀ = 65 nM).³³ From virtual screening against EGFR, the screened thiazole analog, namely 2-(benzo[4,5]imidazo[2,1-b]thiazol-3-yl)-N-(2-hydroxyphenyl) acetamide, was found to be a potent EGFR inhibitor (IC₅₀ = 55 nM) by forming a hydrogen bond with Met769 at the hinge region of EGFR-TK.³¹ Even though several thiazole derivatives have been reported to inhibit JAK2 and EGFR, the aromatic alkyl-amino analogs of thiazole (Fig. 2), possessing antibacterial and anti-cancer activities,³⁴ have not yet been studied in these two proteins.

Another interesting class is chalcones. Chalcones are open-chain flavonoids, biosynthesized in a variety of plant species.³⁵ From a chemical point of view they are 1,3-diphenyl-2-propen-1-ones, which consist of two aromatic rings linked by a three-carbon α,β -unsaturated carbonyl system.³⁵ Chalcone is a special chemical template with wide range of biological activities, among which are anti-cancer,^{36–38} anti-inflammatory,^{39–41} antioxidant,^{41,42} antimicrobial,^{43–45} anti-tubercular,⁴⁶ anti-HIV,^{47,48} antimalarial.⁴⁹ Moreover, it was mentioned in the literatures that chalcones can inhibit kinases essential for tumor cell survival and proliferation such as EGFR,^{50,51} vascular endothelial growth factor receptor-2 (VEGFR-2) and B-Raf (BRAF) kinase.^{52,53}

In this study, taking all mentioned above into account, *in vitro* cytotoxicity screening towards erythroleukemia (TF1 and HEL cells expressing JAK2) and lung carcinoma (A549 and A431 cells expressing EGFR) of thiazole-based chalcones

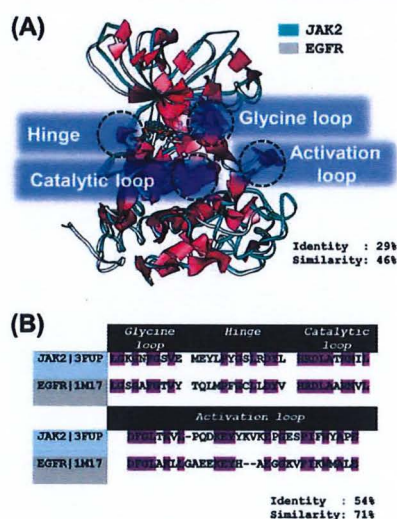


Fig. 1 (A) Superimposition between JAK2 (PDB ID: 3FUP) and EGFR (PDB ID: 1M17) crystal structures. Tofacitinib (white) and erlotinib (dark gray) are shown in a ball and stick model. The sequence alignment of the four conserved regions: catalytic loop, hinge region, glycine loop and activation loop, between JAK2 and EGFR is given in (B), in which the sequence identity is shaded in magenta.

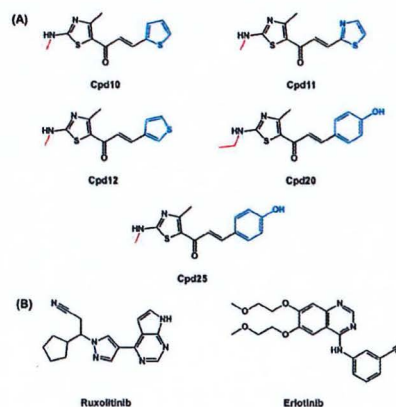


Fig. 2 Chemical structures of (A) the aromatic alkyl-amino analogs of thiazole obtained from a previous study³⁴ and (B) drugs.

Research Article

(Fig. 2) was performed. Subsequently, the kinase inhibitions of the screened compounds towards both proteins were characterized. Finally, the binding interactions at the atomic level of potent compounds were analyzed using molecular docking.

Results

Cytotoxicity

Initially, thiazole derivatives and known drugs (ruxolitinib and erlotinib) at 10 μM were subjected to *in vitro* cytotoxicity screening against TF1 and HEL cell lines expressing JAK2 as well as against A549 and A431 cell lines expressing EGFR (Fig. 3). The results revealed that the HEL erythroleukemia cell line was susceptible to compounds **11** and **12**, whereas the A431 lung cancer cell line was vulnerable to compound **25**. However, TF1 and A549 cells were not sensitive to our thiazole-based chalcone derivatives. Therefore, only these three thiazoles-based chalcones (compounds **11**, **12** and **25**) were selected to evaluate their half maximal inhibitory concentration (IC_{50}) values.

The IC_{50} values of thiazole-based chalcones and the known drugs towards the four cancer cell lines are summarized in Table 1, whereas the IC_{50} curves of these compounds are shown in Fig. S2.† The results revealed that the cytotoxic effect on TF1 cells of compounds **11** (IC_{50} of $30.23 \pm 0.53 \mu\text{M}$) and **12** (IC_{50} of $32.03 \pm 1.07 \mu\text{M}$) was lower than that of ruxolitinib (IC_{50} of $14.35 \pm 2.03 \mu\text{M}$). On the other hand, compounds **11** and **12** (IC_{50} of $\sim 7\text{--}10 \mu\text{M}$) were more susceptible to HEL cells than ruxolitinib (IC_{50} of $18.62 \pm 0.27 \mu\text{M}$) by $\sim 2\text{--}3$ times. In the case of EGFR-expressing cells, the anti-lung cancer potential of compound **25** (IC_{50} of $16.30 \pm 0.78 \mu\text{M}$ and $8.04 \pm 0.90 \mu\text{M}$ for A549 and A431, respectively) was higher ($\sim 2\text{--}6$ fold) than erlotinib used as a reference drug (IC_{50} of $47.74 \pm 6.96 \mu\text{M}$ and $28.70 \pm 6.47 \mu\text{M}$ for A549 and A431, respectively) in both cell lines. In addition, we found that the IC_{50} value of the A431 cell line treated with compound **10** (IC_{50} of $28.49 \pm 0.46 \mu\text{M}$) is similar to erlotinib ($28.70 \pm 6.47 \mu\text{M}$), while the IC_{50} value of the A549 cell line treated with compound **10** (IC_{50} of $62.09 \pm 3.30 \mu\text{M}$) is higher than erlotinib ($47.74 \pm 6.96 \mu\text{M}$). Altogether, these focused thiazole-based chalcones were then subjected to *in vitro* kinase inhibitory activity assay against the JAK2 and EGFR-TK proteins.

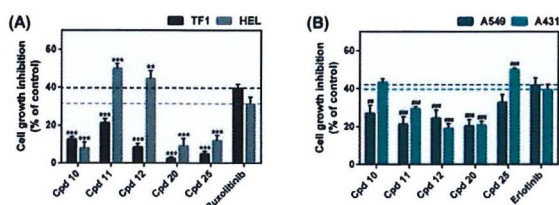


Fig. 3 Cell viability of (A) TF1 and HEL and (B) A549 and A431 cell lines treated with thiazole-based chalcones at 10 μM for 72 h. Data are represented as means \pm SEM ($n = 2$). ** $p < 0.01$, *** $p < 0.001$ vs. ruxolitinib and ## $p < 0.01$, ### $p < 0.001$ vs. erlotinib.

Table 1 The IC_{50} value of thiazole-based chalcones **11**, **12** and **25** towards TF1, HEL, A549 and A431 cancer cell lines

| Compound | IC_{50} (μM) ^a | | |
|-------------|---|-------------------|------|
| | TF1 | HEL | Vero |
| 11 | 30.23 ± 0.53^b | 6.89 ± 0.38^b | >100 |
| 12 | 32.03 ± 1.07^b | 9.96 ± 0.50^b | ND. |
| Ruxolitinib | 14.35 ± 2.03 | 18.06 ± 2.62 | >50 |
| | A549 | A431 | |
| 10 | 62.09 ± 3.30 | 28.49 ± 0.46 | >100 |
| 25 | 16.30 ± 0.78 | 8.04 ± 0.90^c | >100 |
| Erlotinib | 47.74 ± 6.96 | 28.70 ± 6.47 | >6 |

^a Data are shown as means \pm SEM ($n = 3$) and ND; not detected. ^b $p \leq 0.001$ vs. ruxolitinib. ^c $p \leq 0.05$ vs. erlotinib.

In addition, the cytotoxicity to Vero cells, which are normal kidney cells, of compounds **10**, **11** and **25** was investigated in comparison with the known drugs, ruxolitinib and erlotinib (Table 1 and Fig. S3.†). It was found that potent compounds **10**, **11** and **25** showed an IC_{50} value of >100 μM , which is higher than the drugs (>50 μM for ruxolitinib and >6 μM for erlotinib), suggesting that compounds **10**, **11** and **25** have a low toxicity against Vero cells. Note that due to the limited amount of compound **12**, its cytotoxicity towards Vero cells was not performed.

Kinase inhibition

To further support that compounds **11**, **12** and **25** can inhibit the JAK2 and EGFR-TK proteins, the kinase inhibitory activity assays were conducted in comparison to the known inhibitors (ruxolitinib and erlotinib) at 1 μM (Fig. S4.†). As shown in Fig. 4A, the kinase inhibitory activity against JAK2 of compound **11** (IC_{50} of $20.32 \pm 2.07 \text{ nM}$), compound **12** ($17.64 \pm 1.68 \text{ nM}$) and compound **25** (IC_{50} of $33.88 \pm 2.50 \text{ nM}$) was in the range of that of ruxolitinib (IC_{50} of $18.06 \pm 2.62 \text{ nM}$). In the case of EGFR-TK (Fig. 4B), only compound **25** (IC_{50} of $33.66 \pm 2.61 \text{ nM}$) inhibited EGFR-TK activity in a manner similar to erlotinib (IC_{50} of $28.46 \pm 3.09 \text{ nM}$), whereas compounds **11** (IC_{50} of $255.60 \pm 3.10 \text{ nM}$) and **12** (IC_{50} of $143.63 \pm 2.64 \text{ nM}$) showed significantly lower inhibitory activity than erlotinib.

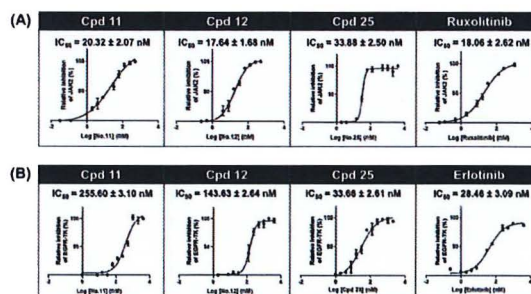


Fig. 4 Kinase inhibitory activity of thiazole-based chalcones towards (A) JAK2 and (B) EGFR-TK. Data are represented as means \pm SEM of three independent experiments.

These results suggested that compound 25 is a dual inhibitor against JAK2 and EGFR, whereas compounds 11 and 12 act as a JAK2 inhibitor (Fig. S6†).

Molecular docking

To investigate the binding mechanism of the focused thiazole derivatives (compounds 11, 12 and 25) towards JAK2 and EGFR-TK in comparison to the known drugs (ruxolitinib and erlotinib), molecular docking was conducted. We found that the fitness score of ruxolitinib in complex with JAK2 (62.13) was higher than those of compounds 11 (56.44), 12 (51.76) and compound 25 (53.57) (Fig. S5†). Similarly, the compound 25/EGFR-TK complex (30.68) gave a fitness score lower than the erlotinib/EGFR complex (36.35).

The binding pattern and the underlying interactions of all focused ligands are shown in Table S1† and Fig. 5 and 6. According to the JAK2 systems, the thiazole core of compounds 11 and 12 aligned well with the pyrrolopyrimidine ring of ruxolitinib at the ATP-binding pocket (Fig. 5A). Moreover, the nitrogen and hydrogen atoms on the thiazole ring of both compounds formed two hydrogen bonds (H-bonds) with Glu930 and Leu932 at the hinge region of JAK2 (Fig. 6A–C), while compound 25 formed H-bonds with Lys858 and Leu932, in a manner similar to ruxolitinib recognition.²⁸ The thiazole ring of compound 11 interacted with Leu855 and Gly856 at the G loop *via* amide- π stacking, while the thiophene group of compound 12 and compound 25 bound to Gly856 through π -sigma interaction. Apart from H-bonds and π interactions, van

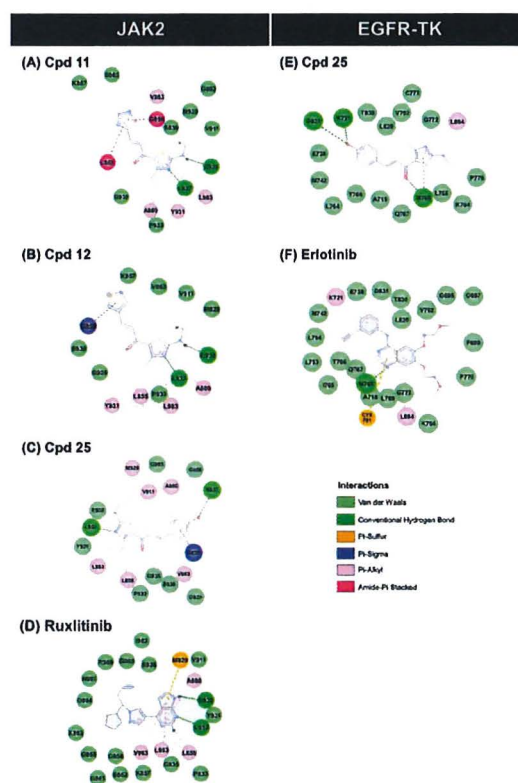


Fig. 6 2D interactions of JAK2 and EGFR-TK complexed with the thiazole-based chalcones and the known drugs. (A–D) JAK2 complexed with compounds 11, 12, 25 and ruxolitinib (E and F) EGFR-TK complexed with compounds 25 and erlotinib.

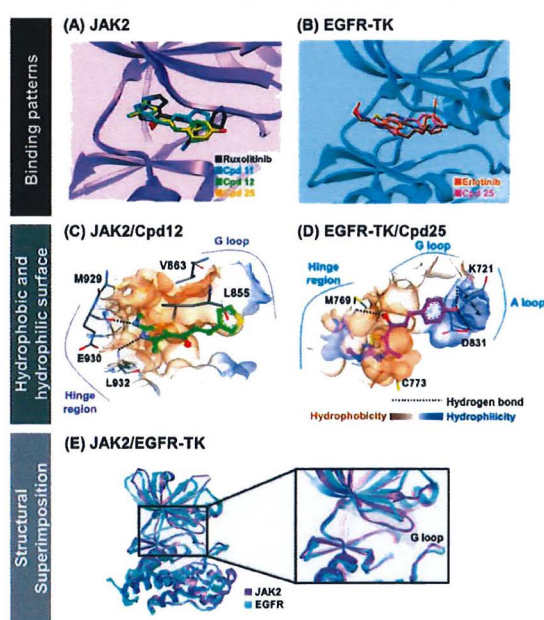


Fig. 5 (A and B) binding patterns of thiazole-based chalcones and known drugs within JAK2 and EGFR-TK. (C and D) Hydrophobic and hydrophilic surfaces of compound 12/JAK2 and compound 25/EGFR-TK complexes. (E) Structural superimposition between JAK2 and EGFR-TK, especially at the ATP-binding pocket.

der Waals (vdW) forces are also important for ligand binding (Table S1†), and the overlapped vdW contacts between the three thiazole-based chalcones and ruxolitinib were as follows: (i) hinge region: Tyr 931, Pro933, Gly935 and Ser936, (ii) G loop: Leu855, Lys857, Gly858, Ser862 and Val863 (π -alkyl), (iii) catalytic loop: Leu983 (π -alkyl), Gly993 and (iv) other regions: Ala880 near the G-loop (π -alkyl) and Val911 near the hinge region.

In the case of compound 25 complexed with EGFR-TK, its thiazole core occupied the hinge region similar to compounds 11, 12 and 25 complexed with JAK2 (Fig. 5A), and overlapped with the quinazoline ring of erlotinib (Fig. 5B). Interestingly, this thiazole analog shared H-bond formation with erlotinib at the hinge region residue Met769 (Fig. 6D and E).⁵⁴ In addition, the hydroxyl group of the phenol ring of compound 25 could form a H-bond with other residues, including Lys721 near the glycine loop. The matched vdW contacts between compound 25 and EGFR-TK were as follows: (i) hinge region: Thr766, Gln767, Leu768, Pro770 and G772, (ii) G loop: Leu694 (π -alkyl), Val702 and Lys704, (iii) catalytic loop: L820 and (iv) other regions: near the G loop (Ala719, Glu738, Met742 and Leu764) and near the activation loop (Thr830).

We further investigated the size of the ligand-binding pocket between JAK2 and EGFR by generating the protein

hydrophobic and hydrophilic surfaces around compounds **12** and **25** (Fig. 5C and D). The results showed that the ATP-binding pocket of JAK2 was smaller than that of EGFR, since the glycine loop of JAK2 was positioned closer to the hinge region than EGFR (Fig. 5E).

Drug-likeness prediction

The potent thiazole-based chalcones against JAK2 and EGFR-TK were further analyzed in terms of drug-likeness by assessing their physicochemical properties (*i.e.*, molecular weight (MW), the numbers of hydrogen bond donors (HBD) and acceptors (HBA), rotatable bond (RB), polar surface area (PSA) and $\text{Log } P$) derived from Lipinski's rule of five (Table 2). The obtained result revealed that compounds **11**, **12** and **25** showed the acceptable value within the criteria of the rules as follows: (i) molecular weight ≤ 500 Da, (ii) hydrogen bond donors ≤ 5 and hydrogen acceptors ≤ 10 , (iii) rotatable bond ≤ 10 , (iv) polar surface area ≤ 140 Å and (v) lipophilicity (expressed as $\text{Log } P$) ≤ 5 .⁵⁵ Therefore, these compounds could likely be developed as promising novel JAK2 and EGFR-TK inhibitors.

Discussion

The thiazole-based chalcones have been previously reported to exhibit antimicrobial and anti-tumor activities,³⁵ and other thiazole derivatives have shown anti-cancer activity against several types of cancer and have been identified as JAK2 and EGFR inhibitors. Therefore, we expected that thiazole-based chalcones can inhibit JAK2 and EGFR-TK activity. Considering the data from the *in vitro* cytotoxic activity of the five thiazole-based chalcone derivatives against erythroleukemia and lung cancer cell lines, we found that compounds **11** and **12** were more susceptible to mutant JAK2-expressing HEL cells rather than the wild-type JAK2-expressing TF1, since the V617F point mutation in JAK2 maintains its open conformation at the activation loop,^{56,57} resulting in higher ligand accommodation.^{58,59} In the case of EGFR-expressing cell lines, only compound **25** significantly inhibited the A431 lung cancer cell line, whereas A549 cells were not sensitive to all thiazole derivatives. In addition, compound **10** showed cytotoxicity to A431 higher than A549. This is because (i) the EGFR expression level found in A431 cells is dramatically higher than that found in A549⁶⁰ and (ii) A549 cells exhibits KRAS mutation, which constitutively activates downstream MAPK signalling pathways, causing a

compensatory mechanism.⁶¹ The cytotoxic effect on cancer cell lines of these thiazole derivatives was due to their inhibitory activity against JAK2 and EGFR-TK, in a manner similar to the known inhibitors (Fig. 4). In addition, both compounds **11** and **25** showed higher IC_{50} than the known drugs in normal kidney Vero cells, suggesting that these thiazole derivatives could be safe for these normal cells, which is consistent with a previous report showing that the cytotoxic effect of thiazole-indenoquinoxaline on normal human cells (WI-38, fibroblast) gave high IC_{50} (>107 μM).⁶² Furthermore, compounds **11** and **12** showed kinase inhibitory activity against JAK2 higher than EGFR, whereas compound **25** inhibited both proteins at a similar level (Fig. 4), indicating that compound **25** acts as a dual inhibitor, and compounds **11** and **12** are JAK2 inhibitors. However, the results from the cell-based assay were inconsistent with kinase inhibition in which compounds **11** and **12** were potent against JAK2-expressing cells, whereas compounds **25** showed good inhibitory activity towards EGFR-expressing cells. This is because cells have several factors involved in cell growth inhibition such as cell permeability and compound degradation within the cell.⁶³ Therefore, compounds with good inhibitory activity from both kinase inhibition and cell-based inhibition were selected to study the binding patterns at the atomic level.

Although the fitness score of compounds **11** and **12** in complex with JAK2 as well as compound **25** in complex with EGFR was lower than that of the known inhibitors, their ligand-protein interactions are similar. It has been reported that the pyrrolopyrimidine moiety of ruxolitinib forms H-bonds with Glu930 and Leu932 of JAK2.⁶⁴⁻⁶⁶ In agreement with this evidence, the thiazole core of compounds **11** and **12** interacted with Glu930 and Leu932 residues at the hinge region of JAK2 *via* hydrogen bonding. The noncovalent pi-alkyl interaction is one of the most important contributions to protein-ligand complexation,⁶⁷ and the glycine loop residues Ala880, Val863 and Leu855 as well as the catalytic residues Leu983 of JAK2 were found to stabilize both thiazoles through pi-alkyl interaction, in correspondence with the reported ATP binding to JAK2, showing that its adenine and ribose moiety are embedded in pockets stabilized by hydrophobic interactions.⁶⁴ The thiazole core of compound **25** points into the hinge region, which is a hydrophobic pocket similar to compounds **11** and **12** within JAK2, while its polar phenol group embedded between the

Table 2 Predicted Lipinski's rule of five for the thiazole-based chalcones and the known drugs. HBD, hydrogen bond donor; HBA, hydrogen bond acceptor; PSA, polar surface area

| Compound | Lipinski's rule of five | | | | | $\text{Log } P$ (≤ 5) | Drug-likeness |
|-------------|-------------------------|------------------|-------------------|------------------------------|---------------------|------------------------------|---------------|
| | MW (≤ 500 Da) | HBD (≤ 5) | HBA (≤ 10) | Rotatable bond (≤ 10) | PSA (≤ 140 Å) | | |
| 11 | 265.35 | 1 | 3 | 4 | 111.36 | 2.47 | Yes |
| 12 | 264.37 | 1 | 2 | 4 | 98.47 | 3.08 | Yes |
| 25 | 274.34 | 2 | 3 | 4 | 90.46 | 2.65 | Yes |
| Ruxolitinib | 306.37 | 1 | 4 | 4 | 83.18 | 2.40 | Yes |
| Erlotinib | 393.44 | 1 | 6 | 10 | 74.73 | 3.20 | Yes |

glycine loop and catalytic loop, which are hydrophilic regions (*e.g.* Asp831 and Lys721).⁶⁸ It has been reported that the *p*-OH group on the phenyl ring of thiazole derivatives can increase the anti-cancer potential.⁶⁹ In accordance with this evidence, the *p*-OH group of compound 25 forms H-bonds with Lys721 near the glycine loop and Asp831 at the activation loop, resulting in higher anti-lung cancer activity than the other analogs (Fig. 3B).

The hinge, deep in the ATP pocket, is an important region called the 'gatekeeper', which controls the access to the 'back-pocket' of the kinase.⁷⁰ The ATP-binding pocket of EGFR was quite larger than that of JAK2; therefore, compound 25 is suitable for EGFR because its phenol moiety at the R₂ position is bulkier than the thiazole/thiophene ring of compounds 11 and 12. This explains why the same series of thiazole derivatives could bind to the different target proteins. Numerous FDA approved drugs consist of a nitrogen-based heterocyclic moiety (*e.g.*, pyrrolopyrimidine for JAK2 inhibitors and quinazolinamine rings for EGFR-TK inhibitors) similar to the adenosine ring of the ATP substrate, which occupies the hydrophobic pocket and forms H-bonds with the hinge region.^{65,71} Therefore, the aromatic alkyl-amino analogs of thiazole-based chalcones in this study could be used as an ATP-competitive inhibitors against JAK2 and EGFR, since they contain the nitrogen-based heterocyclic ring similar to that of ATP and the known kinase inhibitors. Furthermore, all of the potent compounds showed good drug-like physicochemical properties, suggesting that these three thiazole-based chalcones could likely be developed as novel anti-cancer drugs.

Conclusions

In this study, we combined experimental and computational studies to identify novel JAK2 and EGFR inhibitors. *In vitro* cytotoxicity screening results showed that the HEL erythroleukemia cell line was susceptible to compounds 11 and 12, whereas the A431 lung cancer cell line was vulnerable to compound 25. The cytotoxic effect on cancer cell lines of these thiazole-based chalcone derivatives was due to their inhibitory activity against JAK2 and EGFR-TK. From binding interaction analysis, it was found that compounds 11 and 12 formed H-bonds with Leu932 and Glu930 and hydrophobically came into contact with Leu983 at the catalytic site of JAK2, whereas compound 25 formed hydrogen bonds within the ATP-binding pocket of EGFR at Met769 (hinge region), Lys721 (near glycine loop) and Asp831 (activation loop). The bulkiness of the phenol moiety at the R₂ position of compound 25 led to the higher selectivity toward EGFR-TK than compounds 11 and 12. All of the potent thiazole derivatives followed Lipinski's rule of five. Altogether, our study successfully identified novel JAK2 and EGFR inhibitors from the aromatic alkyl-amino analogs of thiazole, which can be used as promising starting points for subsequent drug discovery programs against erythroleukemia and lung cancer.

Materials and methods

Cell lines and chemical reagents

The human erythroleukemia HEL 92.1.7 (ATCC TIB-180) and TF1 (ATCC CRL-2003), and lung carcinoma A549 (ATCC CCL-185) and A431 (ATCC CRL-1555) cell lines, and monkey (*Cercopithecus aethiops*) kidney Vero cell line (ATCC CCL-81) were purchased from the American Type Cell Culture Collection (ATCC, Manassas, VA, USA). Roswell Park Memorial Institute (RPMI), Dulbecco's modified Eagle's medium (DMEM), fetal bovine serum (FBS), penicillin-streptomycin (Pen-Strep), granulocyte-macrophage colony-stimulating factor (GM-CSF) and trypsin were purchased from Life Technologies (California, USA). 3-(4,5-Dimethylthiazol-2-yl)-2,5-diphenyltetrazolium bromide (MTT), dimethyl sulfoxide (DMSO) and JAK2 (SRP0171) were purchased from Sigma-Aldrich (Darmstadt, Germany). PrestoBlue™ cell viability reagent was purchased from Thermo Fisher Scientific (Waltham, MA, USA). The ADP-Glo™ kinase assay kit was purchased from Promega (Wisconsin, USA). Poly (glutyr) peptide (P61-58) was purchased from SignalChem Biotech (Canada). EGFR-TK was obtained from a previous report.⁷² A series of thiazole compounds were kindly provided by Dr. Athina Geronikaki from the Aristotle University of Thessaloniki.³⁴ Note that due to limited amounts of thiazole-based chalcones obtained from a previous study,³⁴ we performed JAK2 and EGFR kinase and cytotoxicity assays as well as a binding pattern study at the molecular level on only five thiazole derivatives (Fig. 2 and ESI† section 7).

Cell cultures

The TF1 cells were grown in complete RPMI-1640 medium supplemented with 10% (v/v) FBS, 100 U mL⁻¹ penicillin, 100 µg mL⁻¹ streptomycin and 2 ng mL⁻¹ GM-CSF. The HEL cells were grown in complete RPMI-1640 medium supplemented with 10% (v/v) FBS, 100 U mL⁻¹ penicillin and 100 µg mL⁻¹ streptomycin. The A549, A431 and Vero cells were grown in complete DMEM medium supplemented with 10% (v/v) FBS, 100 U mL⁻¹ penicillin and 100 µg mL⁻¹ streptomycin. All cells were maintained at 37 °C in a 5% (v/v) CO₂, 95% (v/v) air humidified incubator.

Cytotoxicity in cancer cell lines

The *in vitro* cytotoxicity activity of thiazole derivatives against the TF1 and HEL cells, which are suspension cells, was assessed using the Presto Blue assay, while A549 and A431 cell lines, which are adherent cells, were evaluated using the MTT assay. For preliminary screening, 100 µL of TF1 (50 000 cells per well), HEL (25 000 cells per well), A549 (5000 cells per well) and A431 (5000 cells per well) cell suspension was seeded per well in a 96-well microplate and incubated at 37 °C overnight, and the cells were treated with compounds and known drugs (ruxolitinib and erlotinib) at 10 µM. Then, incubated for 72 h. Subsequently, 10 µL of Presto Blue reagent was added in TF1 and HEL cells and incubated at 37

Research Article

°C for 1 h. The absorbance of the resorufin product was measured. The MTT solution (5 mg mL⁻¹) was added into A549 and A431 cells and incubated at 37 °C for 3 h. The medium was removed, and 50 µL of DMSO was added to each well to lyse the cells and solubilized the formazan crystals. Finally, the absorbance was measured at 570 nm using a microplate reader (Infinite M200 microplate reader, Tecan, Männedorf, Switzerland). Each experiment was performed in duplicate. After screening, the compounds displaying a percentage of cell viability at 10 µM <50 were selected to determine their IC₅₀ value.

In addition, the cytotoxicity of the thiazole derivatives against normal Vero cells (2000 cells per well) was also investigated using the MTT assay.

Kinase inhibition of JAK2 and EGFR-TK

The tyrosine kinase inhibitory activity of JAK2 and EGFR-TK was performed using the ADP-Glo™ kinase assay as previously reported.^{51,72} The first 8 µL of buffer (40 mM Tris-HCl pH 7.5, 20 mM MgCl₂ and 0.1 mg mL⁻¹ bovine serum albumin) was added to a 384-well plate. Then, 5 µL of enzymes (2.5 ng µL⁻¹ for JAK2 and 1.25 ng µL⁻¹ for EGFR) and 2 µL of inhibitors were added, followed by 10 µL of a mixture of 5 µM ATP and 2.5 µM poly(glu-tyr), and incubated for 1 h at room temperature. Next, 5 µL of the ADP-Glo reagent was added and incubated for 40 min. After that, 10 µL of kinase detection reagent was added and incubated at room temperature for 30 min to convert ADP to ATP. ATP was then detected by measuring the luminescence using a microplate reader (Infinite M200 microplate reader, Tecan, Männedorf, Switzerland). All assays were performed in triplicate. The relative inhibition (%) of inhibitors was then calculated and compared to the control with no inhibitor as shown in eqn (1);

$$\begin{aligned} \text{\% Relative inhibition} & \quad (1) \\ & = \frac{[(\text{positive} - \text{negative}) - (\text{sample} - \text{negative})]}{(\text{positive} - \text{negative})} \times 100 \end{aligned}$$

Statistical analysis

The data are represented as mean ± standard error of the mean (SEM). Differences between groups were compared using one-way ANOVA, followed by Tukey's test for multiple comparisons. An independent *t*-test was used for comparison differences between pairing values. The differences in means were determined at the confidence level *P* ≤ 0.05.

Molecular docking

The crystal structures of JAK2 complexed with tofacitinib (PDB ID: 3FUP)⁷³ and EGFR complexed with erlotinib (PDB ID: 1M17)⁷¹ were downloaded from the Protein Data Bank. These structures were chosen because both of them were crystalized with the known drugs. The missing residues of JAK2 (residues 920-923) were built using the SWISS-MODEL server.⁷⁴ The 3D structure of the drugs (ruxolitinib and

erlotinib) were obtained from the ZINC database, whilst the 3D structure of compounds 11, 12 and 25 were generated using the Gaussian 09 program. All the ligands were optimized using the Gaussian 09 program (HF/6-31d) as per the standard protocol.⁷⁵⁻⁷⁷ The protonation state of all studied ligands was characterized using the ChemAxon.⁷⁸

For system validation, the crystalized ligands were defined as a center in the active site for redocking using GOLD programs which are based on genetic algorithm (GA),⁷⁹ and the results are shown in ESI Fig. S1.† The docking protocols were as follows: (i) the JAK2 system was set as 12 Å for sphere docking and GOLD score and ChemScore (rescore) for the scoring function; (ii) the EGFR system was set as 15 Å for sphere docking and ChemScore for the scoring function. All systems were used as 100 docking poses. The binding between proteins and compounds/drugs was visualized using the UCSF Chimera package⁸⁰ and Accelrys Discovery Studio 2.5 (Accelrys Inc.).

Physicochemical predictions

Physicochemical features such as hydrogen bond donors, hydrogen bond acceptors and drug-likeness play an important role in drug discovery and development.⁸¹ Herein, such properties of the potent compounds 11, 12 and 25 were calculated in comparison with drugs (ruxolitinib and erlotinib) using web-based application SwissADME (www.swissadme.ch/).⁸²

Conflicts of interest

There are no conflicts to declare.

Acknowledgements

This work was financially supported by the Ratchadaphiseksomphot Endowment Fund (Grant No. CU_GR_62_96_23_35 for T. R.) and the Thailand Research Fund (DBG6080007 for K.C.). K. S. thanks the Science Achievement Scholarship of Thailand. T. A. acknowledges the 90th Anniversary of Chulalongkorn University Fund (Ratchadaphiseksomphot Endowment Fund). P. Mai. thanks Chulalongkorn University for a short-term visit grant.

Notes and references

- 1 R. J. DeBerardinis, *Genet. Med.*, 2008, **10**, 267-277.
- 2 R. L. Siegel, K. D. Miller and A. Jemal, *Ca-Cancer J. Clin.*, 2019, **69**, 7-34.
- 3 World Health Organization. Cancer. Available online: <http://www.who.int/en/news-room/factsheets/detail/cancer> (accessed on 12 September 2018), 2018.
- 4 A. Dowlati, D. Nethery and J. A. Kern, *Mol. Cancer Ther.*, 2004, **3**, 459-463.
- 5 P. Xu, P. Shen, B. Yu, X. Xu, R. Ge, X. Cheng, Q. Chen, J. Bian, Z. Li and J. Wang, *Eur. J. Med. Chem.*, 2020, **192**, 112155.

- 6 J. J. O'Shea, M. Gadina and R. D. Schreiber, *Cell*, 2002, **109**, S121–S131.
- 7 C. Schindler, D. E. Levy and T. Decker, *J. Biol. Chem.*, 2007, **282**, 20059–20063.
- 8 E. Parganas, D. Wang, D. Stravopodis, D. J. Topham, J. C. Marine, S. Teglund, E. F. Vanin, S. Bodner, O. R. Colamonici, J. M. van Deursen, G. Grosveld and J. N. Ihle, *Cell*, 1998, **93**, 385–395.
- 9 K. J. Morgani and D. G. Gilliland, *Annu. Rev. Med.*, 2008, **59**, 213–222.
- 10 R. L. Levine, M. Wadleigh, J. Cools, B. L. Ebert, G. Wernig, B. J. P. Huntly, T. J. Boggon, L. Wlodarska, J. J. Clark, S. Moore, J. Adelsperger, S. Koo, J. C. Lee, S. Gabriel, T. Mercher, A. D'Andrea, S. Frohling, K. Dohner, P. Marynen, P. Vandenberghe, R. A. Mesa, A. Tefferi, J. D. Griffin, M. J. Eck, W. R. Sellers, M. Meyerson, T. R. Golub, S. J. Lee and D. G. Gilliland, *Cancer Cell*, 2005, **7**, 387–397.
- 11 T. Holbro and N. E. Hynes, *Annu. Rev. Pharmacol. Toxicol.*, 2004, **44**, 195–217.
- 12 K. Choowongkamon, C. R. Carlin and F. D. Sonnichsen, *J. Biol. Chem.*, 2005, **280**, 24043–24052.
- 13 S. Oliveira, P. M. P. Bergen en Henegouwen, G. Storm and R. Schiffelers, *Expert Opin. Biol. Ther.*, 2006, **6**, 605–617.
- 14 J. Schlessinger, *Cell*, 2002, **110**, 669–672.
- 15 P. Mahalapbutr, P. Wonganan, W. Chavasiri and T. Rungrotmongkol, *Cancers*, 2019, **11**, 437, DOI: 10.3390/cancers11040437.
- 16 G. da Cunha Santos, F. A. Shepherd and M. S. Tsao, *Annu. Rev. Pathol.: Mech. Dis.*, 2011, **6**, 49–69.
- 17 E. O. Hexner, C. Serdikoff, M. Jan, C. R. Swider, C. Robinson, S. Yang, T. Angeles, S. G. Emerson, M. Carroll, B. Ruggeri and P. Dobrzanski, *Blood*, 2008, **111**, 5663–5671.
- 18 A. Pardnani, T. Lasho, G. Smith, C. J. Burns, E. Fantino and A. Tefferi, *Leukemia*, 2009, **23**, 1441–1445.
- 19 S. Verstovsek, R. A. Mesa, M. E. Salama, L. Li, C. Pitou, F. P. Nunes, G. L. Price, J. L. Giles, D. N. D'Souza, R. A. Walgren and J. T. Prchal, *Leuk. Res.*, 2017, **61**, 89–95.
- 20 M. H. Cohen, J. R. Johnson, Y. F. Chen, R. Sridhara and R. Pazdur, *Oncologist*, 2005, **10**, 461–466.
- 21 T. S. Mok, Y. L. Wu, S. Thongprasert, C. H. Yang, D. T. Chu, N. Saijo, P. Sunpaweravong, B. Han, B. Margono, Y. Ichinose, Y. Nishiwaki, Y. Ohe, J. J. Yang, B. Chewaskulyong, H. Jiang, E. L. Duffield, C. L. Watkins, A. A. Armour and M. Fukuoka, *N. Engl. J. Med.*, 2009, **361**, 947–957.
- 22 A. Quintas-Cardama, K. Vaddi, P. Liu, T. Manshouri, J. Li, P. A. Scherle, E. Caulder, X. Wen, Y. Li, P. Waeltz, M. Rupa, T. Burn, Y. Lo, J. Kelley, M. Covington, S. Shepard, J. D. Rodgers, P. Haley, H. Kantarjian, J. S. Fridman and S. Verstovsek, *Blood*, 2010, **115**, 3109–3117.
- 23 H. H. Wan, G. M. Schroeder, A. C. Hart, J. Inghrim, J. Grebinski, J. S. Tokarski, M. V. Lorenz, D. You, T. McDevie, B. Penhallow, R. Vuppugalla, Y. P. Zhang, X. M. Gu, R. Iyer, L. J. Lombardo, G. L. Trainor, S. Ruepp, J. Lippy, Y. Blat, J. S. Sack, J. A. Khan, K. Stefanski, B. Slezcka, A. Mathur, J. H. Sun, M. K. Wong, D. R. Wu, P. Li, A. Gupta, P. N. Arunachalam, B. Pragalathan, S. Narayanan, K. C. Nanjundaswamy, P. Kuppusamy and A. V. Purandare, *ACS Med. Chem. Lett.*, 2015, **6**, 850–855.
- 24 W. Liu, J. F. Ning, Q. W. Meng, J. Hu, Y. B. Zhao, C. Liu and L. Cai, *Drug Des., Dev. Ther.*, 2015, **9**, 3837–3851.
- 25 N. Reguart, A. F. Cardona and R. Rosell, *Cancer Manage. Res.*, 2010, **2**, 143–156.
- 26 R. A. Mesa, J. Gotlib, V. Gupta, J. V. Catalano, M. W. Deininger, A. L. Shields, C. B. Miller, R. T. Silver, M. Talpaz, E. F. Winton, J. H. Harvey, T. Hare, S. Erickson-Viitanen, W. Sun, V. Sandor, R. S. Levy, H. M. Kantarjian and S. Verstovsek, *J. Clin. Oncol.*, 2013, **31**, 1285–1292.
- 27 A. B. Methvin and R. E. Gausas, *Ophthalmic Plast. Reconstr. Surg.*, 2007, **23**, 63–65.
- 28 M. Kesarwani, E. Huber, Z. Kincaid, C. R. Evelyn, J. Biesiada, M. Rance, M. B. Thapa, N. P. Shah, J. Meller, Y. Zheng and M. Azam, *Sci. Rep.*, 2015, **5**, 14538.
- 29 C. H. Yun, K. E. Mengwasser, A. V. Toms, M. S. Woo, H. Greulich, K. K. Wong, M. Meyerson and M. J. Eck, *Proc. Natl. Acad. Sci. U. S. A.*, 2008, **105**, 2070–2075.
- 30 Y. L. Chen, C. C. Lin, S. C. Yang, W. L. Chen, J. R. Chen, Y. H. Hou, C. C. Lu, N. H. Chow, W. C. Su and C. L. Ho, *Front. Oncol.*, 2019, **9**, 1–8.
- 31 X. Deng, X. Tan, T. An, Q. Ma, Z. Jin, C. Wang, Q. Meng and C. Hu, *Molecules*, 2019, **24**, 1–13.
- 32 Y. Jin, K. Ding, D. Wang, M. Shen and J. Pan, *Cancer Lett.*, 2014, **353**, 115–123.
- 33 A. C. Hart, G. M. Schroeder, H. Wan, J. Grebinski, J. Inghrim, J. Kempson, J. Guo, W. J. Pitts, J. S. Tokarski, J. S. Sack, J. A. Khan, J. Lippy, M. V. Lorenzi, D. You, T. McDevitt, R. Vuppugalla, Y. Zhang, L. J. Lombardo, G. L. Trainor and A. V. Purandare, *ACS Med. Chem. Lett.*, 2015, **6**, 845–849.
- 34 C. Tratat, M. Haroun, I. Xenikakis, K. Liaras, E. Tsolaki, P. Eleftheriou, A. Petrou, B. Aldhubiab, M. Attimarad, K. N. Venugopala, S. Harsha, H. S. Elsewedy, A. Geronikaki and M. Sokovic, *Curr. Top. Med. Chem.*, 2019, **19**, 356–375.
- 35 B. Orlikova, D. Tasdemir, F. Golais, M. Dicato and M. Diederich, *Genes Nutr.*, 2011, **6**, 125–147.
- 36 C. Karthikeyan, N. S. H. Moorthy, S. Ramasamy, U. Vanam, M. Elangovan, D. Karunakaran and P. Trivedi, *Recent Pat. Anti-Cancer Drug Discovery*, 2014, **10**, 97–115.
- 37 G. Wang, W. Liu, Z. Gong, Y. Huang, Y. Li and Z. Peng, *J. Enzyme Inhib. Med. Chem.*, 2020, **35**, 139–144.
- 38 S. Madhavi, R. Sreenivasulu, J. P. Yazala and R. R. Raju, *Saudi Pharm. J.*, 2017, **25**, 275–279.
- 39 H. Ur Rashid, Y. Xu, N. Ahmad, Y. Muhammad and L. Wang, *Bioorg. Chem.*, 2019, **87**, 335–365.
- 40 J. Wu, J. Li, Y. Cai, Y. Pan, F. Ye, Y. Zhang, Y. Zhao, S. Yang, X. Li and G. Liang, *J. Med. Chem.*, 2011, **54**, 8110–8123.
- 41 K. R. Abdellatif, H. A. Elshemy, S. A. Salama and H. A. Omar, *J. Enzyme Inhib. Med. Chem.*, 2015, **30**, 484–491.
- 42 J. Wang, L. Huang, C. Cheng, G. Li, J. Xie, M. Shen, Q. Chen, W. Li, W. He, P. Qiu and J. Wu, *Acta Pharm. Sin. B*, 2019, **9**, 335–350.
- 43 W. Dan and J. Dai, *Eur. J. Med. Chem.*, 2020, **187**, 111980.
- 44 E. J. Henry, S. J. Bird, P. Gowland, M. Collins and J. P. Cassella, *J. Antibiot.*, 2020, **73**, 299–308.

- 45 S. Burmaoglu, O. Algul, A. Gobek, D. Aktas Anil, M. Ulger, B. G. Erturk, E. Kaplan, A. Dogen and G. Aslan, *J. Enzyme Inhib. Med. Chem.*, 2017, **32**, 490–495.
- 46 R. Anandam, S. S. Jadav, V. B. Ala, M. J. Ahsan and H. B. Bollikolla, *Med. Chem. Res.*, 2018, **27**, 1690–1704.
- 47 H. A. Al-Hazam, Z. A. Al-Shamkani, N. A. Al-Masoudi, B. A. Saeed and C. Pannecouque, *Z. Naturforsch., B: J. Chem. Sci.*, 2017, **72**, 249–256.
- 48 A. L. Cole, S. Hossain, A. M. Cole and O. T. Phanstiel, *Bioorg. Med. Chem.*, 2016, **24**, 2768–2776.
- 49 J. Syahri, E. Yuanita, B. A. Nurohmah, R. Armunanto and B. Purwono, *Asian Pac. J. Trop. Biomed.*, 2017, **7**, 675–679.
- 50 M. Al-Anazi, B. O. Al-Najjar and M. Khairuddean, *Molecules*, 2018, **23**, 1–14.
- 51 K. Sangpheak, L. Tabtimmai, S. Seetaha, C. Rungnim, W. Chavasiri, P. Wolschann, K. Choowongkamon and T. Rungrotmongkol, *Molecules*, 2019, **24**, 1092.
- 52 S. U. Rizvi, H. L. Siddiqui, M. Nisar, N. Khan and I. Khan, *Bioorg. Med. Chem. Lett.*, 2012, **22**, 942–944.
- 53 Q. S. Li, C. Y. Li, X. Lu, H. Zhang and H. L. Zhu, *Eur. J. Med. Chem.*, 2012, **50**, 288–295.
- 54 J. H. Park, Y. T. Liu, M. A. Lemmon and R. Radhakrishnan, *Biochem. J.*, 2012, **448**, 417–423.
- 55 C. A. Lipinski, *Drug Discovery Today: Technol.*, 2004, **1**, 337–341.
- 56 T.-S. Lee, W. Ma, X. Zhang, H. Kantarjian and M. Albitar, *BMC Struct. Biol.*, 2009, **9**, 58.
- 57 T. S. Lee, W. Ma, X. Zhang, F. Giles, H. Kantarjian and M. Albitar, *Cancer*, 2009, **115**, 1692–1700.
- 58 H. Quentmeier, R. A. MacLeod, M. Zaborski and H. G. Drexler, *Leukemia*, 2006, **20**, 471–476.
- 59 E. Senkevitch and S. Durum, *Cytokine+*, 2017, **98**, 33–41.
- 60 W. J. Liu, X. J. Liu, J. Xu, L. Li, Y. Li, S. H. Zhang, J. L. Wang, Q. F. Miao and Y. S. Zhen, *Acta Pharmacol. Sin.*, 2018, **39**, 1777–1786.
- 61 A. Demiray, A. Yaren, N. Karagenc, F. Bir, A. G. Demiray, E. R. Karagur, O. Tokgun, L. Elmas and H. Akca, *Balk. J. Med. Genet.*, 2018, **21**, 21–26.
- 62 E. A. Fayed, Y. A. Ammar, A. Ragab, N. A. Gohar, A. B. M. Mehany and A. M. Farrag, *Bioorg. Chem.*, 2020, **100**, 103951.
- 63 G. Housman, S. Byler, S. Heerboth, K. Lapinska, M. Longacre, N. Snyder and S. Sarkar, *Cancers*, 2014, **6**, 1769–1792.
- 64 T. E. Lin, W. C. HuangFu, M. W. Chao, T. Y. Sung, C. D. Chang, Y. Y. Chen, J. H. Hsieh, H. J. Tu, H. L. Huang, S. L. Pan and K. C. Hsu, *Front. Pharmacol.*, 2018, **9**, 1–14.
- 65 M. Kesarwani, E. Huber, Z. Kincaid, C. R. Evelyn, J. Biesiada, M. Rance, M. B. Thapa, N. P. Shah, J. Meller, Y. Zheng and M. Azam, *Sci. Rep.*, 2015, **5**, 1–19.
- 66 T. Zhou, S. Georgeon, R. Moser, D. J. Moore, A. Caflisch and O. Hantschel, *Leukemia*, 2014, **28**, 471–472.
- 67 H. A. Toupanloo and Z. Rahmani, *Appl. Biol. Chem.*, 2018, **61**, 209–226.
- 68 J. C. Biro, *Theor. Biol. Med. Modell.*, 2006, **3**, 15.
- 69 P. Arora, R. Narang, S. K. Nayak, S. K. Singh and V. Judge, *Med. Chem. Res.*, 2016, **25**, 1717–1743.
- 70 D. Fabbro, S. W. Cowan-Jacob and H. Moebitz, *Br. J. Pharmacol.*, 2015, **172**, 2675–2700.
- 71 J. Stamos, M. X. Sliwkowski and C. Eigenbrot, *J. Biol. Chem.*, 2002, **277**, 46265–46272.
- 72 S. Seetaha, S. Ratanabanyong and K. Choowongkamon, *Appl. Microbiol. Biotechnol.*, 2019, **103**, 8427–8438.
- 73 N. K. Williams, R. S. Bamert, O. Patel, C. Wang, P. M. Walden, A. F. Wilks, E. Fantino, J. Rossjohn and I. S. Lucet, *J. Mol. Biol.*, 2009, **387**, 219–232.
- 74 A. Waterhouse, M. Bertoni, S. Bienert, G. Studer, G. Tauriello, R. Gummienny, F. T. Heer, T. A. P. de Beer, C. Rempfer, L. Bordoli, R. Lepore and T. Schwede, *Nucleic Acids Res.*, 2018, **46**, W296–W303.
- 75 P. Mahalapbutr, K. Thitinthavet, T. Kedkham, H. Nguyen, L. t. h. Theu, S. Dokmaisrijan, L. Huynh, N. Kungwan and T. Rungrotmongkol, *J. Mol. Struct.*, 2019, **1180**, 480–490.
- 76 P. Mahalapbutr, N. Darai, W. Panman, A. Opasmahakul, N. Kungwan, S. Hannongbua and T. Rungrotmongkol, *Sci. Rep.*, 2019, **9**, 10205.
- 77 K. Sanachai, P. Mahalapbutr, K. Choowongkamon, R. P. Poo-Arporn, P. Wolschann and T. Rungrotmongkol, *ACS Omega*, 2020, **5**, 369–377.
- 78 Marvin was used for drawing, displaying and characterizing chemical structures, substructures and reactions, Marvin 17.21.0, ChemAxon (<https://www.chemaxon.com>).
- 79 G. Jones, P. Willett, R. C. Glen, A. R. Leach and R. Taylor, *J. Mol. Biol.*, 1997, **267**, 727–748.
- 80 E. F. Pettersen, T. D. Goddard, C. C. Huang, G. S. Couch, D. M. Greenblatt, E. C. Meng and T. E. Ferrin, *J. Comput. Chem.*, 2004, **25**, 1605–1612.
- 81 F. Cheng, W. Li, Y. Zhou, J. Shen, Z. Wu, G. Liu, P. W. Lee and Y. Tang, *J. Chem. Inf. Model.*, 2012, **52**, 3099–3105.
- 82 A. Daina, O. Michielin and V. Zoete, *Sci. Rep.*, 2017, **7**, 1–13.

**Source of lower anticancer-drug susceptibility due to
T790M/L858R EGFR mutation: Molecular dynamics and
principle component analysis**

Phakawat Chusuth¹, Supot Hannongbua², Thanyada Rungrotmongkol^{1,3}

¹Biocatalyst and Environmental Biotechnology Research unit, Department of Biochemistry,
Faculty of Science, Chulalongkorn University, Bangkok 10330, Thailand

²Computational Chemistry Center of Excellent, Department of Chemistry, Faculty of Science,
Chulalongkorn University, Bangkok 10330, Thailand

³Program in Bioinformatics and Computational Biology, Faculty of Science, Chulalongkorn
University, Bangkok 10330, Thailand

Email: thanyada.r@chula.ac.th, t.rungrotmongkol@gmail.com

Phone: +66-2218-5426. Fax: +66-2218-5418.

Abstract

Tyrosine kinase (TK) domain of epidermal growth factor receptor (EGFR) is the intracellular domain, which is phosphorylated by using ATP as the substrate when the receptor is activated. The downstream signaling cascades, such as Ras/Raf/MAPK and PI3K/AKT pathways, are subsequently stimulated. These pathways regulate cell growth and cell proliferation. The secondary T790M point mutation in the EGFR TK domain co-occurred with pre-existing L858R mutation causes drug resistance in cancer patients. Herein, all-atom molecular dynamics (MD) simulations are employed to investigate the precise role of this secondary mutation causing a high level of resistance to erlotinib. At the same time, principal component analysis (PCA) is used to reveal the change in protein motion due to such mutation. As a result, the secondary mutation has caused the disruption of the middle region, including binding site formation. In the EGFR harboring the T790M/L858R mutation, the protruding of the mutated residue M790 to the drug molecule leads to the quinazoline ring, a core of tyrosine kinase inhibitors (TKIs), swaying out of the pocket concerted with N-lobe movement in the similar direction. It resulted in a lower hydrogen bond interaction with the residue C797, the hot spot position for an oncogenic mutation that overcomes the T790M-targeting EGFR inhibitors (third-generation TKIs), and also a target position for covalently-linked drugs. Therefore, the harboring secondary mutation cannot support the binding of incoming erlotinib through affecting the ligand movement and its N-lobe. The overall data shows the molecular mechanism of how erlotinib resistance associates with the development of T790M mutation in patients.

Introduction

Chemotherapy is the most common treatment for cancers; however, its side effects diminish the quality of the patient's life¹. Targeted therapy is introduced to decrease the side effects of chemotherapy. Instead of killing rapidly-dividing cell likes chemotherapy, the targeted therapy can inhibit specifically at the proteins found in cancer cells or involved in cancer cell growth. Hence, the side effects are lower than chemotherapy². In non-small cell lung cancer (NSCLC), the general protein for a targeted drug is the mutated epidermal growth factor receptor (EGFR). EGFR is the transmembrane receptor that consists of three domains: an extracellular ligand-binding domain, a single transmembrane domain, and an intracellular tyrosine kinase domain³. After binding to its ligands (EGF and TGF- α), EGFR can trigger three main pathways: RAS/RAF/MAPK pathway, PI3K/AKT pathway, and JAK/STAT pathway⁴. All of these pathways involve cell proliferation and apoptotic inhibition. EGFR mutation in the tyrosine kinase (TK) domain causes the autoactivation of downstream pathways, ultimately leading to an uncontrollable increase of the cell. TK domain can be divided into the N- and C-terminal lobes. One of the most common mutations in this domain is L858R substitution, which accounts for 41% in NSCLC⁵.

Erlotinib or Tarceva (trade name, **Figure 1**) is a tyrosine kinase inhibitor (TKI) used to treat NSCLC. It binds at the hinge region between N-lobe and C-lobe of the TK domain. The progression of cancer is inhibited in a period. After that, some patients develop drug resistance against erlotinib. Many possible resistance mechanisms were proposed⁷. One of those is the T790M secondary mutation, which is 50-85% reported in clinical reports after patients resisted to tyrosine kinase inhibitors⁸⁻¹⁰. This mutation occurs in exon 20 and locates at the drug-binding pocket (**Figure 1**). The roles of this mutation in drug resistance were found to enhance ATP binding and thought to be steric to the binding of TKIs since this 790 position is the "gatekeeper"¹¹. However, the molecular mechanism of drug resistance due to the

T790M/L858R mutation, especially the dynamic behaviors and drug-protein interactions, was not well described. Thus, we aim to investigate the source of erlotinib resistance caused by the secondary mutation T790M in EGFR TK domain in active conformation relative to the wild type and primary L858R mutation at atomic level. Herein, all-atom molecular dynamics (MD) simulations together with principle component analysis (PCA) were used to gain insight about structure and dynamics. Apo forms of wild type, L858R and T790M/L858R strains were also simulated in this study for comparison. Note that the drug-target binding affinity in several EGFR TK mutants were previously studied by the *in silico* methods [refs].

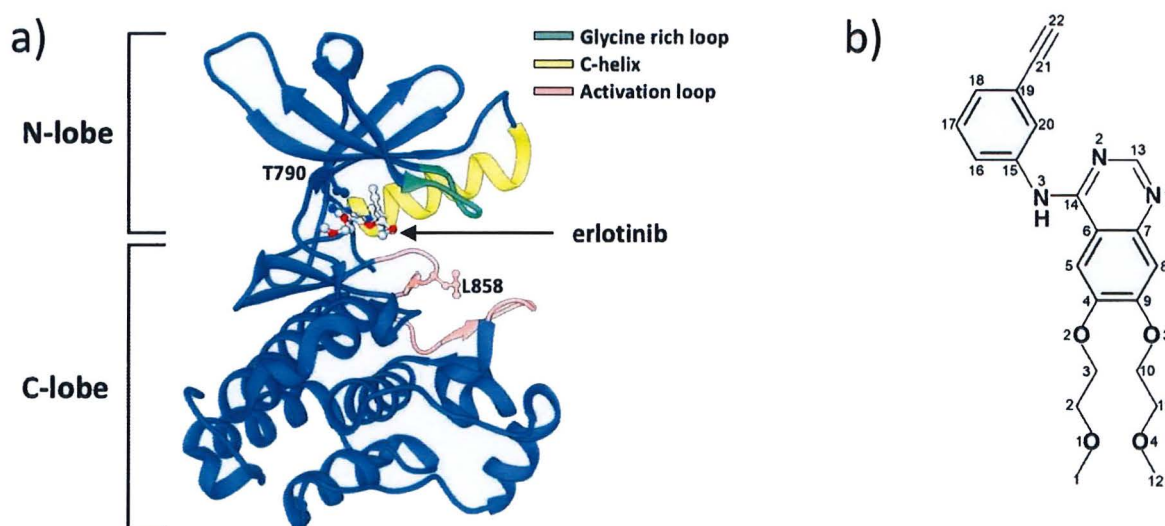


Figure 1. (a) Complex structure of erlotinib binding to EGFR TK domain. (b) Chemical structure of erlotinib where the atomic labels are shown for further discussion.

Results and Discussion

To monitor the stability of the system, the root-mean-square displacements (RMSDs) of all atoms for complex, protein backbone, and erlotinib relative to those of the minimized structure were computed throughout the MD simulations. RMSD plots of all systems are provided in **Figure 2**. RMSD values of all complexes or proteins rapidly increase in the first

10 ns due to their initial steps of simulation, heating, and equilibration. It can be seen that after 120 ns, all systems have reached equilibrium. The fluctuation of wild type-erlotinib (WT-Erlotinib) shows the reduction of RMSD values indicating a more stable structure after drug binding. The other complexes, L858R and T790M/L858R, exhibit a similar pattern of RMSD plot with those in apo forms but differ at its equilibrated values. Based on entire plots, the trajectories from the last 80 ns are selected for further analyses in terms of 2D-RMSD, principal component analysis (PCA), dynamic cross-correlation map (DCCM) and ligand-protein hydrogen bonds to understand the source of drug resistance due to the introduction of the secondary mutation T790M.

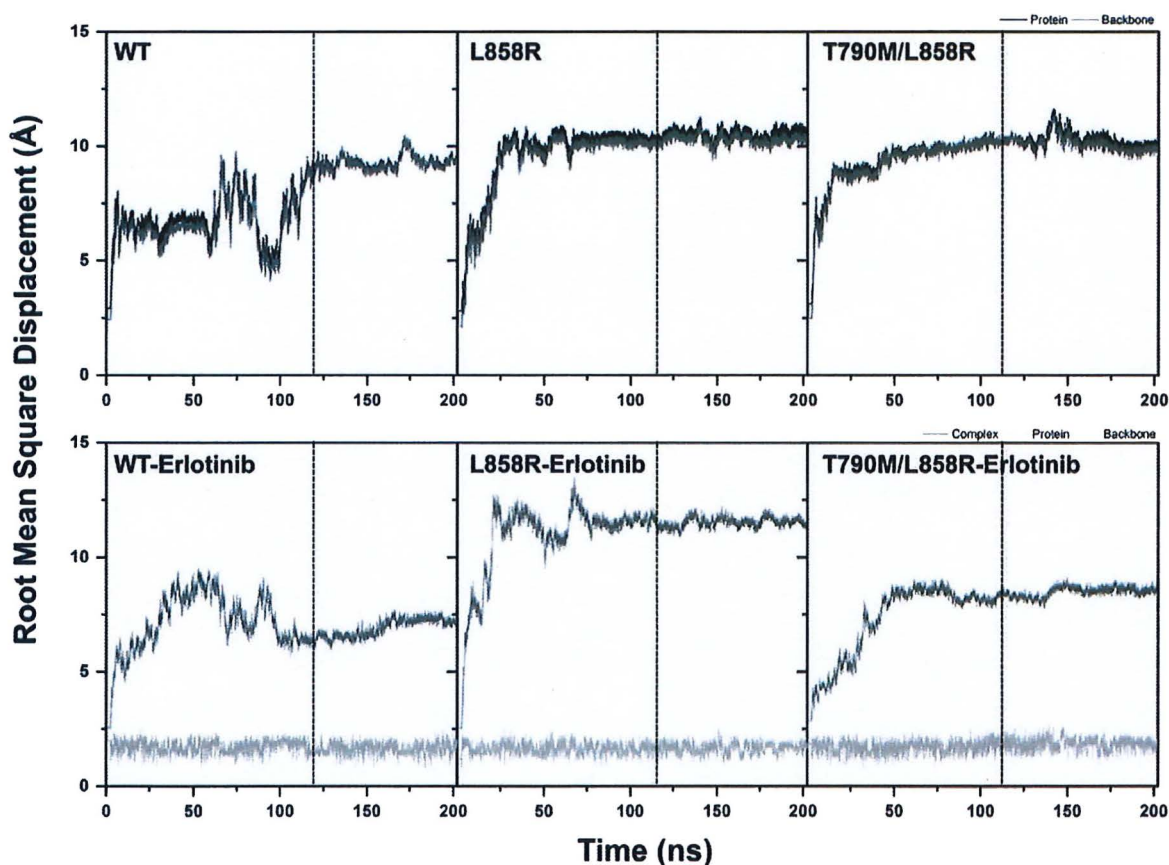


Figure 2. Root-mean square displacement (RMSD) of all six systems: WT, L858R, and T70M/L EGFR TK without and with erlotinib bound. Black, gray, and light gray represent RMSDs of all atoms for protein (apo form) or complex (holo form), backbone, and erlotinib,

respectively. The dashed line indicates the selected period of equilibrated trajectories for further analyses.

Pair-Wise Root Mean Square Displacement Matrix Analysis (2D-RMSD)

2D-RMSD is a useful method to investigate the overview of structural changes at a specific time relative to any time point of the simulation. The 2D-RMSD results for all systems are given and compared in **Figure 3**. Three to four blocks of blue color along the last 80 ns of simulation in WT, L858R, and T790M/L858 suggest a decrease in structural differences. In comparison with apo-wild type, both kinds of mutations in apo forms show a bigger cluster of similar structures and maintain the structure at that stage longer than that of wild type. The reduction of conformational changes is observed when the erlotinib binds to wild type. Similar to those of apo form, T790M/L858R complex has even lower conformational changes (bigger deep blue blocks). In the L858R complex, blue blocks are similar in size with those of apo form but differ by simulation time. The blocks were between 120 to 150 ns and 150 ns to 200 ns. Two blue blocks were shown in T790M/L858R, *i.e.*, one is between 120 to 140 ns; another one is between 140 to 200 ns. Thus, the binding of erlotinib induces stability in all strains with different conformational clusters.

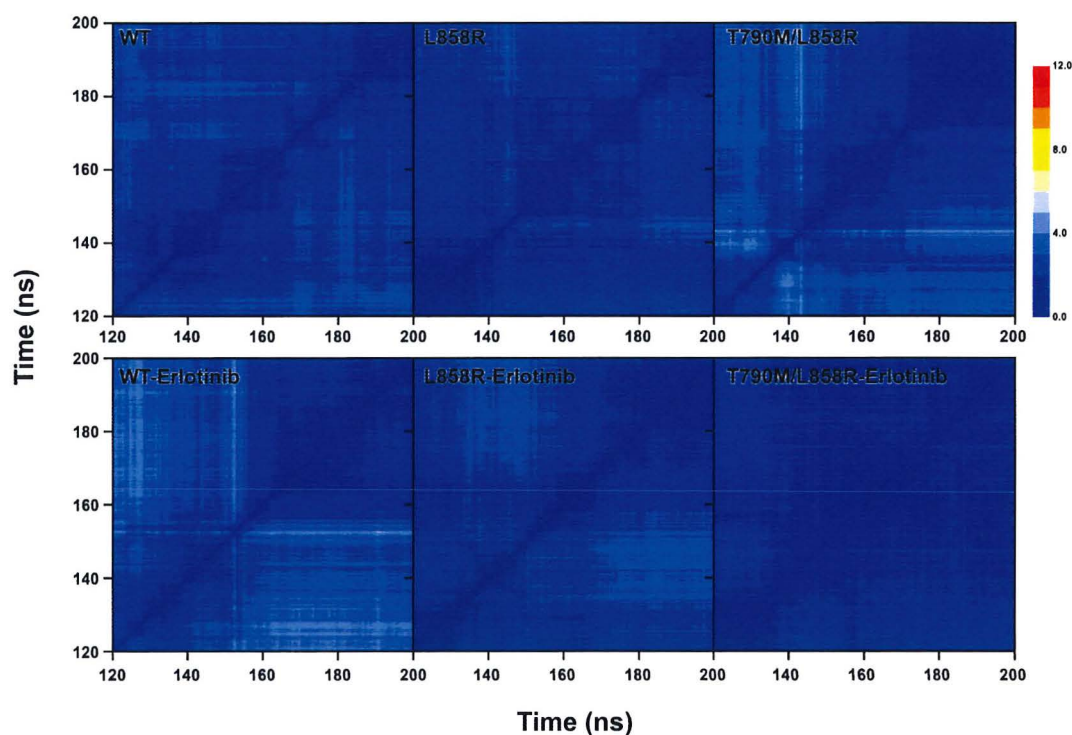


Figure 3. Pair-wise root mean square displacement matrix (2D-RMSD) of all atoms for the six systems: WT, L858R, T790M/L858R, WT-Erlotinib, L858R-Erlotinib, and T790M/L858R-Erlotinib. Each point is the RMSD between two conformations at the same or different time points of simulation. Different colors represent RMSD values. Blue is the lowest RMSD value, 0 Å, while red is the highest RMSD value, 12 Å.

Dynamics Cross-Correlation Map

To examine the correlation of motion between residues, the dynamic cross-correlation matrix (DCCM) is computed over the selected 80 ns trajectories. The C_{ij} elements of matrix vary from -1 to +1, -1 is entirely anti-correlated or opposite in the direction of motion, while +1 is completely correlated or the same direction of motion. Different colors represent C_{ij} values as heat maps in **Figure 4**. The diagonal line (red) is the result of the correlation of each residue with itself. DCCM can give information of the correlation between residues over the

period, but the information of motion from DCCM cannot be visualized as a three-dimensional picture like principal component analysis (PCA) does. The correlation of apo-wild type strain of EGFR TK is divided into four regions, the residues 696-790, 791-860, 875-1000, and 1001-1018, corresponding to N-lobe with juxtamembrane, the upper region of C-lobe, the lower region of C-lobe and C-terminal region, respectively. The N-lobe moves similarly with the upper and lower region of C-lobe, whereas almost the opposite manner to the C-terminus. The correlation of L858R EGFR mutation is similar to that of wild type but with less positive correlation among each region. The correlation block in T790M/L858R double mutation differs from the other apo strains. The positive correlation block is found between the residues 750 to 860 in the middle region of EGFR (lower part of N-lobe, the hinge region, and upper part of C-lobe). Thus, the primary mutation maintains the correlation as that of wild type with a higher degree of independence among regions. In contrast, the secondary mutation promotes the positive correlation in the middle region leading to the dependency between N-lobe and C-lobe connected with the hinge region. In other ways, the secondary mutation keeps the protein regions to behave similarly by controlling the linker region. The binding of erlotinib likely reduces the internal and external positive correlations among the four regions in wild type compared to that of apo form. It also increases positive correlation inside the N-lobe of the L858R strain to become stronger and more prominent, which is similar to that of apo-wild type. Interestingly, the binding of erlotinib to T790M/L858R mutant strain causes the disruption of positive correlation in the middle region, as previously mentioned in the apo system. Hence, the primary and secondary mutations induce the stronger and weaker correlations in the N-lobe and upper part of C-lobe, respectively, after complexation with erlotinib. A similar effect was observed in the previous study, which carried out in wild type and G719S EGFR TK³¹. They found that the stable core was the lower C-lobe region, as we found in the correlation map of wild type and L858R strains. The N-lobe, mostly harboring the mutation hot spots, was

responsible for protein flexibility. Moreover, the oncogenic mutation stabilized the regions around the binding site, including the hinge region, as we observed the correlation formation in the middle region in the secondary mutation.

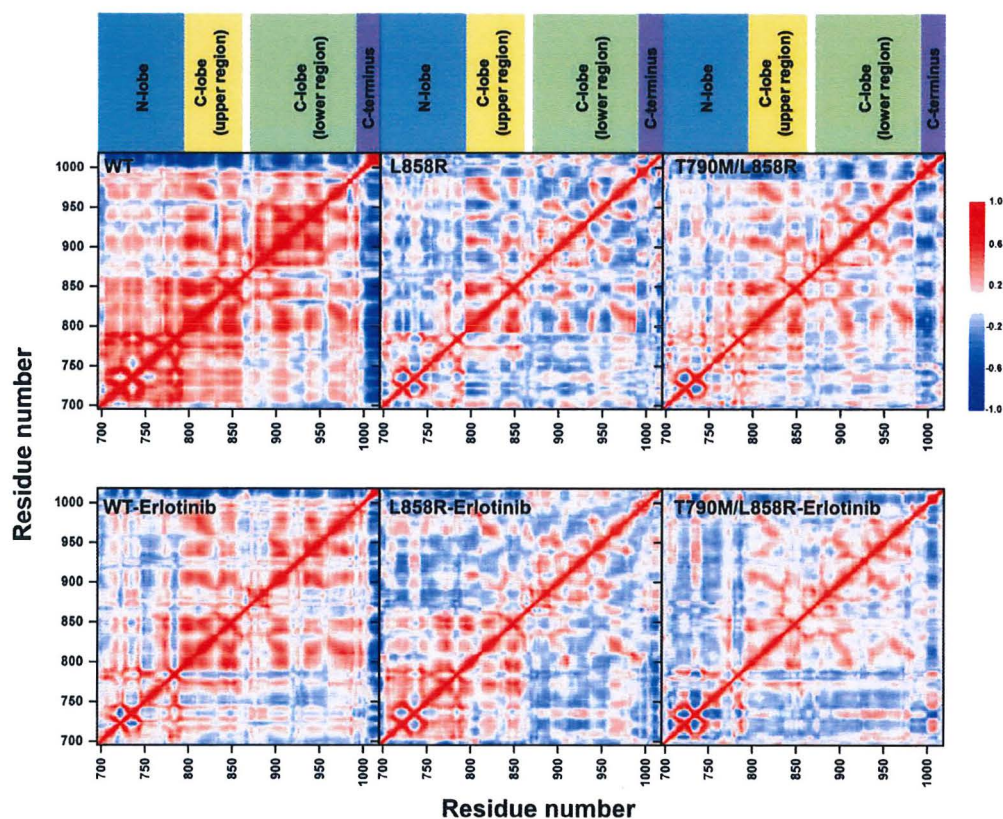


Figure 4. Dynamic cross correlation map (DCCM) represents the correlation between residues by defining C_{ij} value +1 as completely correlated (move in the same direction) and -1 as perfectly anti-correlated (opposite direction). Colors are represented the C_{ij} values from -1 to +1.

Principal Component Analysis

The principal component analysis (PCA) or essential dynamics is a powerful statistical tool to describe the dynamic motions of the structure³²⁻³³, in which a summation of all eigenvalues of each eigenvector in the system is equal to the total variance indicating the fluctuation in the protein. **Figure S2 in Supporting Information** shows the total variance

values of each system. The binding of erlotinib in primary mutation does not reduce the total variance, whereas it is decreased in both wild type and secondary mutation.

The scatter plots between the first and second principal components in **Figure 5**, PC1 and PC2, reveal the different distributions of protein conformations deviating from the averaged structure and its pattern. The zero value corresponds to the averaged structure. Although all plots of apo forms were able to be classified into two to three clusters, the apo-wild type showed the least darkness in each cluster. The conformations of apo-wild type were distributed higher than those of others, suggesting that its structural states were varied. These results are in agreement with those from 2D-RMSD in which multiple states of conformational changes are less observed in both primary and secondary mutations, and no matter they are apo or complexed form.

The first PCA mode (PC1) indicates the highest amplitude of protein motion. The PC1 direction (arrowhead) and its amplitude of motion (length of arrow) for all six systems are depicted in **Figure 6**, together with the protein motion shaded by different colors. The juxtamembrane and C-terminal are the most mobile region in all systems. N-lobe and C-lobe of apo forms tend to move down in all strains with small amplitude except those of T790M/L858R strain, which tends to move up. The binding of erlotinib results in the twisting of N-lobe in wild type and T790M/L858R strain to the right side, but it slightly moves up in the L858R strain. Moreover, the movement to the right side of the N-lobe in T790M/L858R strain with higher amplitude than other complexes was found, indicating the lower stability when erlotinib is bound. This region's correlation is disrupted in DCCM analysis. Thus, the secondary mutation causes the dynamic behavior of N-lobe to be more mobile and disassociation of C-terminus from N-lobe, which resembles wild type strain. However, the stability of the TK domain except for the end of C-terminus and juxtamembrane is in agreement with the previous NMR study suggesting that the kinase domain was rather rigid³⁴.

Motions of ligand, erlotinib, are depicted in **Figure 7**. Erlotinib bound to T790M/L858R sways out of the binding pocket to the right-hand side with a higher amplitude compared to the other strains. The quinazoline ring plays a vital role in this swaying. The mutated residue M790, bigger than that of T790, still protrudes to the drug though it tended to move inside slightly. Residue C797 in the secondary mutation moves in the almost opposite direction with the quinazoline ring (discussed further in the hydrogen bonding section). In contrast, erlotinib is less mobile in wild type and L858R strains. Thus, the secondary mutation T790M causes erlotinib moving out of the binding pocket with a high amplitude of motion in concerted N-lobe translocation.

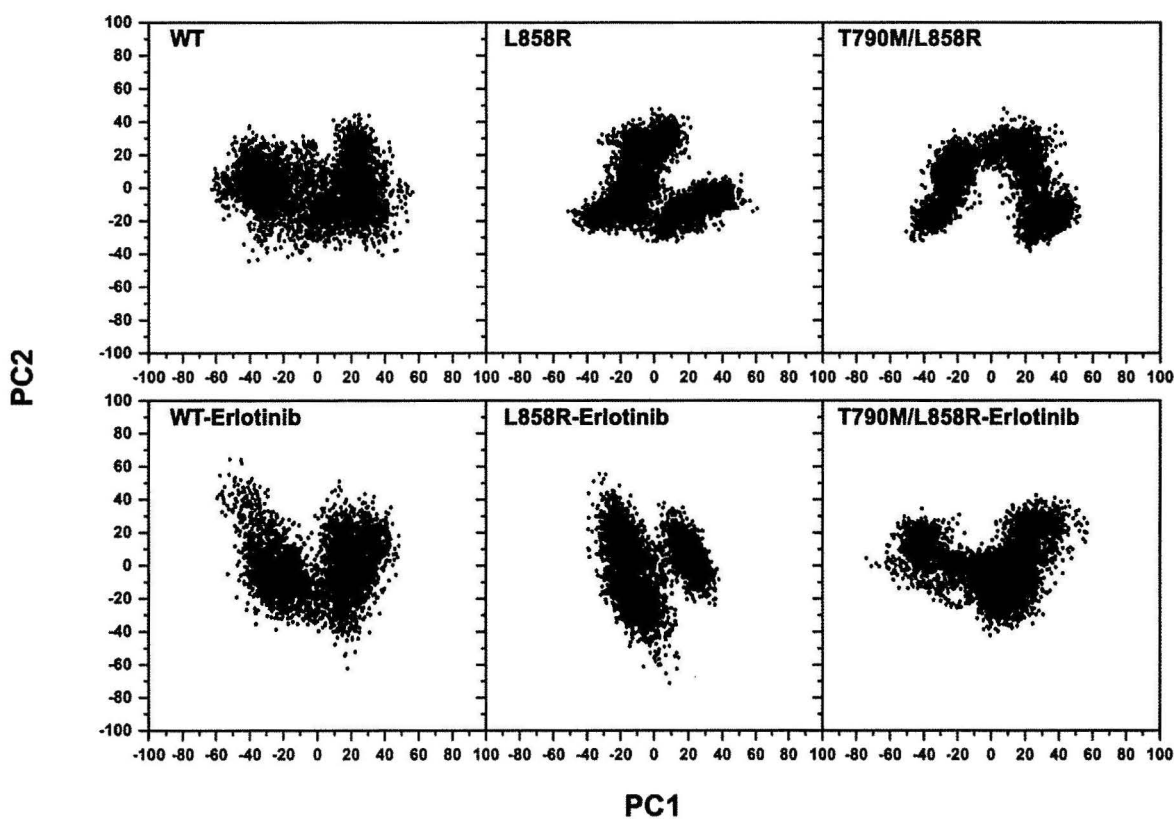


Figure 5. Scatter plot between the first (PC1) and second (PC2) principal components. Zero value corresponds to the averaged structure. The deviation from the averaged structure indicates how much each conformation in simulation differs from the average one when PC1 and PC2 are employed.

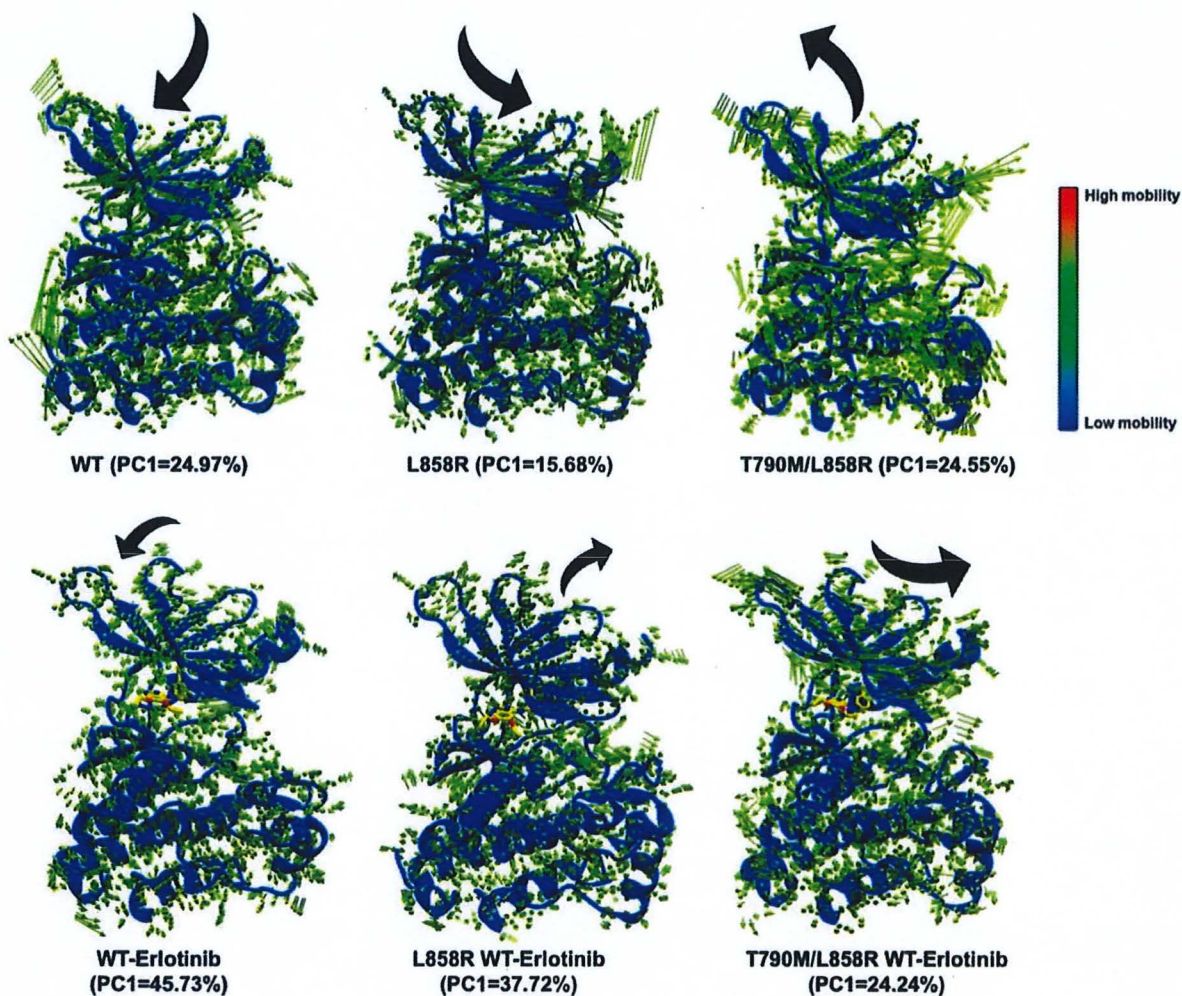


Figure 6. The first principal component (PC1) of each system is demonstrated by arrows (green color) and colors in the protein structure, where its percentage is given in the bracket. The arrowhead indicates the direction of motion while its length reflects the amplitude. The big black arrows show simplified N-lobes' direction of motion, which arrow sizes reflect their amplitudes of motion. The protein mobility is color-scaled by blue to red. Red color indicates the region with high mobility, whereas blue color indicates low mobility.

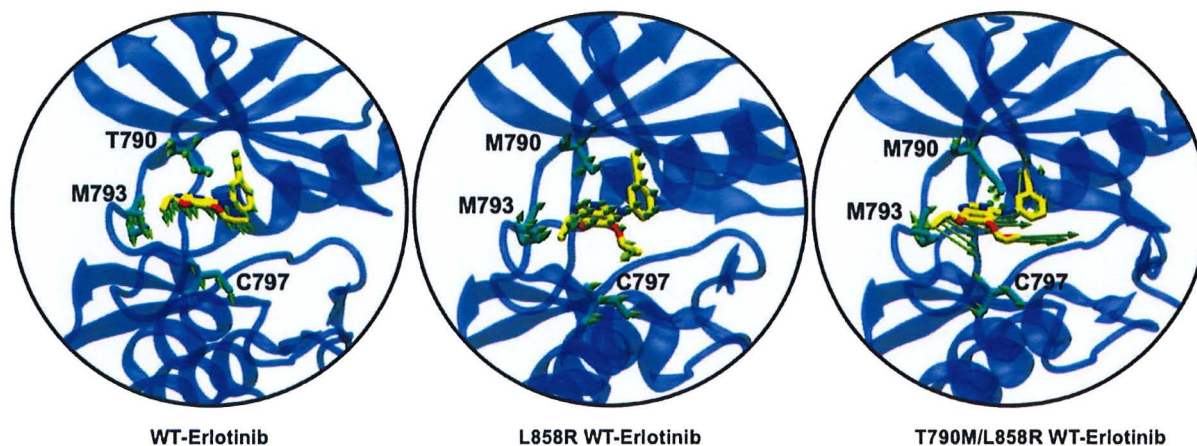


Figure 7. PC1 motion of the three critical residues of the EGFR TK domain, T790M, M793, and C797, as well as erlotinib.

To investigate the difference of protein motion between the two systems, their sets of trajectories are combined for PCA calculation. The PC1 of the combined trajectories from the two considered systems, EGFR TK domain without and with erlotinib bound, is shown in **Figure 8**. The region that exhibits the highest amplitude is focused. The difference of region among all three strains of both apo and complexed forms is mainly the glycine-rich loop (G-loop) and the linkage between N-lobe and C-helix. Apo strains barely differ at the C-lobe, whereas the difference in the N-lobe of complexes is increased, suggesting that the binding of erlotinib influences the motion of N-lobe. Noticeably, the difference between apo and complexed forms of each strain is G-loop in wild type, the linkage between N-lobe and C-helix in L858R, and G-loop in T790M/L858R. The linkage between N-lobe and C-helix in the L858R strain is different from that of the T790M/L858R strain. Altogether, the protein motion seems to mainly differ by its G-loop and also by the linkage between N-lobe and C-helix.

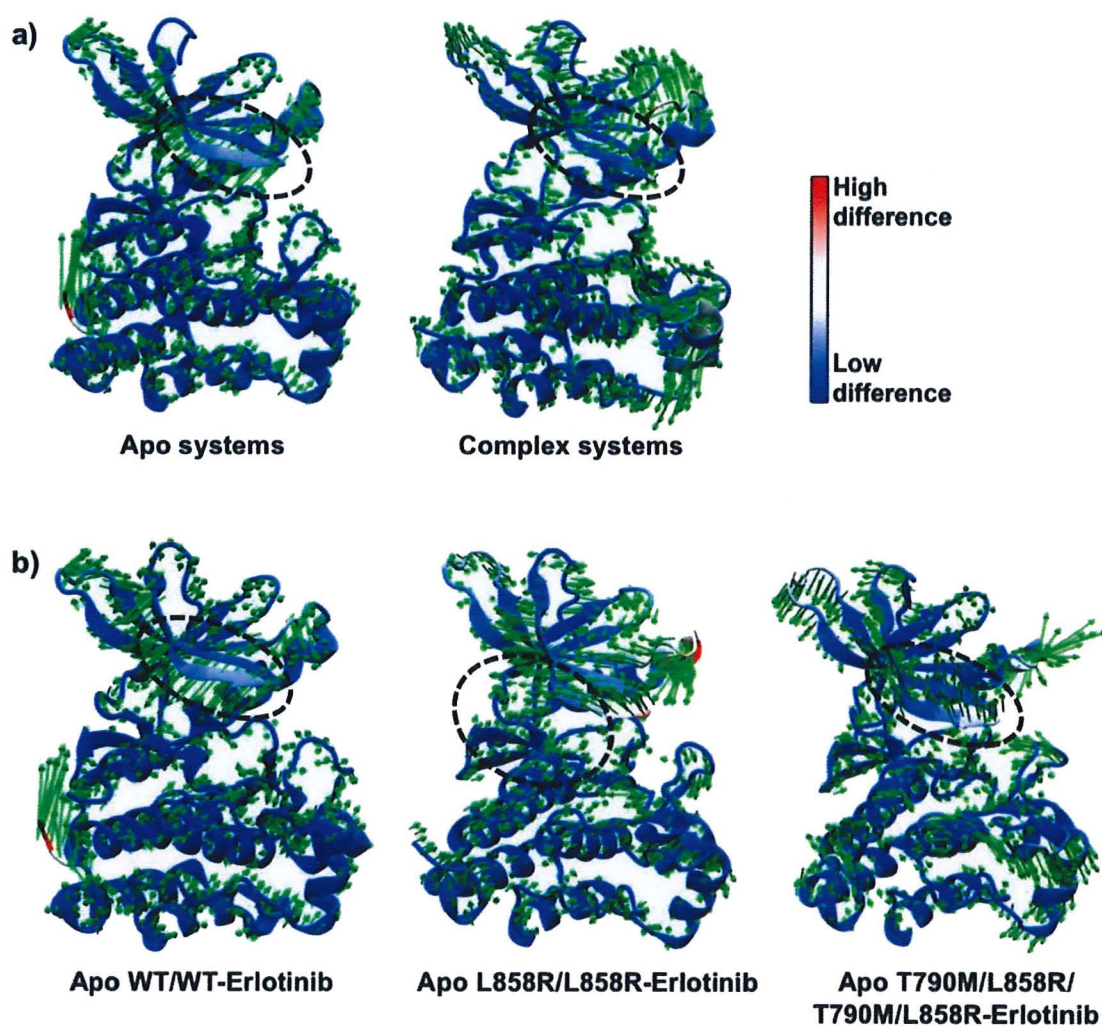


Figure 8. The PC1 of two combined trajectories for (a) apo systems (WT, L858R, T790M/L858R) and complex systems (WT-Erlotinib, L858R-Erlotinib, and T790M/L858R-Erlotinib), and (b) apo and complex systems in each strain. Blue and red colors indicate the region with low and high differences in motion, respectively. The dashed line encloses critical regions of the binding pocket showing different motions.

Hydrogen bonding between erlotinib and EGFR TK domain

To investigate the formation of hydrogen bonds between erlotinib and the residues in the binding site of EGFR TK domain, the hydrogen bond occupation is calculated by using the criteria: 1) the distance between hydrogen bond donor and acceptor is not over than 3.5 Å, and

2) the angle between hydrogen bond donor, hydrogen and hydrogen bond acceptor is larger than 120° . The formation of intermolecular hydrogen bonds of erlotinib with its occupation is drawn in **Figure 9**. In the wild type and L858R strains, erlotinib is stabilized by a strong hydrogen bond with M793 and a weak hydrogen bond with C797. M793 is also found to form hydrogen bonding with co-crystallized ligands and erlotinib analogs in both X-ray crystallography and computation³⁵⁻³⁶. The secondary mutation has not only caused high mobility of erlotinib in the binding site as mentioned above but also led to a reduction in drug-residue C797 interaction, directly resulting in a low binding affinity of erlotinib³⁷⁻³⁸. Moreover, one of the strategies to overcome the drug resistance is to design the covalently-linked drug with C797³⁹ residue, which is an oncogenic mutation hot spot in third-generation of anticancer drug development⁴⁰. Thus, the step of drug resistance development is the decrease of interaction with C797 by causing the second-generation TKIs swaying out of the binding pocket in secondary mutation, and then the C797 itself completely loses its interaction with the T790M-targeting EGFR inhibitors (third-generation TKIs) by mutating to be S797.

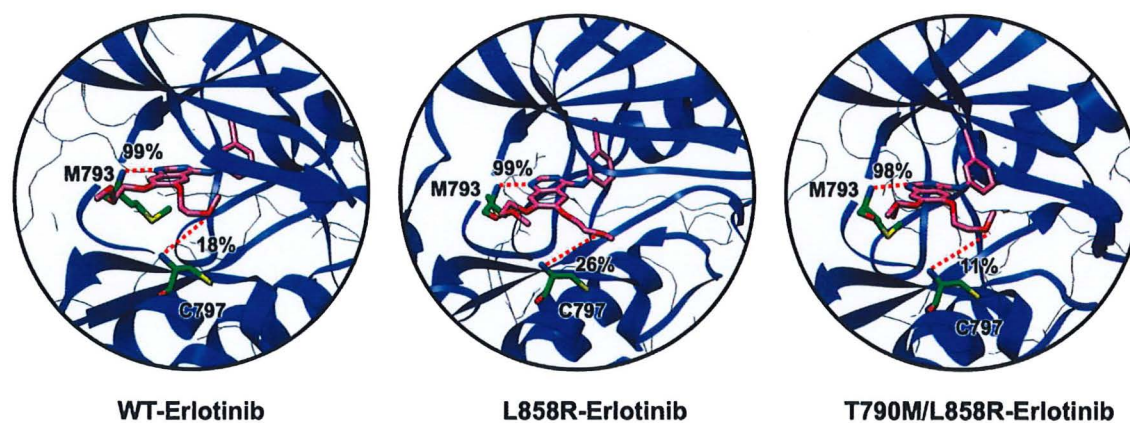


Figure 9. Hydrogen bonding between erlotinib and the two residues of EGFR TK domain in the three complexes represented using the last MD snapshot: WT-Erlotinib, L858R-Erlotinib, and T790M/L858R-Erlotinib.

Conclusions

In this study, we investigated the effect of secondary mutation T790M in the EGFR TK domain (T790M/L858R), which highly caused the erlotinib resistance, by all-atom MD simulations and principal component analysis (PCA). The DCCM results demonstrated that the secondary mutation likely destroyed the stability of middle region formation when there was incoming of erlotinib. From the PCA study, the protruding of T790M closely to the drug affects its quinazoline ring, which is the core of TKIs inhibitor to sway out of the binding pocket and consequently weakens the hydrogen bond interaction with the crucial residue C797. The ligand motion was in the same direction as N-lobe. Besides, the twisting of N-lobe in wild type and secondary mutation cannot be observed in the primary mutation. The structural and dynamic changes due to the introduction of T790M in both the protein itself and the incoming drug systems likely caused the binding affinity of the ligand/protein complex. All obtained data could explain the primary source of erlotinib resistance in the patients who develop the T790M mutation.

Methods

System Preparation

All initial systems were prepared from MODELLER 9v8 program¹²⁻¹⁴ and AMBER 16 package program¹⁵. Homology models of apo-EGFR TK domain in wild type, L858R and L858R/T790M strains, were constructed by using PDB entry code 5EDP as template. Residues M790, A865, A866 and A867 in homology model were changed back to be T790, E865, E866 and K867, respectively, using LEaP module of AMBER 16 program, while the residue M790 remained in homology model of L858R/T790M EGFR TK domain. L858R mutation model was also prepared by LEaP module. All holo forms of EGFR TK domain in complex with erlotinib were constructed by using 1M17.pdb as template. L858R and T790M/L858R

mutations acquired from manual mutation. To mimic the intracellular domain of EGFR, the juxtamembrane region and C-terminal region were also included in all models¹⁶⁻¹⁷. The coordinates of erlotinib in complex with those holo forms were obtained from the co-crystal structure of EGFR TK domain with erlotinib bound (1M17.pdb). The template and erlotinib coordinates for all systems were summarized in **Table 1**.

Table 1. Template and structural coordinates of erlotinib for all studied models.

| System | Template | Coordinates of erlotinib |
|-----------------------|----------|--------------------------|
| WT | 5EDP | - |
| WT-Erlotinib | 1M17 | 1M17 |
| L858R | 5EDP | - |
| L858R-Erlotinib | 1M17 | 1M17 |
| T790M/L858R | 5EDP | - |
| T790M/L858R-Erlotinib | 1M17 | 1M17 |

The protonation state of possible charged residues (Asp, Glu, Lys, Arg and His) for all models was assigned at pH 7.4 with PROPKA3.0¹⁸. Missing hydrogen atoms were added by the LeaP module in AMBER 16, which were then minimized with 1000 steps of steepest descents (SD) and 2000 steps of conjugated gradient (CG). In order to neutralize the system, chloride ions were randomly added. Finally, TIP3P water molecules were filled to construct the system in solution with distance of 13 Å from the protein surface. The AMBER ff14SB force field¹⁹ and the generalized amber force field²⁰ (GAFF) were used to treat for protein and erlotinib, respectively. To obtain the partial atomic charges of erlotinib, the ligand coordinates obtained from the crystallographic structure were optimized by the HF/6-31G* level of theory

by Gaussian09²¹ in according to the standard procedures²²⁻²⁴. Then electrostatic potential (ESP) charges were fitted using the single point energy calculation at the same level of theory on the optimized structure of ligand, which were finally converted to the restrained ESP (RESP) charges using the antechamber module in AMBER 16. The minimization processes of each system were divided into: 1) hydrogen and water minimizations under a restraint on the rest atoms with weight of 10.0 kcal/mol²-Å², 2) minimization under a restraint on the protein backbone atoms with weight of 10.0, 5.0 and 1.0 kcal/mol²-Å², respectively, and 3) minimization on whole system. Each step of minimization consisted of 2500 steps of SD and followed by 2500 steps of CG.

Molecular Dynamics Simulations

All systems were performed by all-atom MD simulation under periodic boundary condition (PBC) by following our previous studies²⁵⁻²⁷. SHAKE algorithm was applied to constrain all covalent bonds involving hydrogen atoms. A non-bonded cutoff of 12 Å was used. Long range electrostatic interactions were treated using particle mesh Ewald (PME). Each system was heated to 310 K for 200 ps with harmonically restrained protein of 10.0 kcal/mol-Å². Subsequently, NVT equilibration was performed for 200 ps. Then, 1 ns of NPT simulation was performed with decreasing restraint weights on the protein position reduced from 10.0 to 5.0 kcal/mol-Å², respectively. After that, the restraint was removed and full MD simulation was carried out until 200 ns by the PMEMD module in AMBER. All results were analyzed by cpptraj module in AMBER 16.

Principal Component Analysis

In order to examine the motion of protein in each system, principal component analysis (PCA) was applied on the 5000 frames from the last 100 ns. To perform PCA, the covariance

matrix size of $3N \times 3N$ is calculated (N is number of atoms) after removal of rotational and translational motions. Then, the covariance matrix is diagonalized to provide eigenvectors describing the dynamic motions of structure, and eigenvalues indicating how much each mode contributes to the entire dynamics.

The probability distribution of the first principal component PC1 was divided into the first 50 ns and the last 50 ns as shown in **Figure S1 of supporting information**. Bin interval was set to 20. The frequency of population was counted when it fell in each bin (x) and was then normalized to provide probability. Let $p(x)$ and $q(x)$ are probability distributions of the last 50 ns and the first 50 ns, respectively. Integral over $p(x)$ and $q(x)$ must be equal to 1, and $p(x) > 0$ and $q(x) > 0$ are for any x . Not every x interval has the overlapping of probability distribution between the first and last 50 ns; however, the percentage is higher than 55% (**Table S1 in supporting information**). Kullback-Liebler divergence²⁸ (D_{KL}) was then employed in the combination with PCA to investigate the convergence between the two probability distributions from the first and last 50 ns using the **eq 1**. If probability distribution $p(x)$ is the same with $q(x)$, D_{KL} is equal to zero. In contrast, if D_{KL} is high or reaches ∞ , it indicates that two populations are different or diverged. It can be seen from the results in **Table S1 of supporting information** that our simulations still showed the partial convergence between the first and last 50 ns of simulation.

$$D_{KL}(p(x)||q(x)) = \sum_{x \in X} p(x) \ln \frac{p(x)}{q(x)} dx \quad (1)$$

Acknowledgement

This study was financially supported by the Ratchadaphiseksomphot Endowment Fund (CU-GR_62_96_23_35), Chulalongkorn University (CU). P.C. thanks Development and Promotion of Science and Technology Talents Project, and Institute for Molecular Science

International Internship Program in Asia (IMS-IIPA). The authors sincerely thank Prof. Saito Shinji for valuable suggestions and comments. The Center of Excellence in Computational Chemistry, CU, was acknowledged for facilities and computing resources.

References

1. Polanski, J.; Jankowska-Polanska, B.; Rosinczuk, J.; Chabowski, M.; Szymanska-Chabowska, A., Quality of life of patients with lung cancer. *Onco Targets Ther* **2016**, *9*, 1023-8.
2. Baudino, T. A., Targeted Cancer Therapy: The Next Generation of Cancer Treatment. *Curr Drug Discov Technol* **2015**, *12* (1), 3-20.
3. Songtawee, N.; Gleeson, M. P.; Choowongkomon, K., Computational study of EGFR inhibition: molecular dynamics studies on the active and inactive protein conformations. *J Mol Model* **2013**, *19* (2), 497-509.
4. Normanno, N.; De Luca, A.; Bianco, C.; Strizzi, L.; Mancino, M.; Maiello, M. R.; Carotenuto, A.; De Feo, G.; Caponigro, F.; Salomon, D. S., Epidermal growth factor receptor (EGFR) signaling in cancer. *Gene* **2006**, *366* (1), 2-16.
5. Tetsu, O.; Hangauer, M. J.; Phuchareon, J.; Eisele, D. W.; McCormick, F., Drug Resistance to EGFR Inhibitors in Lung Cancer. *Chemotherapy* **2016**, *61* (5), 223-35.
6. Wang, X.; Goldstein, D.; Crowe, P. J.; Yang, J. L., Next-generation EGFR/HER tyrosine kinase inhibitors for the treatment of patients with non-small-cell lung cancer harboring EGFR mutations: a review of the evidence. *Onco Targets Ther* **2016**, *9*, 5461-73.
7. Huang, L.; Fu, L., Mechanisms of resistance to EGFR tyrosine kinase inhibitors. *Acta Pharm Sin B* **2015**, *5* (5), 390-401.
8. Pao, W.; Miller, V. A.; Politi, K. A.; Riely, G. J.; Somwar, R.; Zakowski, M. F.; Kris, M. G.; Varmus, H., Acquired resistance of lung adenocarcinomas to gefitinib or erlotinib is associated with a second mutation in the EGFR kinase domain. *PLoS Med* **2005**, *2* (3), e73.
9. Onitsuka, T.; Uramoto, H.; Nose, N.; Takenoyama, M.; Hanagiri, T.; Sugio, K.; Yasumoto, K., Acquired resistance to gefitinib: the contribution of mechanisms other than the T790M, MET, and HGF status. *Lung Cancer* **2010**, *68* (2), 198-203.
10. Costa, D. B.; Nguyen, K. S.; Cho, B. C.; Sequist, L. V.; Jackman, D. M.; Riely, G. J.; Yeap, B. Y.; Halmos, B.; Kim, J. H.; Janne, P. A.; Huberman, M. S.; Pao, W.; Tenen, D. G.; Kobayashi, S., Effects of erlotinib in EGFR mutated non-small cell lung cancers with resistance to gefitinib. *Clin Cancer Res* **2008**, *14* (21), 7060-7.
11. Yun, C. H.; Mengwasser, K. E.; Toms, A. V.; Woo, M. S.; Greulich, H.; Wong, K. K.; Meyerson, M.; Eck, M. J., The T790M mutation in EGFR kinase causes drug resistance by increasing the affinity for ATP. *Proc Natl Acad Sci U S A* **2008**, *105* (6), 2070-5.
12. Webb, B.; Sali, A., Comparative Protein Structure Modeling Using MODELLER. *Curr Protoc Bioinformatics* **2016**, *54*, 5 6 1-5 6 37.
13. Sali, A.; Blundell, T. L., Comparative protein modelling by satisfaction of spatial restraints. *J Mol Biol* **1993**, *234* (3), 779-815.
14. Fiser, A.; Do, R. K.; Sali, A., Modeling of loops in protein structures. *Protein Sci* **2000**, *9* (9), 1753-73.

15. D.A. Case, R. M. B., D.S. Cerutti, T.E. Cheatham, III, T.A. Darden, R.E. Duke, T.J. Giese, H. Gohlke, A.W. Goetz, N. Homeyer, S. Izadi, P. Janowski, J. Kaus, A. Kovalenko, T.S. Lee, S. LeGrand, P. Li, C. Lin, T. Luchko, R. Luo, B. Madej, D. Mermelstein, K.M. Merz, G. Monard, H. Nguyen, H.T. Nguyen, I. Omelyan, A. Onufriev, D.R. Roe, A. Roitberg, C. Sagui, C.L. Simmerling, W.M. Botello-Smith, J. Swails, R.C. Walker, J. Wang, R.M. Wolf, X. Wu, L. Xiao and P.A. Kollman *AMBER 2016*, University of California San Francisco, 2016.
16. Jura, N.; Zhang, X.; Endres, N. F.; Seeliger, M. A.; Schindler, T.; Kuriyan, J., Catalytic control in the EGF receptor and its connection to general kinase regulatory mechanisms. *Mol Cell* **2011**, *42* (1), 9-22.
17. Arkhipov, A.; Shan, Y.; Das, R.; Endres, N. F.; Eastwood, M. P.; Wemmer, D. E.; Kuriyan, J.; Shaw, D. E., Architecture and membrane interactions of the EGF receptor. *Cell* **2013**, *152* (3), 557-69.
18. Dolinsky, T. J.; Nielsen, J. E.; McCammon, J. A.; Baker, N. A., PDB2PQR: an automated pipeline for the setup of Poisson-Boltzmann electrostatics calculations. *Nucleic Acids Res* **2004**, *32* (Web Server issue), W665-7.
19. Maier, J. A.; Martinez, C.; Kasavajhala, K.; Wickstrom, L.; Hauser, K. E.; Simmerling, C., ff14SB: Improving the Accuracy of Protein Side Chain and Backbone Parameters from ff99SB. *J Chem Theory Comput* **2015**, *11* (8), 3696-713.
20. Wang, J.; Wolf, R. M.; Caldwell, J. W.; Kollman, P. A.; Case, D. A., Development and testing of a general amber force field. *J Comput Chem* **2004**, *25* (9), 1157-74.
21. M. J. Frisch, G. W. T., H. B. Schlegel, G. E. Scuseria, M. A. Robb, J. R. Cheeseman, G. Scalmani, V. Barone, G. A. Petersson, H. Nakatsuji, X. Li, M. Caricato, A. Marenich, J. Bloino, B. G. Janesko, R. Gomperts, B. Mennucci, H. P. Hratchian, J. V. Ortiz, A. F. Izmaylov, J. L. Sonnenberg, D. Williams-Young, F. Ding, F. Lipparini, F. Egidi, J. Goings, B. Peng, A. Petrone, T. Henderson, D. Ranasinghe, V. G. Zakrzewski, J. Gao, N. Rega, G. Zheng, W. Liang, M. Hada, M. Ehara, K. Toyota, R. Fukuda, J. Hasegawa, M. Ishida, T. Nakajima, Y. Honda, O. Kitao, H. Nakai, T. Vreven, K. Throssell, J. A. Montgomery, Jr., J. E. Peralta, F. Ogliaro, M. Bearpark, J. J. Heyd, E. Brothers, K. N. Kudin, V. N. Staroverov, T. Keith, R. Kobayashi, J. Normand, K. Raghavachari, A. Rendell, J. C. Burant, S. S. Iyengar, J. Tomasi, M. Cossi, J. M. Millam, M. Klene, C. Adamo, R. Cammi, J. W. Ochterski, R. L. Martin, K. Morokuma, O. Farkas, J. B. Foresman, and D. J. Fox *Gaussian 09*, Gaussian, Inc: Wallingford CT, USA, 2016.
22. Meeprasert, A.; Hannongbua, S.; Rungrotmongkol, T., Key binding and susceptibility of NS3/4A serine protease inhibitors against hepatitis C virus. *J Chem Inf Model* **2014**, *54* (4), 1208-17.
23. Meeprasert, A.; Khuntawee, W.; Kamlungsua, K.; Nunthaboot, N.; Rungrotmongkol, T.; Hannongbua, S., Binding pattern of the long acting neuraminidase inhibitor laninamivir towards influenza A subtypes H5N1 and pandemic H1N1. *J Mol Graph Model* **2012**, *38*, 148-54.
24. Sangpheak, W.; Khuntawee, W.; Wolschann, P.; Pongsawasdi, P.; Rungrotmongkol, T., Enhanced stability of a naringenin/2,6-dimethyl beta-cyclodextrin inclusion complex: molecular dynamics and free energy calculations based on MM- and QM-PBSA/GBSA. *J Mol Graph Model* **2014**, *50*, 10-5.
25. Kaiyawet, N.; Rungrotmongkol, T.; Hannongbua, S., Effect of halogen substitutions on dUMP to stability of thymidylate synthase/dUMP/mTHF ternary complex using molecular dynamics simulation. *J Chem Inf Model* **2013**, *53* (6), 1315-23.
26. Rungnim, C.; Arsawang, U.; Rungrotmongkol, T.; Hannongbua, S., Molecular dynamics properties of varying amounts of the anticancer drug gemcitabine inside an open-ended single-walled carbon nanotube. *Chemical Physics Letters* **2012**, *550* (Supplement C), 99-103.

27. Khuntawee, W.; Rungrotmongkol, T.; Hannongbua, S., Molecular dynamic behavior and binding affinity of flavonoid analogues to the cyclin dependent kinase 6/cyclin D complex. *J Chem Inf Model* **2012**, *52* (1), 76-83.
28. Kullback, S., and R. A. Leibler, On Information and Sufficiency. *The Annals of Mathematical Statistics* **1951**, *22* (1), 79-86.
29. Kaus, J. W.; Pierce, L. T.; Walker, R. C.; McCammont, J. A., Improving the Efficiency of Free Energy Calculations in the Amber Molecular Dynamics Package. *J Chem Theory Comput* **2013**, *9* (9).
30. Steinbrecher, T.; Joung, I.; Case, D. A., Soft-core potentials in thermodynamic integration: comparing one- and two-step transformations. *J Comput Chem* **2011**, *32* (15), 3253-63.
31. Paladino, A.; Morra, G.; Colombo, G., Structural Stability and Flexibility Direct the Selection of Activating Mutations in Epidermal Growth Factor Receptor Kinase. *J Chem Inf Model* **2015**, *55* (7), 1377-87.
32. David, C. C.; Jacobs, D. J., Principal component analysis: a method for determining the essential dynamics of proteins. *Methods Mol Biol* **2014**, *1084*, 193-226.
33. Mahalaputr, P.; Chusuth, P.; Kungwan, N.; Chavasiri, W.; Wolschann, P.; Rungrotmongkol, T., Molecular recognition of naphthoquinone-containing compounds against human DNA topoisomerase II α ATPase domain: A molecular modeling study. *Journal of Molecular Liquids* **2017**, *247* (Supplement C), 374-385.
34. Kaplan, M.; Narasimhan, S.; de Heus, C.; Mance, D.; van Doorn, S.; Houben, K.; Popov-Celeketic, D.; Damman, R.; Katrukha, E. A.; Jain, P.; Geerts, W. J. C.; Heck, A. J. R.; Folkers, G. E.; Kapitein, L. C.; Lemeer, S.; van Bergen En Henegouwen, P. M. P.; Baldus, M., EGFR Dynamics Change during Activation in Native Membranes as Revealed by NMR. *Cell* **2016**, *167* (5), 1241-1251 e11.
35. Stamos, J.; Sliwkowski, M. X.; Eigenbrot, C., Structure of the epidermal growth factor receptor kinase domain alone and in complex with a 4-anilinoquinazoline inhibitor. *J Biol Chem* **2002**, *277* (48), 46265-72.
36. Yun, C. H.; Boggon, T. J.; Li, Y.; Woo, M. S.; Greulich, H.; Meyerson, M.; Eck, M. J., Structures of lung cancer-derived EGFR mutants and inhibitor complexes: mechanism of activation and insights into differential inhibitor sensitivity. *Cancer Cell* **2007**, *11* (3), 217-27.
37. Balius, T. E.; Rizzo, R. C., Quantitative prediction of fold resistance for inhibitors of EGFR. *Biochemistry* **2009**, *48* (35), 8435-48.
38. Bello, M., Binding mechanism of kinase inhibitors to EGFR and T790M, L858R and L858R/T790M mutants through structural and energetic analysis. *Int J Biol Macromol* **2018**, *118* (Pt B), 1948-62.
39. Schwartz, P. A.; Kuzmic, P.; Solowiej, J.; Bergqvist, S.; Bolanos, B.; Almaden, C.; Nagata, A.; Ryan, K.; Feng, J.; Dalvie, D.; Kath, J. C.; Xu, M.; Wani, R.; Murray, B. W., Covalent EGFR inhibitor analysis reveals importance of reversible interactions to potency and mechanisms of drug resistance. *Proc Natl Acad Sci U S A* **2014**, *111* (1), 173-8.
40. Smith, S.; Keul, M.; Engel, J.; Basu, D.; Eppmann, S.; Rauh, D., Characterization of Covalent-Reversible EGFR Inhibitors. *ACS Omega* **2017**, *2* (4), 1563-1575.